

BULGARIAN CHEMICAL COMMUNICATIONS

2012 Volume 44 / Number 3

*Journal of the Chemical Institutes
of the Bulgarian Academy of Sciences
and of the Union of Chemists in Bulgaria*

BULGARIAN CHEMICAL COMMUNICATIONS

A quarterly published by

THE BULGARIAN ACADEMY OF SCIENCES

and

THE UNION OF CHEMISTS IN BULGARIA

Volume 44, Number 3

ИЗВЕСТИЯ ПО ХИМИЯ

Тримесечно издание на

БЪЛГАРСКА АКАДЕМИЯ НА НАУКИТЕ

и

СЪЮЗ НА ХИМИЦИТЕ В БЪЛГАРИЯ

Том 44, Книга 3

2012

Editor-in-Chief:

V. Beschkov

EDITORIAL BOARD

Ch. Bonev, P.R. Bontchev, L. Boyadzhiev, I. Gutzow, I. Havezov, E. Ivanova, P. Peshev, K. Petkov, K. Petrov, L. Petrov, I. Pojarlieff, S. Rakovsky, D. Stoychev, L. Terlemezyan, D. Tsalev, D. Vladikova, D. Yankov

Members from abroad:

J. M. Albella (Spain), S. Berger (Germany), J. C. Breakman (Belgium), J. Etourneau (France), M. Farina (Italy), K. Friedrich (Germany), J. Gyenis (Hungary), A. J. Kirby (United Kingdom), T. Kowalska (Poland), K. Kutchitsu (Japan), A. Lasia (Canada), O. V. Mazurin (Russia), B. Mutafschiev (France), E. Peter Kündig (Switzerland), S. De Rosa (Italy), T. F. Tadros (United Kingdom), K. Valko (Hungary)

Language editor: E. Ivanova

The annual subscription (for 4 issues) for vol. 44 (2012) is € 160. – including postage, handling and packaging charge.

Payments should be delivered to:

*Editorial Board of Bulgarian Chemical Communications, Institute of Chemical Engineering,
Bulbank, IBAN: BG57BFTB76303400001748; BIC - BFTBBGSF (for Euro €).*

HVB Bank Biochim, IBAN: BG77BACX96603119903312; SWIFT BIC - BACXBGSF (for local currency BGN).

This issue is published with the financial support of the National Science Fund at the Ministry of Education and Science of Bulgaria.

Removal of divalent heavy metal ions from aqueous solutions by Dowex HCR-S synthetic resin

B.A. Fil*, A. E. Yilmaz, R. Boncukcuoğlu, S. Bayar

Ataturk University, Faculty of Engineering, Department of Environmental Engineering, 25240, Erzurum-Turkey

Received December 23, 2011; revised May 16, 2012

Ion exchange technology is currently the best way to remove heavy metals from water and wastewater. In this study, we investigated heavy metal ions as cadmium (Cd^{2+}), nickel (Ni^{2+}) and zinc (Zn^{2+}) removal from aqueous solutions using synthetic resin. Batch experiments on the removal efficiency of heavy metal ions at under different conditions such as initial solution pH, stirring speeds, temperatures, initial concentrations and resin dosages of synthetic wastewater solutions were carried out. The maximal exchange levels attained were as follows: 99.76% Cd^{2+} , 93.66% Ni^{2+} and 83.10% Zn^{2+} onto Dowex HCR-S synthetic resin at 293 K, 250 mg L^{-1} initial metal concentration, ion exchange time of 60 min, 400 rpm stirring speed, pH: 6.0 and 2 g resin dosage.

Keywords: zinc; cadmium; nickel; heavy metals; ion exchange; Dowex HCR-S

INTRODUCTION

Fast industrialization has affected to rise up disposal of heavy metals into the environment. The exceeding increase in the use of the heavy metals over the past few decades has unavoidable consequence in an increased flow of metallic substances in the aquatic environment.

Toxic heavy metal ions get introduced to wastewater through various industrial activities such as mining, refining ores, fertilizer industries, tanneries, batteries, paper industries, pesticides etc. [1]. Heavy metals are not biodegradable and tend to be accumulated in living organism, causing various diseases and disorders; therefore, they must be removed before discharge to natural resources [2, 3].

A number of technologies have been developed over the years to remove heavy metals from industrial wastewater. The most important technology includes coagulation/flocculation [4], chemical precipitation [5], adsorption [6], ion-exchange [7], biosorption [8], electrochemical processes [9] and membrane technology [10].

Ion exchange can be used to remove heavy metals from wastewater using an ion exchange resins as synthetic ones derived from guaran [11], Chelex 100 [12], clinoptilolite [13], Amberlite (IR 120, 200, and 252 ZU) [14], Dowex M-4195 [15], Lewatit [16], indion BSR [17], Amberlite IR-96 and Dowex 1x8 [18], and Dowex 50W [19].

In the present study, ion exchange of Cd^{2+} , Ni^{2+} and Zn^{2+} on Dowex HCR S/H strongly acidic cation exchanger resin is examined. The purpose of this study, is examine the interest for different heavy metals of the resin. The parameters that influence adsorption such as initial nickel concentration, stirring speed, resin dosage, temperature, pH and contact time were investigated.

2. MATERIALS AND METHODS

Synthetic Dowex HCR S/H in hydrogen form was obtained from Fluka Co. The properties of Dowex HCR S/H are given in Table 1. The heavy metal solutions of Zn (II), Ni (II) and Cd (II) chloride (analytical grade from Sigma Co) were prepared in double-distilled water.

To study the effect of important parameters like contact time, stirring speed, resin amount, pH, initial metal concentration and temperature on the removal of Cd (II), Ni (II) and Zn (II) by Dowex HCR S/H, experiments were conducted at room temperature except those in which the effect of temperature. The parameters chosen in the experiments were given in Table 2.

A batch system was used for removing by the exchange reaction of heavy metal ions from wastewater. Experimental period was determined as 60 min result of the preliminary tests. The temperature of the reactor was controlled with a HAAKE D8 thermostat connected to reactor. The experimental set up is shown in Figure 1 [20].

* To whom all correspondence should be sent:
E-mail: baybarsalifil2@gmail.com

Table 1. Properties of Dowex HCR-S resin

Parameters	Value
Type	Strong acid cation
Change capacity	1.8 meq/ml
Particulate size	300 μm – 1200 μm
pH	0 – 14
Max. operating temperature	100 $^{\circ}\text{C}$
Ionic form	H^+
Ionic density	1.22 g/cm^3
Physical form	Uniform particle size, spherical beads

Table 2. Experimental parameters

Parameter	Studied ratio
Initial metal concentration mg/L	25, 50, 100, 250, 500 and 1000
Adsorbent dosage (g/500 ml)	0.25, 0.50, 1.00, 1.50 and 2.00
pH	3.0, 4.0, 5.0 and 6.0
Stirring speed (rpm)	200, 300, 400, 500 and 600
Solution temperature (K)	293, 313, 333 and 353

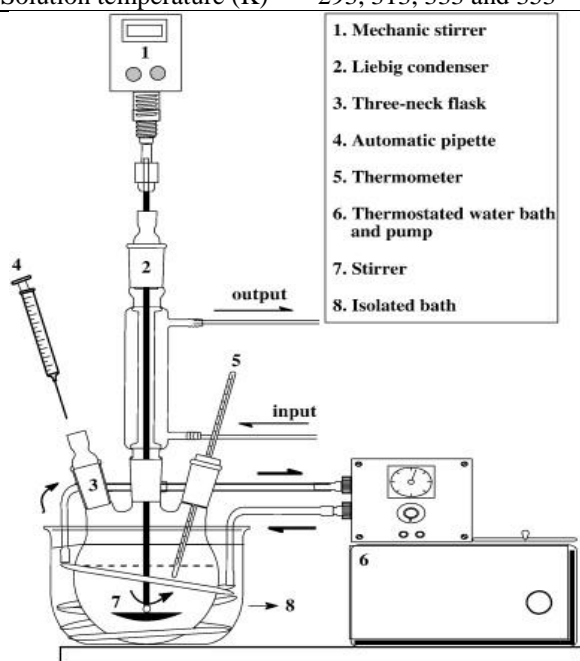


Fig. 1. Experimental set up.

Kinetic experiments were made by using 500 ml of heavy metal solutions (Cd^{2+} , Ni^{2+} and Zn^{2+}) of various concentrations. Samples were taken at different time intervals and remaining metal concentrations were analyzed. The remaining metal concentration in solution with atomic absorption spectrometers (AAS – 6800) device was decided. The amount of metal removal onto Dowex HCR S/H was calculated from the percent efficiency equation as follows:

$$\% \text{ efficiency} = \left(\frac{C_0 - C_t}{C_0} \right) \times 100 \quad (1)$$

where C_0 (mg L^{-1}) is the initial metal concentration, C_t (mg L^{-1}) is the concentration of metal ions in solution at time t .

3. RESULTS AND DISCUSSION

3.1 Effect of pH on ion exchange process

In order to establish the effect of pH on the ion exchange of zinc (II), cadmium (II) and nickel (II) ions on to synthetic resin, the batch equilibrium

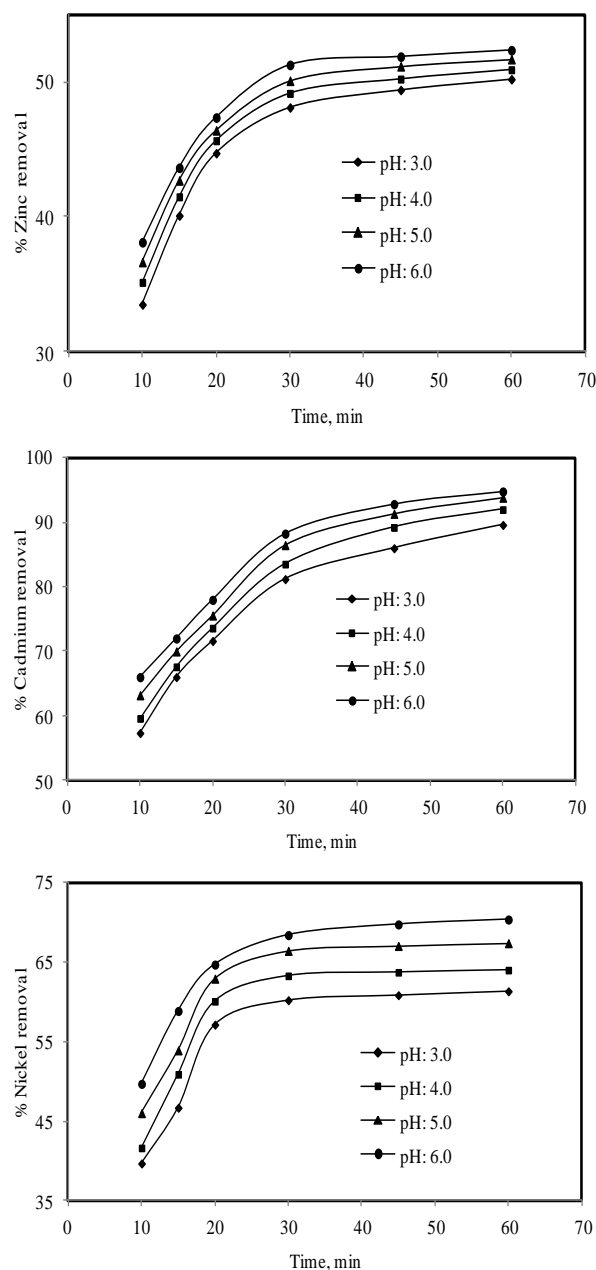


Fig. 2. The effect of initial pH on removal efficiency for the here metal ions (250 mg L^{-1} initial metal concentration, 293 K solution temperature, 400 rpm stirring speed, 1 g/500 ml resin dosage).

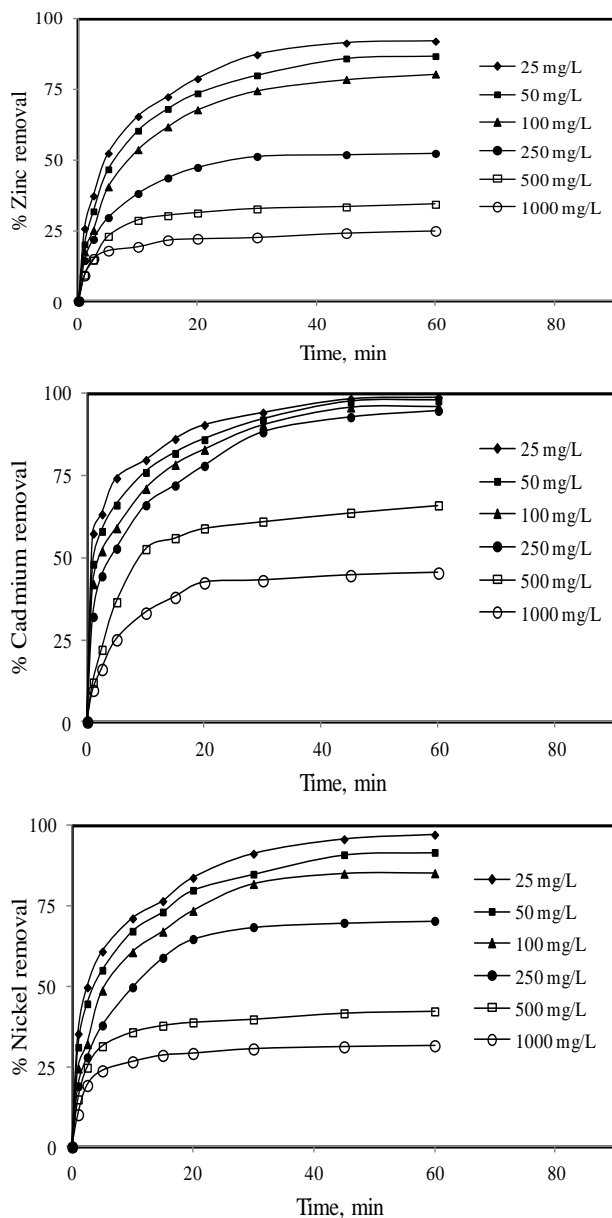


Fig. 3. The effect of initial metal concentration on removal efficiency (pH 6.0, 293 K solution temperature, 400 rpm stirring speed, 1 g/500 ml resin dosage).

studies at different pH values were carried out in the range of 3.0 – 6.0 for a constant resin amount of 1 g/L and initial metal concentrations of 250 mg/L at 293 K (Fig. 2). Because of precipitation of heavy metal ions, high values of pH were not studied. Fig. 2 shows the change in metal uptake by synthetic resin at different initial pH levels. It can be seen from Fig. 2 that the pH of the aqueous solution is an important control parameter in the ion exchange process [12]. The percentage of removal metals increased with pH from 3 to 6 with maximum binding occurring pH 6. At pH 6, 52.336% for zinc, 94.777% for cadmium and 70.359% for nickel.

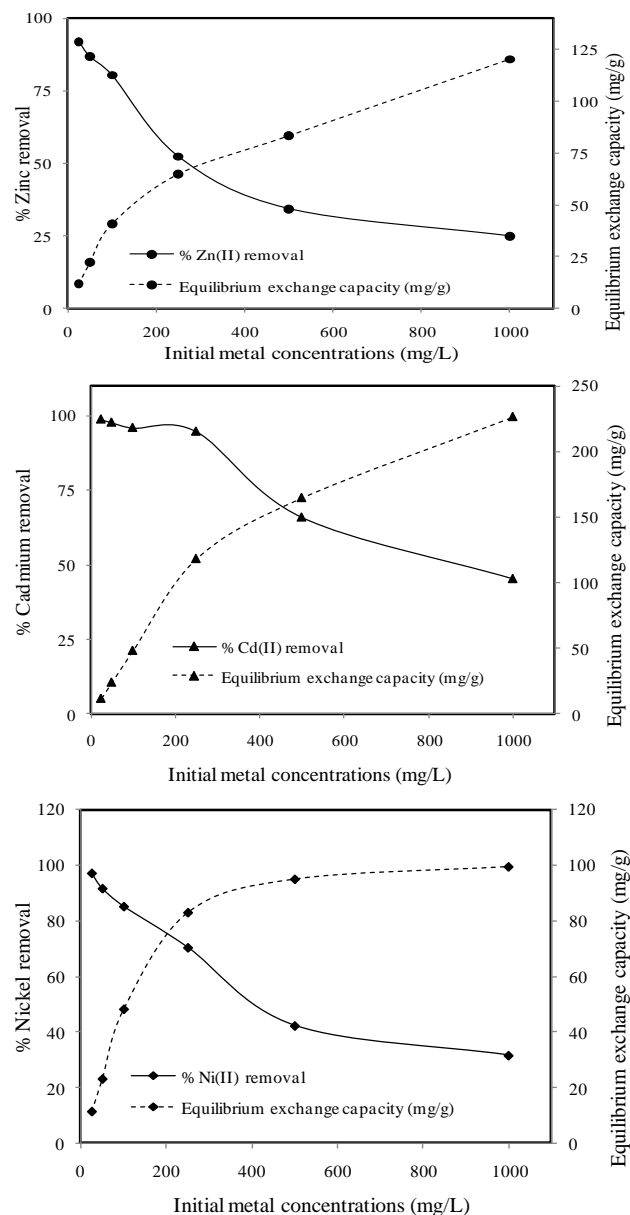


Fig. 3a. The effect of initial metal concentration on removal efficiency and exchange capacity (pH 6.0, 293 K solution temperature, 400 rpm stirring speed, 1 g/500 ml resin dosage).

3.2 Effect of initial metal concentrations on ion exchange process

Half litre of each of the three metal solutions (Zn^{2+} , Cd^{2+} and Ni^{2+}) of different concentrations ranging from 25 to 1000 mg/L with 1 g of synthetic resin was stirred at 400 rpm and ambient temperature (293 K) for a contact period of 1 h. The results obtained are shown in Fig. 3 and Fig. 3a and indicate that all the curves have the same shape.

It was also realized that the capacity of metal removal by Dowex HCR S/H at the equilibrium increased with the initial concentration of metal but the percent removal decreased with the increase in initial metal concentration from 92.09% for 25

mg/L of Zn to 24.849% for 1000 mg/L of Zn, from 98.842% for 25 mg/L of Cd to 45.338% for 1000 mg/L of Cd and from 97.167% for 25 mg/L of Ni to 31.500% for 1000 mg/L of Ni. Similar results were obtained for Ni (II) on Lewatit resin [16] and Cd (II) on Duolite ES 467 resin [21]. Apparently, the initial heavy metal concentrations played an important role in affecting the capacity of metal exchange onto synthetic resin. The higher the heavy metal concentrations, the stronger the driving forces of the concentration gradient, and therefore the higher the adsorption capacity. In general, the percentage of metal removal increased rapidly up to approximately 10 min and thereafter, rose slowly before attaining a saturation value.

3.3 Effect of solution temperature on ion exchange process

The effect of solution temperatures onto heavy metal removal is shown in Fig. 4. The removal of heavy metal ions as Zn^{2+} , Cd^{2+} and Ni^{2+} increased slightly increasing temperature from 293 K to 353 K. It is seen from Fig. 4 that when synthetic resin for Zn (II) was used with an increase in temperature from 293 to 353 K, the ion exchange efficiency capacity increased from 52.366% to 59.280% for the initial metal concentration of 250 mg L^{-1} ; in the case of Cd (II) and Ni (II), the efficiency increased from 94.777% to 98.719% and from 70.359% to 74.680 for the same initial metal concentrations and pH 6.0. This indicated that the exchange reaction was endothermic in nature and ions exchange mechanism favors higher temperatures [7]. An increase in the removal with the rise in temperature may be explained by active site onto synthetic resin being more active at high temperatures. Additionally, an increase in temperature results for mobility of the ions being increased and a decrease in the retarding forces acting on the adsorption ions [22].

3.4 Effect of resin dosage on ion exchange process

The percentage efficiency of each of the three heavy metal ions at different doses of Dowex HCR S/H strongly acidic resin is shown in Fig. 5 and Fig. 5a. The degree (%) of removal efficiency increased as the resin dose was increased. It might be concluded that by increasing the resin dose, the removal efficiency of heavy metal ions increased, while ion exchange density decreased with increase in resin dose. The decrease in ion exchange density may be due to the fact that some adsorption sites may remain unsaturated during the adsorption process whereas the number of sites available for adsorption increases by increasing the resin doses

and that results in the increase of removal efficiency [23]. It could be seen from Fig. 5 when increased resin dosage from 0.25 to 2.00 g, removal efficiency increased from 22.143% to 88.099% for Zn (II), from 42.625% to 99.757% for Cd (II) and from 27.591% to 93.665% for Ni (II).

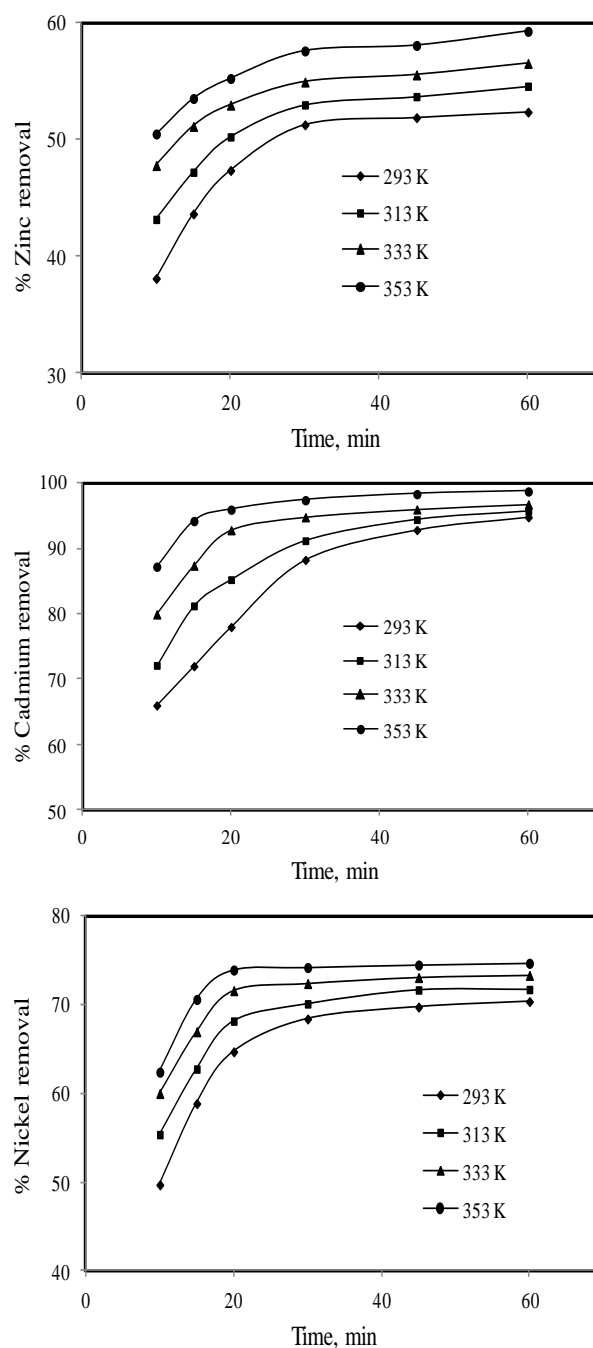


Fig. 4. The effect of solution temperature on removal efficiency (pH 6.0, 1 g/500 ml resin dosage, 400 rpm stirring speed and 250 mg L^{-1} initial metal concentrations).

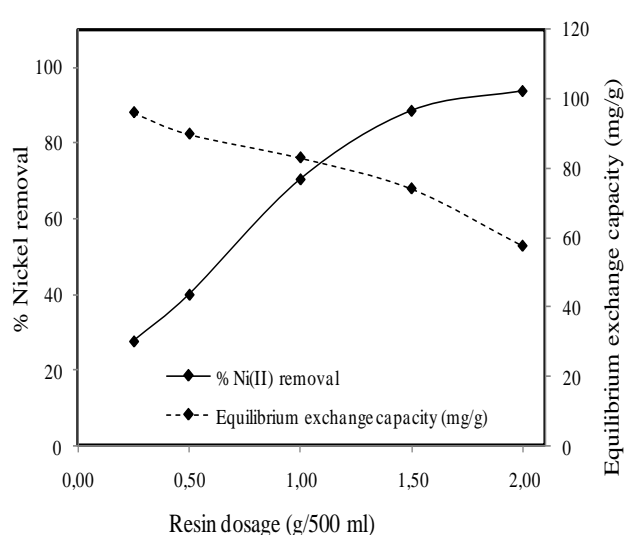
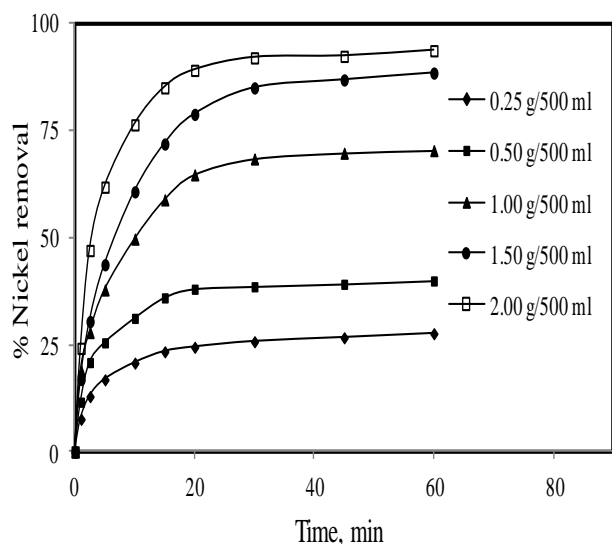
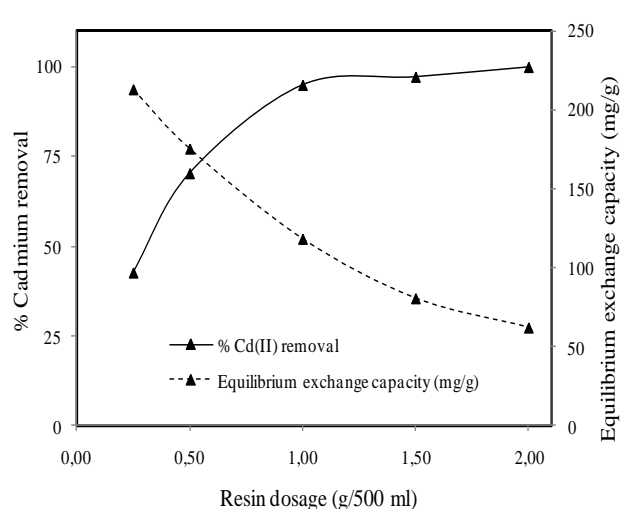
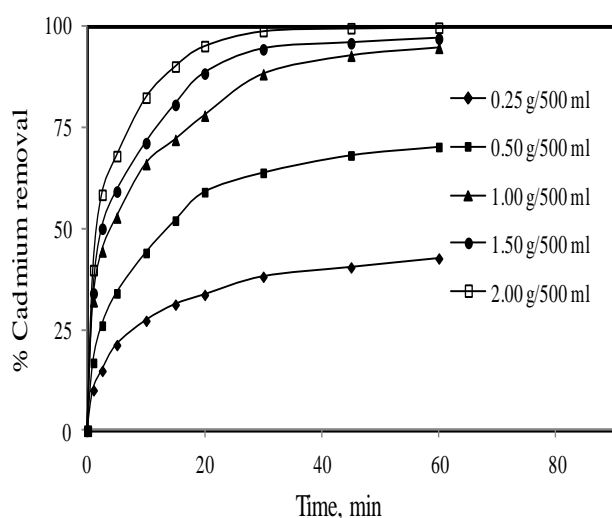
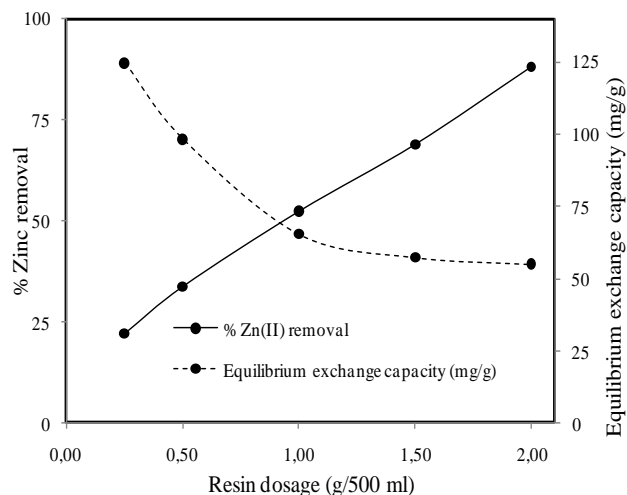
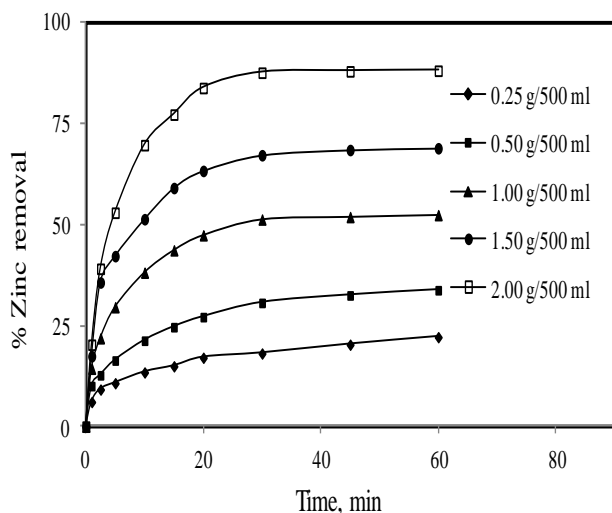


Fig. 5. The effect of resin dosage on removal efficiency (pH 6.0, 293 K solution temperature, 400 rpm stirring speed and 250 mg L⁻¹ initial metal concentrations).

Fig. 5a. The effect of resin dosage on removal efficiency and exchange capacity (pH 6.0, 293 K solution temperature, 400 rpm stirring speed and 250 mg L⁻¹ initial metal concentrations).

3.5 Effect of stirring speed on ion exchange process

Experimental results regarding the effect of agitation speed (200, 300, 400, 500 and 600 rpm) were presented. It is clear that stirring is found to be appropriate for maximum exchange of metal ion from the synthetic wastewater. The removal of metal ions using Dowex HCR S/H reaches 56.622% for Zn (II), 98% for Cd (II) and 73.805% for Ni (II) at 600 rpm, (Fig. 6). The effect of the

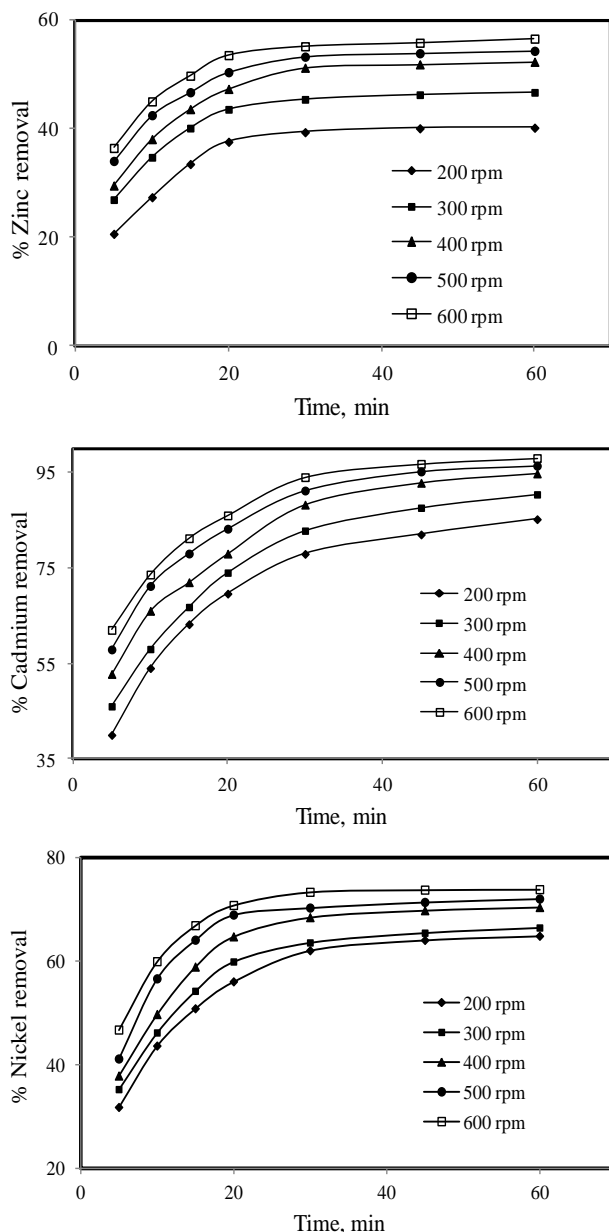


Fig 6. The effect of stirring speed on removal efficiency (pH 6.0, 1 g/500 ml resin dosage, 293 K solution temperature and 250 mg L⁻¹ initial metal concentration).

Agitation speed was examined at agitation speeds of range of 200–600 rpm. Stirring speeds higher than 600 rpm were not studied due to the effect of centrifugal forces on the system will increase. It is

obvious that agitation increased metal removal from aqueous solutions. This is due to the fact that metal ions, through their transportation to the solid phase, come on resistance at the liquid phase, through the boundary layer. The moving induced by the stirring of suspensions during experiments leads to a reducing of the boundary layer thickness and to a consequent decrease of the transportation resistance of metal ions. This increases the transfer rate of the ions and, thus, the ion exchange rate of the Zn (II), Cd (II) and Ni (II) ions [21].

CONCLUSION

The batch experiments presented in this study revealed that the Dowex HCR-S strongly acidic cationic synthetic resin could be effectively used as adsorbent for removing heavy metals. Treatment of heavy metal ions from aqueous solution was found to increase by increasing the resin dosage, stirring speed, temperature and solution pH. Increase of initial metal concentration decreases removal efficiency but the percent removal decreases with the increase in initial metal concentration. According to the heavy metal removal studies by using Dowex HCR-S strongly acidic cationic synthetic resin, the selectivity sequence could be given as Cd (II) > Ni(II) > Zn(II) at all studying parameters such as initial solution pH, stirring speeds, temperatures, initial concentrations and resin dosages of synthetic wastewater solutions.

REFERENCES

- 1 F. Fu, Q. Wang, *J. Environ. Manag.*, **92**, 407 (2011).
- 2 R.M. Schneider, C.F. Cavalin, M.A.S.D. Barros, C.R.G. Tavares, *Chem. Eng. J.*, **132**, 355 (2007).
- 3 M.H. Jnr, A.I. Spiff, *Acta Chim. Slov.*, **52**, 174 (2005).
- 4 F.M. Pang, P. Kumar, T.T. Teng, A.K. Mohd Omar, K.L. Wasewar, *J. Taiwan Inst. Chem. Engrs*, **42**, 809 (2011).
- 5 S. Mauchauffée, E. Meux, *Chemosphere*, **69**, 763 (2007).
- 6 N. Caliskan, A.R. Kul, S. Alkan, E.G. Sogut, I. Alacabey, *J. Hazard. Mater.*, **193**, 27 (2011).
- 7 I.H. Lee, Y.-C. Kuan, J.-M. Chern, *J. Chin. Inst. Chem. Eng.*, **38**, 71 (2007).
- 8 A.H. Hawari, C.N. Mulligan, *Bioresource Technol.*, **97**, 692 (2006).
- 9 F. Akbal, S. Camci, *Chem. Eng. Technol.*, **33**, 1655 (2010).
- 10 Z.V. P. Murthy, L.B. Chaudhari, *Chem. Eng. J.*, **150**, 181 (2009).
- 11 M. Ahuja, A.K. Rai, *Carbohydr. Polym.*, **33**, 57 (1997).

- 12 L.-C. Lin, R.-S. Juang, *Chem. Eng. J.*, **132**, 205 (2007).
- 13 Ö. Can, D. Balköse, S. Ülkü, *Desalination*, **259**, 17 (2010).
- 14 S. Kocaoba, *Environ. Eng. Sci.*, **25**, 697 (2008).
- 15 C.V. Diniz, V.S.T. Ciminelli, F.M. Doyle, *Hydrometallurgy*, **78**, 147 (2005).
- 16 N. Dizge, B. Keskinler, H. Barlas, *J. Hazard. Mater.*, **167**, 915 (2009).
- 17 A. Agrawal, K.K. Sahu, *Adsorp. Sci. Technol.*, **22**, 107 (2004).
- 18 S. Edebalı, E. Pehlivan, *Chem. Eng. J.*, **161**, 161 (2010).
- 19 E. Pehlivan, T. Altun, *J. Hazard. Mater.*, **134**, 149 (2006).
- 20 M.H. Karaoğlu, M. Doğan, M. Alkan, *Desalination*, **256**, 154 (2010).
- 21 K.S. Rao, G.R. Chaudhury, B.K. Mishra, *Int. J. Miner. Process*, **97**, 68 (2010).
- 22 M.A. Stylianou, V.J. Inglezakis, K.G. Moustakas, S.P. Malamis, M. D. Loizidou, *Desalination*, **215**, 133 (2007).
- 23 B. Alyüz, S. Veli, *J. Hazard. Mater.*, **167**, 482 (2009).

ОТСТРАНЯВАНЕ НА ДВУВАЛЕНТНИ ЙОНИ НА ТЕЖКИ МЕТАЛИ ОТ ВОДНИ РАЗТВОРИ СЪС СИНТЕТИЧНА ЙОНООБМЕННА СМОЛА DOWEX HCR-S

Б.А. Фил, А.Е. Йилмаз, Р. Бонджукджуоолу, С. Баяр

Университет „Ататюрк“, Факултет по инженерство, Департамент по екологично инженерство, 25240 Ерзурум, Турция

Постъпила на 23 декември, 2011 г.; преработена на 16 май, 2012 г.

(Резюме)

В момента йонообменните технологии предоставят най-добрия начин за отстраняване на тежки метали от водата и отпадъчните води. В тази работа ние изследваме отстраняването на йоните на тежки метали като кадмий (Cd^{2+}), никел (Ni^{2+}) и цинк (Zn^{2+}) от водни разтвори с помощта на синтетична йонообменна смола. Проведени са в периодични условия експерименти върху ефективността на отстраняване на металните йони от синтетични отпадъчни води при различни условия – начална стойност на рН, скорост на разбъркване, температура, начални концентрации и количество смола. Максимални степени на извличане се постигат както следва: 99.76% Cd^{2+} , 93.66% Ni^{2+} и 83.10% Zn^{2+} върху Dowex HCR-S при 293 К, начална концентрация на металните йони 250 mg L^{-1} , контактно време от 60 минути, скорост на разбъркване 400 об/мин, рН 6.0 и 2 г смола/500 мл.

Optimization of reaction conditions for synthesis C-tetramethylcalix[4]resorcinarene

D. Plachkova-Petrova¹, P. Petrova¹, St. Miloshev^{1*}, Ch. Novakov²

¹ University of Chemical Technology and Metallurgy, Department of Polymer Engineering,, 1756 Sofia, Bulgaria

² Institute of Polymers, Bulgarian Academy of Sciences, 1113 Sofia, Bulgaria

Received January 18, 2012; revised July 16, 2012

A new alternative method for the synthesis of calix[4]resorcinarenes has been shown. The optimal parameters for obtaining a C-tetramethylcalix[4]resorcinarene as a representative of the class of calix[4]resorcinarenes have been determined by varying the reaction conditions. It has been demonstrated that cyclic products can be prepared under certain conditions using catalytic amounts of mineral acid. It has been found that *cis-cis* (*cccc*) and *trans-trans* (*rttt*) isomers of C-tetramethylcalix[4]resorcinarene can be synthesized selectively by changing the ratio of water-organic phase, i.e. by changing the polarity of the medium. The reaction products have been separated using semi preparative liquid chromatography and characterized by gel permeation chromatography (GPC), nuclear magnetic resonance (¹H NMR), ultraviolet (UV) and fourier transform infrared (FTIR) spectroscopy.

Key words: C-tetramethylcalix[4]resorcinarene, polycondensation, resorcinol, acetaldehyde

INTRODUCTION

Resorcinarenes, the cyclic compounds belonging to calixarenes group are products of a polycondensation reaction between resorcinol and acetaldehyde (Figure 1) [1–9]. The presence of two hydroxide groups in the benzene rings, forming the macro cycle determines their relatively easy participation into large number of chemical interactions. Recently there has been a growing interest in the use of resorcinol based calixarenes and especially the calix[4]resorcinarene that have proved to be valuable for many applications in chemistry, biology and medicine [10–12].

Usually the synthesis of calix[4]resorcinarene is carried out by acid activated polycondensation in the presence of mineral acids and various alcohols. Concentrated hydrochloric acid in equimolar quantities to other reagents is the most used catalyst. Isolation of final cyclic products has been done through different approaches ranging a practical yield. Some authors reported for preparation of isolated products of relatively high yields in the presence of acid as a catalyst and in the presence of adequate solvents (methanol, ethanol) [13–15]. Reported reaction conditions (temperature, reaction time, sequence of reagents addition, etc.) have been varied widely, which leads to contradictory conclusions.

Therefore the aim of the present work is to

investigate and optimize the route to the synthesis of C-tetramethylcalix [4]resorcinarene.

The effect that the catalyst amount has on polycondensation and subsequent cyclization of oligomeric products has been traced in the course our research. The influence of the polarity of the medium on product composition has been also investigated. A procedure for optimization the isolation of cyclic products has been worked out as well.

EXPERIMENTAL

Materials

The reagents were purchased from Fluka (resorcinol and acetaldehyde), Merck (hydrochloric acid (37%)) and Lab-Scan (ethanol (96%), methanol, tetrahydrofurane (THF)).

Syntheses

Syntesis of calix[4]resorcinarene in ethanol medium using different amount of catalyst. The synthesis was performed according to methodology analogous to the one suggested by Ito and coworkers [16].

Resorcinol 15,46mmol (1,71g) and 20ml of ethanol were placed into a two-necked flask fitted with a reflux condenser and stirrer. The mixture was homogenized till complete dissolving of the resorcinol. The solution was placed into an ice bath and 15.46mmol (0,86ml) of acetaldehyde in 10ml of ethanol were added in a separating funnel for 10min. Then the required amount of hydrochloric

* To whom all correspondence should be sent:

E-mail: stmiloshev@yahoo.com

acid (0.01 – 30.15 mmol) was added taking care that the temperature of the reaction medium did not increase highly. Having added the catalyst the reaction solution was heated at 75°C for 5 to 24h. Then the resulting mixture was cooled to room temperature. The precipitate formed was filtered, washed with hot water (to neutral pH of washing water fractions) and dried under vacuum at 40°C.

Synthesis of calix[4]resorcinarene in ethanol/water medium using catalytic amount of hydrochloric acid. A series of syntheses was conducted using the optimal catalytic amounts of hydrochloric acid found experimentally and varying the ratio of ethanol/water in the reaction medium.

Resorcinol 0,3 mol (33,03g), 0,3mol (13,23ml) acetaldehyde and 120 ml ethanol/water mixture of different ratios were placed into a two-necked flask fitted with reflux condenser and stirrer. Acid catalyst (4 mol % compared to the other reagents concentrated hydrochloric acid) was added to the homogenized solution. The reaction solution was heated at 75°C under stirring for at least 1h. Then the resulting mixture was cooled to room temperature. The precipitate formed was filtered and recrystallized from methanol/water (v/v=50/50) solution. The reaction products were isolated using semi preparative liquid chromatography and characterized by GPC and ¹H NMR.

Instrumentation

Gel permeation chromatography (GPC). GPC experiments were performed on a chromatography line consisting of a tunable absorbance detector M 484, a differential refractive index detector M 410 (all Millipore Co., Waters Chromatography Division), a U6K universal injector and a set of three UltraStyragel gel columns (Waters) with nominal pore sizes of 100Å, 500Å and linear. THF was used as an eluent at 45°C and a flow rate of 1.0 ml.min⁻¹. Molecular weight characteristics were calculated using a calibration curve constructed with monodisperse poly(vinylpyridine) standards on a station for collection and processing of data through Clarity software. 1,3-dihydroxybenzene was used as an internal standard.

High-performance liquid chromatography (HPLC). The chromatograms were taken on a HP 1100 chromatography line (Agilent Technologies) equipped with a diode array UV detector, and a Kinetex C18 column with 2.6 pore size. Acetonitrile/water (68/32 v/v) mixture was used as an eluent at 30°C and a flow rate of 0,7 ml.min⁻¹.

Semi preparative liquid chromatography. The chromatographic separation was achieved on a

chromatography line consisting of M501 pump, a tunable absorbance detector M 490 (all Millipore Co., Waters Chromatography Division), a U6K universal injector and a semi preparative chromatographic column “μBondapak”C18 with a nominal pore size of 10 μm. A mixture of acetonitrile (A)/methanol (B)/phosphoric acid (0.5% water solution) (C) was used as an eluent. The samples were separated by running a linear gradient scheme as shown in Table 1.

Table 1. Gradient elution scheme

Time, (min)	Solvent mixture, %		
	A (%)	B (%)	C (%)
0	20	20	60
6	30	30	40
10	60	10	30
20	60	40	0
30	20	20	60

Ultraviolet spectroscopy (UV). UV spectra of the samples were recorded on a HP 1100 chromatography line (Agilent Technologies) equipped with a diode array UV detector in the course of chromatographic studies.

Fourier transform infrared spectroscopy (FTIR) Infrared spectra of the samples were recorded on a Bruker Vector 22 FT-IR spectrometer using potassium bromide pellet technique.

Nuclear magnetic resonance spectroscopy (¹H NMR). ¹H NMR spectra were recorded on a Bruker Avance DRX 250 (250 MHz) instrument. The samples were dissolved in deuterated solvent (dimethyl sulfoxide-d₆). Trimethylsilane was used as an internal NMR standard.

RESULTS AND DISCUSSION

Influence of catalyst amount on the yield of the reaction products

The reaction of polycondensation of resorcinol and acetaldehyde was carried out with different amounts of hydrochloric acid as a catalyst (0,01 to 1,00 mol per mol phenolic compound). It was found that reaction products of different composition and amount are obtained depending on the amount of hydrochloric acid used as shown on Figure 1. Increasing the acid amount (up to equimolar) led to a higher content of higher molecular weight linear oligomeric products (Figure 1a). That became an obstacle to obtaining cyclic products in the next stage of the process. Using a catalytic amount of catalyst resulted into the formation of predominantly cyclic product (Figure 1b).

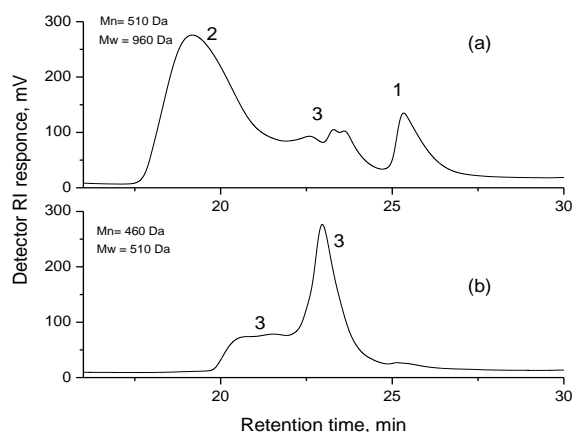


Fig. 1. GPC chromatograms of products obtained at 24h reaction time of polycondensation process catalyzed by hydrochloric acid: a) 1.0 mol per mol phenolic compound; b) 0.04 mol per mol phenolic compound (1- low molecular weight oligomers; 2- high molecular weight oligomers; 3- cyclic products).

Therefore, it was interesting to determine the minimum effective catalyst amount whereupon the reaction of polycondensation and oligocyclization proceeded at a comparable rate. Under the selected reaction conditions (see experimental section) a maximum yield of cyclic product was obtained with about 0,04 mol hydrochloric acid per mol phenolic compound as illustrated in Figure 1b. Further studies were performed with that ratio.

Influence of medium polarity on the yield and composition of the reaction products

Our previous investigations as well as data in the literature demonstrated the influence that polarity of reaction medium had on the composition of the polycondensation products obtained [10].

To determine the effectiveness of influence of medium polarity on the yield and composition of the reaction products the ethanol/water ratio was varied in a wide range – from pure ethanol to neat water solutions. Dielectric constant was used as an effective feature for the polarity of the medium. According to the literature [16–21] the dependence changes linearly with a change of ethanol or water in their mixtures. This dependence can be illustrated with the average values varying in the range of 3–5 units as shown in Figure 2. The reduction of the amount of ethanol in the reaction medium increases its polarity.

The polycondensation process performed in the span of 24 h was monitored by GPC technique. Due to the strong reactivity of resorcinol the polycondensation process begins almost immediately upon reaching 75°C. Reaching this

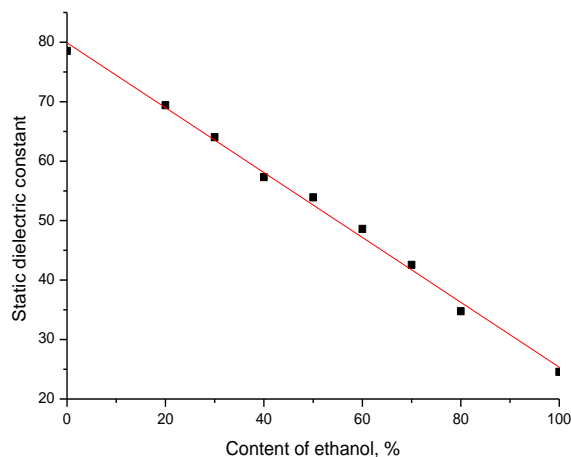


Fig. 2. Plot of the dielectric constant versus ethanol content in ethanol / water mixture (constructed on data cited in [16-21]).

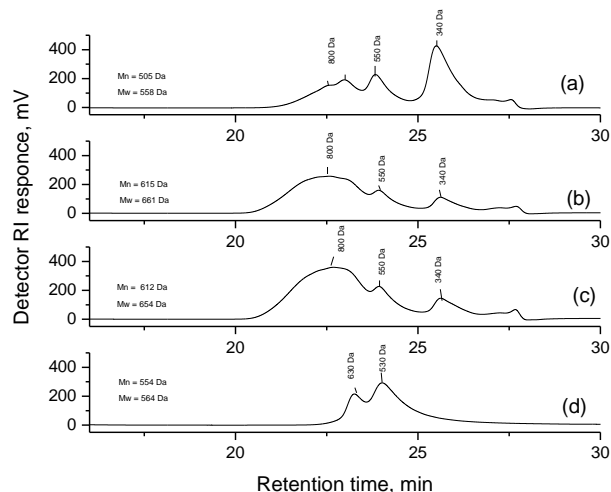


Fig. 3. GPC traces of reaction products obtained with hydrochloric acid (0.04 mol/mol phenolic compound) in ethanol/water mixture (20/80 v/v) at temperature 75°C for reaction time as follows: a) 0h; b) 2h; c) 5h; d) 24

temperature is considered to be conditional zero of the reaction. At this moment the products of different molecular weight are already formed as seen in Figure 3a. Their fractional composition changes with increasing the reaction time.

Semi preparative liquid chromatography of reaction mixtures is used to clarify the mechanism of the polycondensation process as well as to define the products obtained. The fractionation of the products obtained at conditional zero and at 24 h reaction time was carried out. The fractions collected were analyzed by GPC chromatography and ^1H NMR spectroscopy as shown in Figure 4 and Figure 5, respectively.

It was found fractions of molecular weight of about 200, 340, 550 Da and those within range 800-

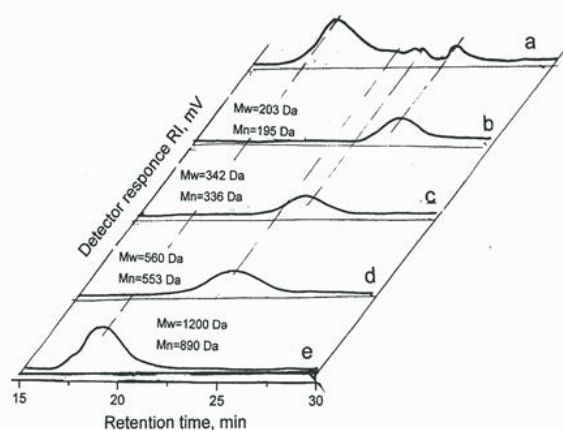


Fig. 4. GPC traces of reaction products obtained with hydrochloric acid (0.04 mol/mol phenolic compound) in ethanol/water mixture (30/70 v/v) at 75°C for 20h reaction time (a) and of fractioned products (b), (c), (d), (e) separated and isolated by semi preparative liquid chromatography.

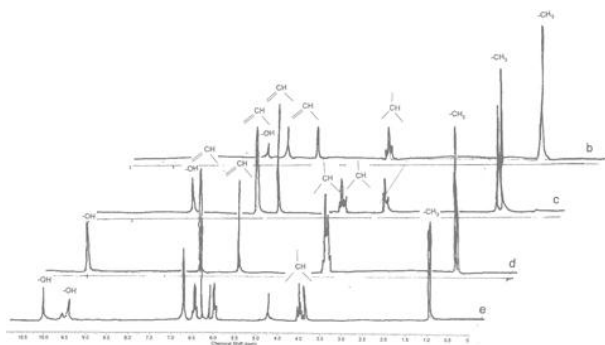


Fig.5. ^1H NMR spectra of fractionated by semi preparative liquid chromatography reaction products (b), (c), (d), (e) (see Fig. 4 caption).

1300 Da regardless of the ratio of ethanol/water reaction mixtures to be the dominant (Figure 4). In the ^1H NMR spectrum of fraction 4 (Figure 5e) with experimentally determined average number molecular mass (Mn) is 890 Da (Figure 4e) multiple signals within the ranges of 1.32 – 1.39 (36H), 4.11- 4.30 (8H) and 4.69 (4H) ppm were observed. They can be attributed to protons of methyl and methine groups connecting aromatic rings, respectively. The total number of experimentally determined protons does not exactly correspond to the theoretically calculated ratio of protons in the elementary unit of the polymers obtained. Taking into account that finding as well as the high polydispersity index of the fraction ($D=1.348$) one can conclude that it consists of oligomeric chains with different numbers of elementary units. Furthermore, the observed resonance signals at 9.40 and 10.01 ppm in NMR spectra (Figure 5e) are attributable to the protons of hydroxyl groups. Most probably the signal at 9.40

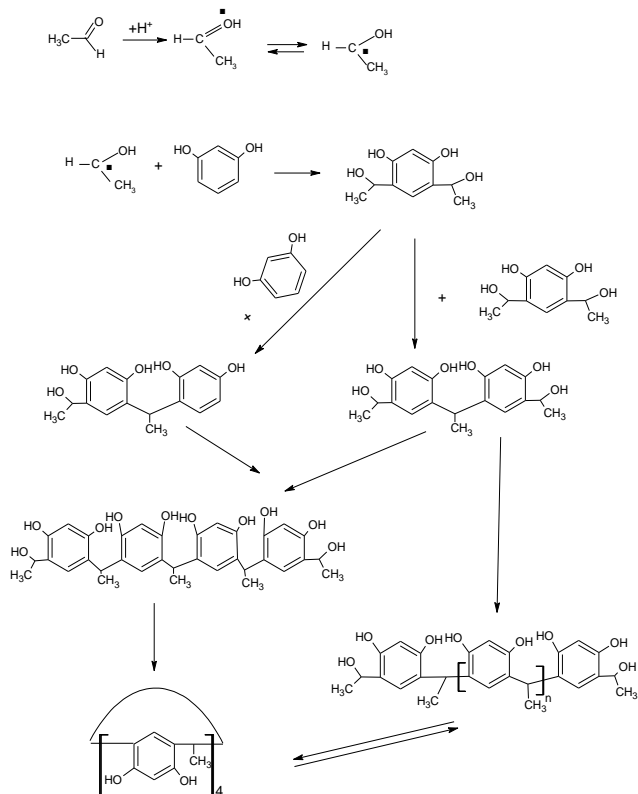
ppm corresponds to dihydroxyalkyl oligomeric product while the signal at 10.01 ppm is attributed to the corresponding cyclic oligomeric product.

The ^1H NMR spectrum of fraction 1 (Figure 5b) having a molecular mass of about 200 Da as determined by GPC (Figure 4b) signals at 6.57 and 7.27 ppm which can be attributed to protons of the aromatic rings. The chemical shift at 7.78 ppm is estimated as a signal corresponding to four protons of hydroxyl groups. The presence of these signals and others at 4.94 ppm (2H) and 1.41 ppm (6H) attributed to the protons of methine and methyl groups in alkyl substitute suggest that the product obtained is a dihydroxyalkyl derivative of resorcinol. Besides, the experimentally found molecular mass of 195 Da corresponds well to the theoretically calculated one of 198 Da.

In the ^1H NMR spectrum of fraction 2 (Figure 4c and 5c) multiple signals at 1,37 – 1,43 (9H), 4,05 (1H) and 5,05 (2H) ppm, respectively, were observed which can be attributed also as protons of methine and methyl groups. The resonance signals at 6,54 (2H) and 7,01(2H) ppm are referred to protons in the aromatic ring. Taking into account their number as well as other signal at 8,52 (6H) ppm corresponding to protons in hydroxyl groups it is presumed that the product obtained comprise dimers of dihydroxyalkyl derivative of resorcinol as main component. The theoretically calculated molecular mass of 334 Da matches the experimentally found one (336 Da) which also supports the supposed structure of the product obtained.

The multiple resonance signals at 1,28 – 1,30 (12H) and at 4,43 – 4,47 (4H) ppm observed in ^1H NMR spectrum of fraction 3 (Figure 5d) are attributed to protons of methine and methyl groups. The other signals observed at 6,43 (4H) and at 7,30 (4H) ppm corresponds to protons of the aromatic ring while that one at 10,00 (8H) ppm – to protons of hydroxyl groups. The experimentally found molecular mass of 553 Da is in good agreement with the theoretically calculated one of 544 Da which implies the C-tetramethylcalix [4] resorcinarene as a reaction product formed.

All separated fractions obtained at different stages of process of C-tetra-methylcalix [4] resorcinarene isolation were characterized by GPC chromatography and ^1H NMR spectroscopy. Well-established structures of the products obtained give grounds to suggest the most likely mechanism of the polycondensation and oligocyclization processes presented in Scheme 1.



Scheme 1. Proposed mechanism of the process of polycondensation and oligocyclization.

The proposed mechanism of propagation of oligomeric chains occurs mainly through dihydroxyalkyl derivative of resorcinol and its dimer product. A similar pattern is typical for polycondensation of p-substituted phenols [22] which ensures the formation of linear oligomers.

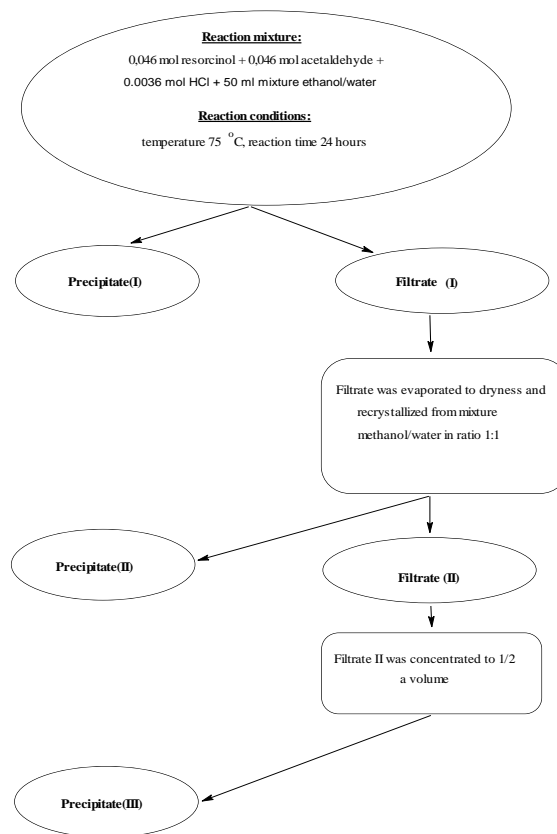
Considering the composition dependency of fractionation products allow the following conclusions:

1) Increasing the polarity of the reaction medium leads to an increase of oligocyclization which yields predominantly C-tetramethylcalix [4]arene products, respectively;

2) In contrast, decreasing the polarity, i.e. more ethanol in ethanol/water mixture, the longer reaction time is needed for the process of hydrolysis to proceed with hence for formation of "high molecular" weight oligomeric products.

Optimization of C-tetramethylcalix[4]arene isolation obtained by varying polarity of the medium

It is found from the above studies that the reaction mixtures after 24 hours time contain mainly cyclic products but in a quantity less than expected one. In order to optimize the procedure of



Scheme 2. A route to separation and isolation of C-tetramethylcalix[4]arene

isolation of C-tetramethylcalix[4]arene in a maximum quantity the following scheme was used (Scheme 2).

Initially, the precipitate (I) was separated from the reaction mixture. The filtrate was evaporated to dryness and recrystallized from methanol/water mixture. A new residue (II) and filtrate (II) were collected. The methanol was evaporated from the filtrate (II) and additional precipitate (III) was collected. Following this procedure, the cyclic product obtained was almost completely isolated. The products yielded from the process run at different polarity of the medium ranged from 42% to almost quantitative (99%).

All products obtained at different stages of the procedure for the isolation of C-tetramethylcalix [4] arene are subjected to fractionation using semi preparative liquid chromatography. The fractions collected were characterised by HPLC, GPC, IR and ¹H NMR techniques to define the structure of products obtained. The summarized data are presented in Table 2.

As seen from Table 2 the increased medium polarity (at minimum ethanol content in ethanol/water mixtures) increases the formation of cyclic products. Their maximum yield is reached at

Table 2. Composition of separated and isolated products obtained upon various polarity of the reaction medium

	Ethanol/water solvent composition ratio								
	0:100	20:80	30:70	40:60	50:50	60:40	70:30	80:20	100:0
Fractionated products content in precipitate 1 (%)									
L1*	58,83	-	-	-	-	-	-	6,81	30,60
L2**	-	17,43	-	-	-	-	-	-	-
C1***	18,80	48,34	58,69	33,95	25,83	21,21	31,26	5,58	-
C2****	-	-	19,78	4,25	-	-	-	-	-
Fractionated products content in precipitate 2 (%)									
L1*	-	-	-	1,45	0,65	-	5,47	-	1,33
L2**	-	-	-	-	-	-	-	-	2,62
C1***	14,74	25,45	18,20	19,93	18,36	17,88	32,56	44,93	22,05
C2****	-	-	-	4,05	1,23	1,17	7,84	9,23	4,43
Fractionated products content in precipitate 3 (%)									
L1*	-	-	-	-	-	-	-	-	-
L2**	-	-	-	-	-	-	-	-	-
C1***	-	3,18	-	-	-	-	-	-	-
C2****	5,18	4,70	1,19	2,70	2,07	1,36	3,20	1,43	2,30
Total content of fractionated products (%)									
Total:	97,35	99,10	97,86	64,88	48,12	41,62	75,57	68,05	63,83
Content of oligocyclic isomers (%):									
C1***	33,54	76,97	76,89	53,88	44,19	39,09	63,82	50,51	22,05
C2****	5,18	4,70	20,97	11,00	3,30	2,53	11,04	10,66	6,73
Total:	38,72	81,67	97,86	64,88	47,49	41,62	74,86	61,17	28,78

*L1-Linear hydroxyl- and dihydroxyl derivatives of molecular mass up to 400 Da; **L2- Linear oligomers of molecular mass over 800 Da; *** C1 – rccc-isomer of C-tetramethylcalix[4]arene; **** C2- rttt-isomer of C-tetramethylcalix[4]arene

30 % ethanol content. Generally, an increase in medium polarity increases twice the content of linear low molecular weight hydroxyl and dihydroxyl derivatives which facilitates the subsequent cyclization. It should be noted that the comparable amount of cyclic product is obtained in both extreme cases (pure ethanol or water solution)

The existence of fractions of comparable molecular masses in some of precipitated products was found (for example C1 (553 Da) and C2 (556 Da) fractions). In addition, the existence of two peaks at different elution volumes but with identical UV spectra in HPLC eluograms (similar to those shown in Figure 4) are observed. Moreover, the IR spectra of these products were in a good agreement with each other.

A triplet signal at 1.28 – 1.32ppm in ¹H NMR spectrum of C1 fraction was observed (analogous to Figure 5). The spectrum of C2 fraction showed the existence of triplet signal at 1.54 ppm. In both cases, these peaks correspond to 12 protons and can be attributed to the signals characteristic for the protons of methyl groups. The observed signals at 4.48 ppm (C1 fraction) and at 4.54 ppm (C2 fraction) correspond to 4 protons assigned for the protons of methine groups. Singlet signals observed at about 10.0 ppm (C1 fraction, Figure 5e) as well

as those at 9.8ppm and 8.9 ppm (C2 fraction, Figure 5d) both corresponding to 8 protons were assigned to the protons of hydroxyl groups of resorcinol since their disappearance in spectrum upon addition of deuterated water. Therefore, these products can be referred to rccc– and rttt-isomers of C-tetramethylcalix[4]arene, respectively. Regardless of their equal theoretical molecular weight (544 Da) due to the difference in hydrodynamic volumes a shift in elution volumes was observed on chromatogram.

The growing interest in the optimization of the reaction conditions for the synthesis of C-tetramethylcalix[4]resorcinarene is not accidental. These products may serve as receptors of ionic and neutral species [23] and as building blocks of supramolecular chemistry structures of, i.e. as components of capsules [24], cavitand [24,25], and nanotubes [26,27]. The C-tetramethylcalix[4]resorcinarene isomers and their derivatives are applicable in the molecular recognition reactions [28], separation procedures [29] and as mimetics of biological processes [30].

CONCLUSIONS

The influence of the acid catalyst (hydrochloric acid) on the yield and structure of the products

obtained in the course of polycondensation of resorcinol and acetaldehyde was studied. It has been shown that cyclic oligomeric products of quantitative yields are obtained under certain reaction conditions and catalytic amounts of hydrochloric acid.

The influence of the polarity of the medium on the composition of the obtained products has been investigated. It has been found that by altering of polarity of the reaction medium the formation of cis- or trans-isomers of cyclic oligomeric products can be controlled selectively. A possible mechanism of the polycondensation and oligocyclization processes is proposed. The structure of the products obtained has been defined.

An optimized procedure for the separation and isolation of the cyclic C-tetramethylcalix[4]arene products has been proposed. It has been shown that the cyclic product of quantitative yield is formed by running the synthesis in alcohol - water reaction mixture containing 30% ethanol.

Acknowledgment: *The authors would like to express their gratitude to the National Science Fund of the Ministry of Education, Youth and Science of Bulgaria for the financial support under contract BU X-304/2007 and Research and Development Fund of University of Chemical Technology and Metallurgy, Sofia, Contract 10793. Ch. Novakov acknowledges the financial support by the National Science Fund of Bulgaria through contract DCVP-02/2/2009, National Centre for New Materials UNION.*

REFERENCES

1. S.S. Zhu, H. Staats, K. Brandhorst, J. Grunenberg, F. Gruppi, E. Dalcanale, A. Liitzen, K. Rissanen, C.A. Schalley, *Angew. Chem. Inter. Ed.*, **47**, 788 (2008).
2. A. Wzorek, W. Iwanek, J. Mattay, *Tetrahedron: Asymmetry*, **18**, 815 (2007).
3. G.A. Gainanova, E.P. Zhiltsova, L.A. Kudryavtseva, S. Lukashenko, I. Knyazeva, A. Burilov, V. Kovalenko, L. Awakumova, A. Konovalov, *Russian J. of Gen. Chem.*, **40**, 77 (2007).
4. A. Wzorek, W. Iwanek, Chirality of resorcinarenes, in: *Synthetic Receptors in Molecular Recognition*, V. Rybachenko (eds), Schidnij Wydawnicyj Dim, Donetsk, Ukraine, 2007, p. 105.
5. O.D. Fox, J. Cookson, E.J.S. Wilkinson, M.G.B. Drew, E.J. MacLean, S.J. Teat, P.D. Beer, *J. Am. Chem. Soc.*, **128**, 6990 (2006).
6. D. Yang, S.W. Chang, C.K. Ober, *J. Mater. Chem.*, **16**, 1693 (2006).
7. B. Botta, F. Caporuscio, I. D'Acquarica, G.D. Monache, D. Subissati, A. Tafi, M. Botta, A. Filippi, M. Speranza, *Chem.-A Eur. J.*, **12**, 8096 (2006).
8. H. Mansikkamaki, S. Busi, M. Nissinen, A. Ahman, K. Rissanen, *Chem.-A Eur. J.*, **12**, 4289 (2006).
9. A.R. Burilov, L.I. Vagapova, M.A. Pudovik, T.N. Pashirova, I.S. Ryzhkina, L.A. Kudryavtseva, A.P. Timosheva, W.D. Habicher, A.I. Konovalov, *Russian Chem. Bull.*, **55**, 920 (2006).
10. W. Sliwa, T. Zujewska, B. Bachowska, *Pol. J. Chem.*, **77**, 1079 (2003).
11. D.J. Cram, J.M. Cram, *Monographs in Supramolecular Chemistry*, RSC, London, **4**, 162 (1989).
12. D.M. Rudkevich, W. Verboom, D.N. Reinhoudt, *J. Org. Chem.*, **59**, 3683 (1994).
13. R.J.M. Egberink, P.L.H.M. Cobben, W. Verboom, S. Harkema, D.N. Reinhoudt, *J. Includ. Phenom. Mol.*, **12**, 151 (1992).
14. L.M. Tunstad, J.A. Tucker, E. Dalcanale, J. Weiser, J.A. Bryant, J.C. Sherman, R.C. Helgeson, C.B. Knobler, D.J. Cram, *J. Org. Chem.*, **54**, 1305 (1989).
15. E.U. Thodenvan Velzen, J.F.J. Engbersen, J.N. Reinhoudt, *J. Am. Chem. Soc.*, **116**, 35597 (1994).
16. H. Ito, T. Nakayama, M. Sherwood, D. Miller and M. Ueda, *Chem. Mater.*, **20**, 341 (2008).
17. S.M. Puranik, A.C. Kumbharkhane, S.C. Mehrotra, *Proc. Natl. Acad. Sci. India A.*, **63**, 415 (1993).
18. S.M. Puranik, A.C. Kumbharkhane, S.C. Mehrotra, *J. Mol. Liq.*, **73**, 59 (1994).
19. A. Chaudhari, A.G. Shankarwar, B.R. Arbad, S.C. Mehrotra, *J. Solution Chem.*, **33**, 313 (2004).
20. T. Sato, R. Buchner, *J. Phys. Chem. A*, **108**, 5007 (2004).
21. R.J. Sengwa, Madhvi, S. Sankhla, S. Sharma, *J. Solution Chem.*, **35**, 1037 (2006).
22. C. Gonzalez, L. Castedo, *Synthesis of phenols*, in: *The Chemistry of Phenols*, Z. Rappaport (eds), Wiley, 2003, p.396.
23. A.F. D. de Namor, W. Aparicio-Aragon, N. Nwogu, A. El Gamouz, O. E. Piro, E. E. Castellano, *J. Phys. Chem. B*, **115** (21), 6922 (2011).
24. C. Bonaccorso, G. Sgaltata, G. Grasso, V. Zito, D. Sciotto, G. Arena, *Chem. Commun.*, **47**, 6117 (2011).
25. W. Sliva, T. Girek, *J. Incl. Phenom. Macromol.*, **66**, 15 (2010).
26. V.G. Organo, D.M. Rudkevich, *Chem. Commun.*, **38**, 3891 (2007).
27. S. Kennedy, Ch.M. Beavers, S.J. Teat, S.J. Dalgano, *New J. Chem.*, **35**, 28 (2011).

28. J.Rebek Jr., *PNAS*, **106**, 10423 (2009)
29. D. Zhang, X. Cao, D.W. Purkiss, R.A. Bartsch, *Org. Biomol. Chem.*, **5**, 1251 (2007)
30. A. Dondoni, A. Marra, *Chem. Rev.*, **110**, 4949 (2010).

ОПТИМИЗАЦИЯ НА РЕАКЦИОННИТЕ УСЛОВИЯ ЗА СИНТЕЗ НА С-ТЕТРАМЕТИЛКАЛИКС[4]РЕЗОРЦИНАРЕНИ

Д. Плачкова-Петрова¹, П. Петрова¹, Ст. Милошев^{1*}, Хр. Новаков²

¹ Химикотехнологичен и металургичен университет, Департамент по технология на полимерите, 1756 София

² Институт по полимери, Българска академия на науките, 1113 София

Постъпила на 18 януари, 2012 г.; приета на 16 юли, 2012 г.

(Резюме)

Показан е нов алтернативен метод за синтез на каликс[4]резорцинарени. Определени са оптималните параметри за получаване на С-тетраметилкаликс[4]резорцинарени, като представител на класа на каликс[4]резорцинарени, чрез вариране на реакционните условия. Показано е, че тези циклични продукти могат да бъдат получени при определени условия, използвайки каталитично количество минетарна киселина. Установено е, че цис-цис (ccss) и транс-транс (tttt) изомери на С-тетраметил-каликс[4]резорцинарени може да бъдат синтезирани селективно чрез промяна на съотношението на водно-органичната фаза, т.е. чрез промяна полярността на средата. Реакционните продукти са разделени чрез полупрепаративна течна хроматография и охарактеризирани чрез гел-протикваща хроматография (GPC), ядрено магнитен резонанс (¹H NMR), ултравиолетова (UV) и Фурие преобразуваща инфрачервена (FTIR) спектроскопия.

Structural and spectroscopic characterization of 2-amino-3, 5-dibromopyridine

A. G. Chapkanov^{1*}, B. B. Ivanova²

¹Department of Chemistry, Faculty of Mathematics and Natural Sciences, South-West University "Neofit Rilski", 2700 Blagoevgrad, Bulgaria

²University of Sofia "St. Kl. Ohridsky", Faculty of Chemistry, 1164 Sofia, Bulgaria

Received June 5, 2012; Accepted July 23, 2012

The correlation between the structure and spectroscopic properties of 2-amino-3, 5-dibromopyridine (**1**) is studied, using the methods as single crystal X-ray diffraction, IR- and UV-spectroscopy. The X-ray diffraction investigation showed that, the unit cell contains 4 molecules, forming dimmers by means of the NH...N hydrogen bonding. In particular, the linear-dichroic IR-spectroscopy coupled with the orientation technique of solid samples as liquid crystal suspension is applied for identification of the IR-bands, characteristic for the structural fragments. The presence of dimmers formation in the unit cell assumed Fermiresonance splitting effect of the $V_{\text{NH}_2}^s$ of (**1**) in the solid-state IR-spectra. Quantum chemical calculations are performed in order to obtain the electronic structure and spectroscopic properties of the compound studied (**1**).

Keywords: 2-amino-3, 5-dibromopyridine, Crystal structure, Linear-Dichroic Infrared Spectroscopy (IR-LD), Quantum chemical calculations.

INTRODUCTION

The substituted aminopyridines are N-heterocyclic amines possessing biological activity. Their action and biological effect as K^+ and Ca^{2+} channel inhibitor and the role of the transition metal complexes and coordination capability has been discussed systematically [1–6]. It is known, that aminopyridines are weak bases and they can exist in neutral or protonated cationic form at physiological pH. This characteristic however complicates the elucidation of the mechanism and the site of action [7, 8]. On the other hand any *in vivo* studies are based on the detail investigations and correlations between the structure and spectroscopic properties *in vitro*. In our previously works [9–13] it was established the influence of the protonation on the charge redistribution in pyridinium ring and the effect on the optical and magnetic properties, as well the self-association of different substituted pyridines in solution and solid state applying various methods for analysis. As a part of our systematic study of pyridine derivatives in this paper is presented structural and spectroscopic investigation of the titled compound, which structure is shown in Scheme 1. For that purpose were used different methods as a single crystal X-ray diffraction, comparatively

characterization by means of Inrand UV-



Scheme 1. Chemical diagram of 2-amino-3,5-dibromopyridine (**1**)

spectroscopy in particular, the linear-dichroic infrared (IR-LD) spectroscopy. Quantum chemical calculations at the DFT, MP2 and CIS levels of theory using 6-311++G**basis set are employed for predicting and supporting of the experimentally observed properties.

EXPERIMENTAL

Materials and methods

Starting compound (**1**) is trade product (Sigma-Aldrich). The suitable for the single Xray diffraction measurements crystals were obtained by recrystallization from ethanol.

The IR-spectra were measured using a Bomem-Michelson 100 FT-IR-spectrometer (4000 – 400 cm^{-1} , $\pm 2 \text{ cm}^{-1}$ resolution, 150 scans) equipped with a Perkin Elmer wire-grid polarizer. The non-polarized solid state IR spectra were recorded using KBr disk technique.

The oriented samples were obtained as suspension in a nematic 4'-cyano-4'-alkyl-bicyclohexyl mixture (ZLI-1695 in the Merck

* To whom all correspondence should be sent:

E-mail: chapkanov@swu.bg

notation), mesomorphic at room temperature. The poor IR spectrum makes possible to record the guest-compound bands in the whole 4000–400 cm^{-1} range. The presence of an isolated nitrile stretching IR-band at 2233 cm^{-1} additionally serves as an orientation indicator. The effective orientation of the solid state sample was achieved through the following procedure: about 5 mg of the compound studied was added to the appropriate liquid crystal substance until a slightly viscous mixture is obtained. The suspension thus prepared was pressed between two KBr-plates rubbed out in advance in one direction by means of fine sandpaper. The grinding of the prepared mull in the rubbing direction promotes an additional orientation of the sample [14–17].

The UV-VIS spectra of the compound studied as 1.10^{-4} mol/l solutions (1-cm quartz cell) in acetonitrile were recorded on Evolution 300 spectrometer (Thermo Scientific, USA) with ± 2 nm resolution.

The X-ray diffraction intensities were measured on a Bruker Smart X2S diffractometer, using microsource Mo-K \cdot radiation and employing the ω -scan mode. The data were corrected for Lorentz and Polarization effects. An absorption correction based on multiple scanned reflections [18]. The crystal structures were solved by direct methods using SHELXS-97 [19]. The crystal structures were refined by full-matrix least-squares refinement against F^2 [18–21]. Anisotropic displacement parameters were introduced for all nonhydrogen atoms. The hydrogen atoms attached to carbon were placed at calculated positions and refined allowing them to ride on the parent carbon atom.

Quantum chemical calculations were performed with GAUSSIAN 98 and Dalton 2.0 program packages [22, 23]. The output files were visualized using the GausView03 program [24]. The geometry of (1) was optimized at two levels of theory: second-order Moller-Pleset perturbation theory (MP2) and density functional theory (DFT) using the 6-311++G** basis set. The DFT method employed is B3LYP, which combines Becke's three-parameter nonlocal exchange function with the correlation function of Lee, Yang and Parr. The molecular geometries of the studied species were fully optimized by the force gradient method using Bernys' algorithm. For every structure the stationary points found on the molecule potential energy hypersurfaces were characterized using standard analytical harmonic vibrational analysis. The absence of the imaginary frequencies, as well as of negative eigenvalues of the second-derivative

matrix, confirmed that the stationary points correspond to minima of the potential energy hypersurfaces. The calculation of the vibrational frequencies and infrared intensities were checked to establish which kind of performed calculations agree the best with the experimental data. The empirical scaling factors 0.9614 and 0.8929 are made to achieve better correspondence between the experimental and theoretical values. The UV spectra in the gas phase and in acetonitrile solution are obtained by CIS/6-311++G** and TDDFT calculations at the same basis set. We use the methods of Hartree-Fock theory and density functional theory, systematically explained in [25–29].

RESULTS AND DISCUSSION

Crystal and molecular structure of (1)

The X-ray diffraction investigation of the 2-amino-3, 5-dibromopyridine (1) was carried out. The obtained crystallographic data show, that compound (1) crystallizes in the monoclinic space group $P2_1/n$. The presented in Fig. 1 an ORTEP plot illustrates the structure at the 50% thermal ellipsoids. The unit cell of the compound (1) contains 4-molecules, which form dimmers by means of the NH...N hydrogen bonding (3.041 Å) as is shown in Fig. 2.

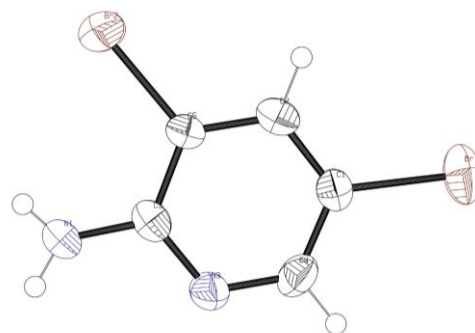


Fig. 1. ORTEP plot of (1) at the 50% thermal ellipsoids; Hydrogen atoms are shown as spheres of arbitrary radii.

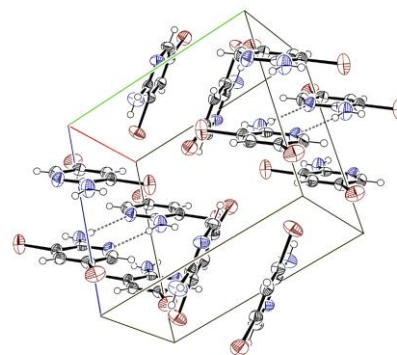


Fig. 2. Unit cell contents and hydrogen bonding scheme in (1).

The asymmetric hydrogen bonding type with participation of the NH₂-group proposes an observation of the Fermi-resonance splitting effect [30–33] of the ν_s NH₂ in the corresponding solid-state IR-spectra of (**1**). The performed quantum chemical calculations of the molecular geometry of (**1**) show a good correlation of the obtained bond lengths and angles, in comparing with the experimental crystallographic data. The obtained difference of 0.012 Å and 1.0(2) ° is a good background for the next vibrational spectral analysis.

Vibrational and IR-LD spectral analysis

The calculated IR-spectrum of (**1**) is shown in Fig. 3. From the spectrum can be see that, the most typical in this respect are the characteristic bands of the pyridine skeleton vibrations at 1619 cm⁻¹, 1587 cm⁻¹, 1496 cm⁻¹ and out-of-plane peak at 966 cm⁻¹ assigned according to Wilson notation [34] as **8a**, **8b**, **19a** and **11- γ CH**, respectively. Comparing with the data of other pyridine derivatives [14–18], the presence of the Br-substituents leads to the higher-frequency shifting of the in-plane skeleton vibrations. The band at 1360 cm⁻¹ belongs to ν_{C-N} vibration. Comparing the theoretical and experimental IR-bands a difference of 2 cm⁻¹ is obtained for the above stated frequencies. Significantly different are the IR-bands for the NH₂-vibrations, as a result of the participation of the group in the intermolecular interactions.

The theoretical IR-bands of $\nu^{as}_{NH_2}$, $\nu^s_{NH_2}$, δ_{NH_2} and ω_{NH_2} are at 3505 cm⁻¹, 3385 cm⁻¹, 1619 cm⁻¹ and 377 cm⁻¹ (Fig. 3).

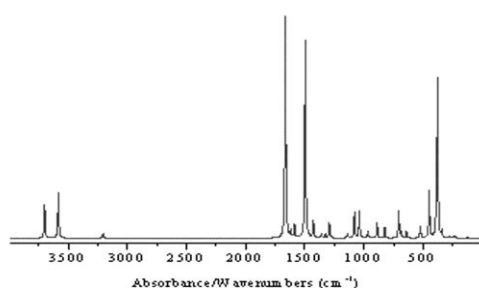


Fig. 3. Calculated IR-spectrum of (**1**).

The corresponding bands at the experimental solid-state spectrum are at 3464 cm⁻¹, 3280/3210 cm⁻¹, 1627 cm⁻¹ and 700 cm⁻¹, respectively (Fig. 4.1). The band of $\nu^s_{NH_2}$ is Fermi resonance splitted [25–29]. However, both bands are with the same sign in the corresponding difference IR-LD spectrum in Fig. 4.2. Direct proof of this statement follows by the obtained elimination of these

maxima at the same dichroic ratio (Fig. 4.3). The last elimination leads to strong reduction of the band at 1627 cm⁻¹ of δ_{NH_2} as a result of the difference of the transition moments of the $\nu^s_{NH_2}$ and δ_{NH_2} an angle of 12.3(1)° according the crystallographic data. The elimination of the $\nu^{as}_{NH_2}$ leads to the reduction of the i.p. maxima at 888 and 706 cm⁻¹, which is also in accordance with the calculated resulting transition moments (Fig. 4.4). The elimination of the o.p. band at 960 cm⁻¹ leads to disappearance of the bands at 824 cm⁻¹ and 687 cm⁻¹, which directly shows their belonging to the same symmetry class (Fig. 4.5).

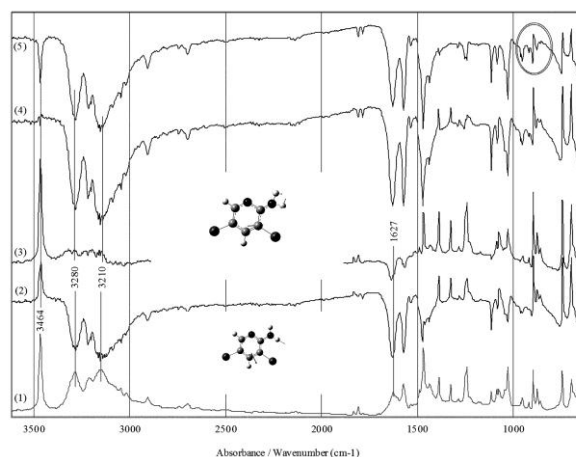
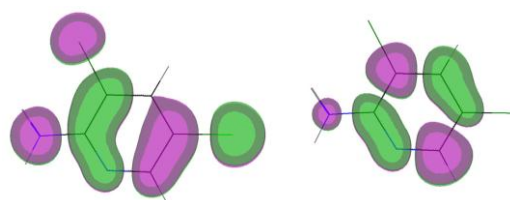


Fig. 4. Non-polarized IR-(1), difference (2) and reduced IR-LD spectra of (**1**) after the elimination of the bands at 3280 cm⁻¹ (3), 3464 cm⁻¹ (4) and 687 cm⁻¹ (5).

UV-spectral data

In accordance with the data literature [35, 36] the electronic spectrum of 2-amino pyridine poses two characteristic bands at 242 nm ($\epsilon = 11000$ L mol⁻¹cm⁻¹) and 262^{sh} nm ($\epsilon = 788$ L mol⁻¹cm⁻¹) belonging to pyridine aromatic system. Other result is observed looking on the UV–VIS spectrum of 2-amino-3, 5-dibromopyridine. The spectrum of (**1**) contains one broad band at 255 nm ($\epsilon = 10160$ L mol⁻¹cm⁻¹) as a result of the presence and influence of the bromine atoms as a substituents in the 2-amino pyridine structure. These data are in a good agreement with the theoretically predicted electronic spectrum. The HOMO-LUMO Mos gaps of (**1**) are given in the Scheme 2 and correlated well with the obtained experimental data.



Scheme 2. HOMO and LUMO MOs gaps of (**1**)

CONCLUSION

In this work is has performed structural and spectroscopic analysis of 2-amino-3,5-dibromopyridine by means of X-ray diffraction, IR- and linear-polarized IR-spectroscopy of oriented colloid suspensions in nematic host, UV–VIS spectroscopy and theoretical calculations. It was established the presence of dimers formation by NH...N hydrogen bonding in the unit cell, which proposes Fermi-resonance splitting effect of the ν_s NH₂ of (**1**) in the solid-state IR-spectra. The quantum chemical calculations of (**1**) show a good agreement of the obtained data (bond lengths and angles) with the experimental crystallographic data.

SUPPLEMENTARY MATERIAL

Crystallographic data for the structural analysis have been deposited with the Cambridge Crystallographic Data Centre, CCDC 761691. Copies of this information may be obtained from the Director, CCDC, 12 Union Road, Cambridge, CB2 1EZ, UK (Fax: +44 1223 336 033; e-mail: deposit@ccdc.cam.ac.uk or <http://www.ccdc.cam.ac.uk>)

Acknowledgements: The author thanks for the single crystal X-ray diffraction measurements on the Bruker Smart X2S (Sofia University St. Kl. Ohridski) a donation of the Alexander von Humboldt Foundation

REFERENCES

1. P Gisele, C.A.Carlos, C. Yara, *Eur. J. Pharmacol.* **469**, 57 (2003).
2. A. Nino, C. Munoz-Caro, *Biophys. Chem.* **91**, 49 (2001).
3. C. Munoz-Caro, A. Nino, *Biophys. Chem.* **96**, 1 (2002).
4. S. Akyuz, *J. Mol. Struct.* **482**, 171 (1999).
5. Y. Buyukmurat, S. Akyuz. *J. Mol. Struct.* **651**, 533 (2003).
6. P. Zimmermann. W. Buhr, C. Brehm, A. Palmer, M. Feth, J. Senn-Bilfinger, W. Simon, *Bioorg. Med. Chem. Lett.* **7**, 5374 (2007).
7. H. Meves, H. Pichon, *J. Physiol. Lond.* **251**, 60 (1979).
8. J. Raust, S. Goulay-Dufay, M. Le Hoang, D. Pradeau & F. Guyon, *J. Pharmaceut. Biomed. Anal.* **43**, 83 (2007).
9. B. Koleva, R. Nikolova, A. Chapkanov, S. Zareva, T. Kolev, H. Mayer-Figge, M. Spiteller, W.S. Sheldrick, *Polish J. Chem. Techn.* **11**, 35 (2009).
10. A. Chapkanov, S. Zareva, R. Nikolova, T. Kolev, B. Koleva, E. Trendafilova, *Collect. Czech. Chem. Commun.* **74**, 1295 (2009).
11. A. Chapkanov, *Struct. Chem.* **21**, 29 (2010).
12. B. Ivanova M. Arnaudov, H. Mayer-Figge, *Polyhedron*, **24**, 1624 (2005).
13. B. Koleva, E. Trendafilova, M. Arnaudov, W. Sheldrick, H.Mayer-Figge, *Trans. Met. Chem.* **31**, 866 (2006).
14. T. Kolev, M. Spiteller, B. Koleva, *Amino Acids* **39**, 309 (2010).
15. B. Ivanova, M. Arnaudov, P. Bontchev, *Spectrochim. Acta*, **60A**, 855 (2004).
16. B. Ivanova, V. Simeonov, M. Arnaudov, D. Tsalev, *Spectrochim Acta*, **67A**, 66 (2007).
17. B. Koleva, T. Kolev, V. Simeonov, T. Spasov, M. Spiteller, *J. Incl. Phenom.*, **61**, 319 (2008).
18. G. Sheldrick, *Acta Cryst.* **64A**, 112, (2008)
19. Sheldrick GM, SHELXL-97, Program for Crystal Structure Solution, University of Cottingen, Germany, 1997.
20. R. Blessing, *Acta Cryst.* **51A**, 33 (1995).
21. 21A. L. Spek, *J. Appl. Cryst.* **36**, 7, (2003).
22. Frisch M.J., Trucks G.W., Schlegel H.B., Scuseria G.E., Robb M.A., Cheeseman J.R., Zakrzewski V.G., Montgomery J.A., Stratmann R.E., Burant J.C., Dapprich S., Millam J.M., Daniels A.D., Kudin K.N., Strain M.C., Farkas O., Tomasi J., Barone V., Cossi M., Cammi R., Mennucci B., Pomelli C., Adamo C., Clifford S., Ochterski J., Petersson G.A., Ayala P.Y., Cui Q., Morokuma K., Salvador P., Dannenberg J.J., Malick D.K., Rabuck A.D., Raghavachari K., Foresman J.B., Cioslowski J., Ortiz J.V., Baboul A.G., Stefanov B.B., Liu G., Liashenko A., Piskorz P., Komaromi I., Gomperts R., Martin R.L., Fox D.J., Keith T., Al-Laham M.A., Peng C.Y., Nanayakkara A., Challacombe M., Gill P.M.W., Johnson B., Chen W., Wong M.W., Andres J.L., Gonzalez C., Head-Gordon M., Replogle E.S., Pople J.A. Gaussian 98, Gaussian, Inc., Pittsburgh, PA, 1998.
23. Dalton 2.0 Program Package, <http://www.kjemi.uio.no/software/dalton/dalton.html>
24. GausView03, <http://www.softwarecientifico.com/paginas/gaussian.htm>
25. B. Koleva, T. Kolev, R.W. Seidel, H. Mayer-Figge, M.Spiteller, W.S. Sheldrick, *J. Phys. Chem.* **112A**, 2899 (2003).
26. B. Koleva, T. Kolev, R.W. Seidel, M. Spiteller, H. Mayer-Figge and W.S. Sheldrick, *J. Phys. Chem.* **113A**, 308 (2009).
27. T. Kolev, B. Koleva, R.W. Seidel, M. Spiteller and W.S. Sheldrick, *Cryst. Growth Des.* **9**, 3348 (2009).
28. T. Kolev, T. Tsanev, S. Kotov, H. Mayer-Figge, M. Spiteller, W.S. Sheldrick, B. Koleva, *Dyes & Pigments* **82**, 95 (2009).
29. T. Kolev, B. Koleva, M. Spiteller, W.S. Sheldrick, H. Mayer-Figge, *J. Phys. Chem.* **111A**, 1084 (2007).
30. B. Koleva, T. Kolev, R.W. Seidel, Ts. Tsanev, H. Mayer-Figge, M. Spiteller, W.S. Sheldrick, *Spectrochim. Acta*, **71A**, 695 (2008).

31. B. Ivanova, H. Mayer-Figge, *J. Coord. Chem.* **58**, 653 (2005).
32. B. Koleva, E. Trendafilova, M. Arnaudov, W. Sheldrick, H. Mayer-Figge, *Trans. Met. Chem.* **31**, 866 (2006).
33. T. Kolev, B. Koleva, T. Spasov, E. Cherneva, M. Spitteller, W.S. Sheldrick, H. Mayer-Figge, *J. Mol. Struct.* **875**, 372 (2008).
34. G. Varsanyi, *Vibrational Spectra of Benzene Derivatives*, Academia Kiado, Budapest, 1969.
35. S. Smrckova, K. Juricova, V. Prutianpv, *Collect. Czech. Chem. Commun.* **59**, 2057 (1994)
36. S.F. Mason, *J. Chem. Soc.* 219 (1960).

СТРУКТУРНО И СПЕКТРОСКОПСКО ОХАРАКТЕРИЗИРАНЕ НА 2-АМИНО-3,5-ДИБРОМОПИРИДИН

А. Г. Чапкънов^{1*}, Б. Б. Иванова²

¹Катедра "Химия", Природо-Математически факултет, Югозападен университет „Н. Рилски“, 2700 Благоевград²³ Катедра "Аналитична химия", Химичен факултет, СУ „Св. Климент Охридски“, 1164 София

Постъпила на 5 юни, 2012 г.; приета на 23 юли, 2012 г.

(Резюме)

Изследвана е взаимната зависимост между структура и спектроскопските свойства на 2-амино-3,5-дибромопиридин използвайки методите на рентгено-структурния анализ, ИЧ- и УВ-спектроскопията. Данните от рентгено-структурния анализ показват, че елементарната клетка съдържа 4 молекули, образувайки димери чрез NH...N водородно свързване. Отделно е приложена линейно-дихроичната ИЧ-спектроскопия в съчетание с техниката на ориентирани твърди проби като суспензия в течен кристал за идентифициране на ИЧ-ивиците, характерни за съответните структурни фрагменти. Наличието и образуването на димери в елементарната клетка предполага ефекта на Ферми резонансното разцепване на ν^s NH₂ на (**1**) в ИЧ-спектъра в твърдо състояние. Извършените квантово-химични изчисления са с цел да бъдат получени електронната структура и спектроскопските свойства на изучаваното съединение (**1**).

Articles, presented at the 6th Bulgarian Peptide
Symposium,
Sofia, September 29th – October 1st, 2011

Collected and edited by
E. Naydenova and L. Vezekov

Novel cysteic acid s-amides substituted in the sulfonamide function. Synthesis and modifications

S.S. Pancheva, R.H. Kalauzka, E.S. Jovcheva, T.A. Dzimbova, E.P. Popgeorgieva, T.I. Pajpanova*

Institute of Molecular Biology "Roumen Tsanev", Bulgarian Academy of Sciences, 1113 Sofia, Bulgaria

Received June 10, 2012; accepted August 3, 2012

In the present work we reported the synthesis of several analogues **5a-e** of cysteic acid S-amides with substituted sulfonamide function, where fully protected D,L-cysteic acid S-chlorides were treated with the required aliphatic amines to give a series of new derivatives which could be considered as structural sulfoanalogues of leucine, isoleucine and norleucine, respectively. We presented here new method for preparation of D,L-cysteic acid S-chlorides. Various modifications with N_α- and C_α- protective groups useful in peptide synthesis have been successfully achieved. These novel compounds are of potential interest in structure-activity studies, easily applied in solid phase, as well as in conventional synthesis of biologically active peptides.

Keywords: Amino acids, Cysteic acid S-amides, Aliphatic amines, Alkaline protease, Antimetabolites

INTRODUCTION

Increasing the likelihood of a chance discovery, which is still a major route in drug development, it seems prudent to consider synthetic transformations of side-chain groups of the natural amino acids as an alternative strategy for the preparation of biologically active analogues and its incorporation in peptides. The relationship between the antagonist and the natural metabolite is one in which the β-carboxyl group of aspartic is replaced by the sulfo-group in the analogue. Accordingly, the sulfonamide or substituted sulfonamide derivatives of cysteic acid were obtained in the similar manner by different authors, [1-4] based on oxidative chlorination of the disulfide bond in the cystine molecule, followed by replacement of the chlorine atom in the sulfochloride by an amino group. Due to its structural similarity to asparagine, S-cysteine sulfonamide was suspected to have the ability to act as antagonist [5] and the early structure-activity relationship studies with the cysteic acid S-amide [6] aimed at developing inhibitors of L-asparagine synthetase and potential antitumor agents with substituted sulfonamide moiety [7,8]. It was found that they inhibit growth of asparagine - dependant mutants of some microorganisms [9], exhibit fairly wide range of other antibacterial activities as well as possess a low [10], or moderate antineoplastic activity [11]. However, very little was done for the

application of the cysteic acid S-amide and its derivatives with substituted sulfonamide function, as structural sulfoanalogues of the appropriate natural amino acids in the peptide design [12]. The synthesis of sulfoanalogues of lysine [13] and arginine [14], as well as their incorporation in some model biologically active peptides have been achieved [15,16]. Most of the cysteine sulfonamide containing oligopeptides, synthesized by classical methods of peptide chemistry, displayed higher antibacterial activity than cysteine sulfonamide [11,17].

On the basis of the above data and continuing our research program on new nonproteinogenic acids, we considered to synthesize several new structurally related cysteic acid S-amides in order to verify whether such kind of substitution could improve the biological activity of this class of compounds.

In this paper we report the synthesis of the following new nonproteinogenic cysteic acid-S-amides: cysteic acid S-(N,N-dimethyl) amide (**5a**), cysteic acid S-(N-methyl, N-ethyl) amide (**5b**), cysteic acid S-(N-methyl) amide (**5c**), cysteic acid S-(N-ethyl) amide (**5d**), and cysteic acid S-(N-propyl) amide (**5e**). They could be considered as structural sulfoanalogues of the corresponding natural amino acids - leucine, isoleucine and norleucine, respectively and named as following - **sLeu**, **sIle** and **sNle** (sNle₁, sNle₂ and sNle₃) (Fig. 1.):

* To whom all correspondence should be sent:
E-mail: tamara@bio21.bas.bg

EXPERIMENTAL

Melting points were determined on a Büchi melting point apparatus and are uncorrected. Elemental analysis was compatible for all new products synthesized. Electron spray mass spectra

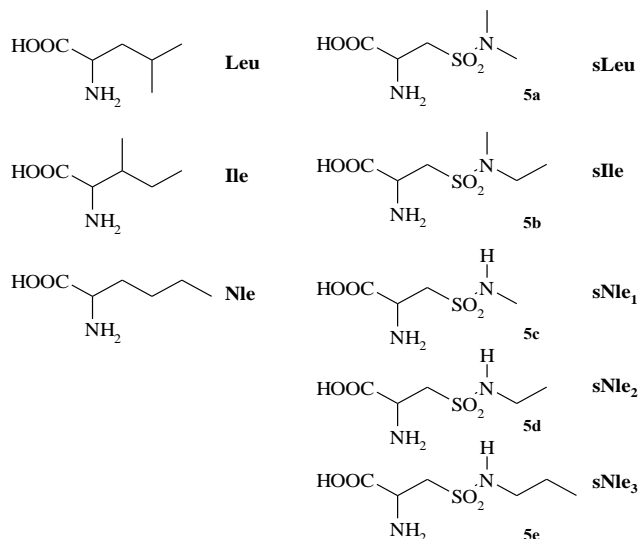


Fig. 1. Structures of the sulfoanalogues of natural amino acids Leu, Ile, Nle.

(ESMS) were done on a Vestec 201 single quadrupole mass spectrometer using AcOH:H₂O:MeCN (4:46:50) as a solvent. ESMS spectra of the products were in agreement with the composition of each compound. Optical rotation was measured with a Perkin-Elmer polarimeter 241 (sodium lamp, 589nm). Thin-layer chromatography (TLC) was run on precoated silica gel plates (60F-254, Merck) with the following solvent systems: (a) 1-butanol : AcOH : H₂O (4:1:5), upper phase; (b) 1-butanol : AcOH : H₂O (4:1:1); (c) 1-butanol : AcOH : H₂O : pyridine (15:3:3:10); (d) chloroform : methanol (7:3); (e) 1-butanol : AcOH : H₂O (2:1:1). Loads of 10-15 µg were applied and chromatograms were developed at a minimum length of 10 cm. Compounds were visualized by UV, ninhydrin as well as the chlorine gas procedure for the RI-starch reagent. Analytical HPLC was performed on a Waters 810 instrument under the following conditions: gradient/solvent system A - 90:10 to 30:70 0,05% aqueous TFA : 0,05% TFA in MeCN, linear gradient over 60 min at 1.0 ml/min and B: 60:40 to 15:85 H₂O/H₃PO₄ (pH 3): MeCN, linear gradient over 30 min at 1.0 ml/min. In both cases a Mickrosorb C₁₈ column (Rainin Instrument Co., Inc) was used. Overall yields are calculated from the starting amino acid.

General procedure for synthesis of fully protected cysteic acid S-amides(compounds 2a-e)

Na-Z-D,L-cysteic acid S-chloride ethyl ester, **1** (3.49 g, 10 mmol) dissolved in 15 ml CHCl₃ was added dropwise to an ice-cold solution (DMF, 15 ml) of appropriate aliphatic amine (dimethylamine, methylethylamine, methylamine, ethylamine and propylamine) hydrochloride (30 mmol) previously converted to a free base by treatment with Et₃N (30 mmol). The mixture was stirred for 2-3 h at 0°C. After completion of the reaction (TLC-monitoring) the solvent was removed under reduced pressure, and the evaporated residue was precipitated twice from DMF/hot water and acetone light petroleum consecutively.

Enzymatic resolution of parent Na-Z-D,L-cysteic acids S-amides ethyl esters (2a-e). Preparation of compounds 3a-e end 4a-e

The amino acid **2a-e** (10 mmol) was dissolved in a mixture of DMF (40 ml) and water (60ml) containing 30 mmol NaHCO₃. Alkaline protease from *Bacillus subtilis* DY strain (0.2 g) was added and the mixture was stirred for about 4 hours (TLC monitoring) at 37°C. After removal of the solvents under reduced pressure, water was added to the residue, pH was adjusted to 9 with 5% NaHCO₃, and the mixture was extracted with ethyl acetate (3 x 70 ml). The combined organic phases were washed with water, dried with Na₂SO₄, and the solvent was evaporated under reduced pressure. The isolated D-esters were crystallized from DMF/H₂O and/or recrystallized from CHCl₃/light petroleum. The aqueous phase was acidified with 5 % NaHSO₄ solution to pH 3 and extracted with ethyl acetate (3 x 70 ml). The combined organic phases were washed with water, dried with Na₂SO₄, and the solvent was evaporated under reduced pressure. The resulting L-enantiomers were crystallized from MeOH or 2-PrOH.

General procedure for removing of Na-Z-protective groups from L-enantiomers (4a-e). Preparation of compounds 5a-e

Na-Z-L-cysteic acid S-[N-(R₁R₂)] amide (5 mmol) was hydrogenated on Pd/C in 4,4% formic acid/ MeOH (50 ml). After completion of the reduction (1 hour), the Pd was filtered off and the solution was concentrated under reduced pressure. The residue solidified upon consecutive treatment with MeOH and dry diethyl ether. The solid

products were obtained as white foams and were directly used for the next modifications.

*General procedure for synthesis of N_α-substituted Boc-sulfonamide derivatives.
Compounds 6a-e*

Each of the solid products **5a-e** (10 mmol) was dissolved in a mixture of 2-PrOH (30 ml), water (10 ml) and Et₃N (4.2 ml, 30 mmol) with stirring. (Boc)₂O (2.9 ml, 13 mmol) was added dropwise and kept stirring until completion of the reaction (12 hours, TLC monitoring). The organic solvent was evaporated under reduced pressure, and the cooled aqueous solution was acidified to pH 2 - 3 with 0,5% NaHSO₄. The resulting mixture was extracted with ethyl acetate (3 x 40 ml). The organic layers were combined, washed with brine, dried over Na₂SO₄ and evaporated under reduced pressure. The products were recrystallized from DCM in a high purity.

Synthesis of methanesulfonate of Z-Ser-OEt, 9

To stirred solution of Z-Ser-OEt (2.67 g, 10 mmol) in CH₂Cl₂ (20 ml) in the presence of DIPEA (1.9 ml, 11 mmol) was added at 0°C a solution of methanesulfonyl chloride (0.8 ml, 10.4 mmol) in CH₂Cl₂ (10 ml). The mixture was stirred at room temperature for 20 minutes, then the solvent was evaporated under reduced pressure. The residue was treated with ethyl acetate (20 ml) and water (20 ml). The organic layer was separated, washed consecutively with aqueous 5 % NaHCO₃ (3 x 10 ml) and brine (3 x 10 ml), dried over anhydrous Na₂SO₄ and filtered. The solvent was removed under reduced pressure to give **9** (3.1g, 91%) which then was used for the next steps without further purification.

Synthesis of fully protected cysteic acid, 10

Sodium sulfite (1.7 g, 13.5 mmol) was added to a solution of **9** (3.45 g, 9 mmol) in a mixture of water : dioxane (1:1, 20 ml) and the mixture was stirred at room temperature for 24 hours. Dioxane was evaporated under reduced pressure, aqueous solution was acidified to pH 3 and **10** was left to crystallize at 4°C. Product (**10**) was obtained in 2.94 g (89%).

Synthesis of sulfonyl chloride of N- and C-protected cysteic acid, 1

The SOCl₂ (1.4 ml, 19.4 mmol) was added slowly to CH₂Cl₂ (10 ml) at 0°C. The ice bath was removed and **10** (2.94 g, 8.8 mmol) in CH₂Cl₂ (10

ml) was added dropwise over one minute. The mixture was stirred for 1 hour at room temperature and then solvent was removed by evaporation under reduced pressure. Residue crystallized from absolute ethanol to give key intermediate, **1** (1.4 g, 45%).

RESULTS AND DISCUSSION

To our knowledge, until now only the single synthesis of L-cysteic acid S-(N,N-dimethyl) amide (**5a**), employing a similar approach to ours has been published [12]. On the other hand, our special interest concerns the synthesis of corresponding suitable protected sulfonamide derivatives (**4-7a-e**, Fig. 2), useful clues for the design of more potent and selective biologically active compounds.

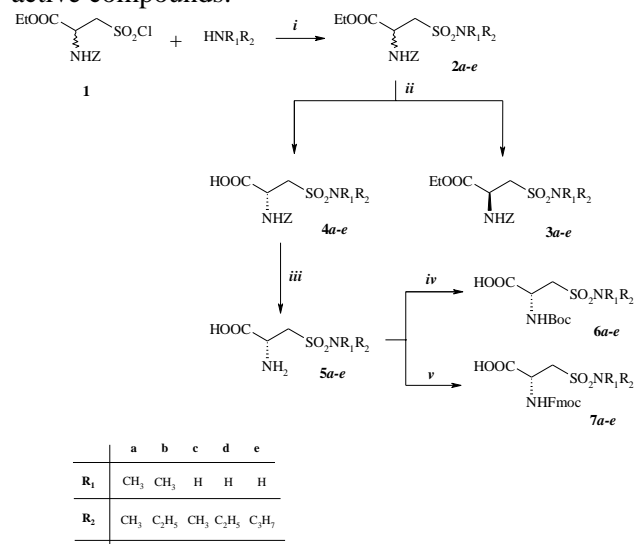


Fig. 2. Synthesis of protected sulfonamides. *Reagents and condition: i) CHCl₃/DMF/-5°C; ii) Bac. Subt. DY/DMF-H₂O/NaHCO₃/37°C; iii) 10% Pd/C/MeOH/HCOOH; iv) (Boc)₂O/i-PrOH-H₂O/5% Na₂CO₃; v) Fmoc-OSu/Dioxan-H₂O/NaHCO₃.*

The synthetic route chosen for preparation of the required compounds is illustrated in Fig. 2. The key intermediate **1** was obtained according to the well-known procedures previously described [4,7], based on oxydative chlorination of the disulfide bond in the cysteic molecule, followed by replacement of the chlorine atom in the sulfochloride by an amino group. In addition we present also a new synthetic route for preparation of the key initial compound – sulfonyl chloride of cysteic acid **1** (Fig. 3). On the first step mesylated N- and C-protected serine was obtained. Preparation of this compound was done in the presence of N,N-diisopropylethylamine (DIPEA) as a base in CH₂Cl₂. Methanesulfonyl

chloride was added to the reaction mixture at 0°C and the process continue at room temperature for additional 20 minutes. Product was obtained easily by simple washing of its organic solution in very good yield of 91%. Next step of this synthetic scheme is preparation of *N*- and *C*-protected cysteic acid. It was made by reaction of methanesulfonate with sodium sulfite in water : dioxane mixture for 24 hours at room temperature. *N*- and *C*-protected cysteic acid was obtained in good yield (89%), after evaporation of dioxane and consecutive acidifying of the aqueous solution. Sulfonyl chloride **1** was synthesized in reaction of **10** with SOCl₂ with moderate yield of 45%.

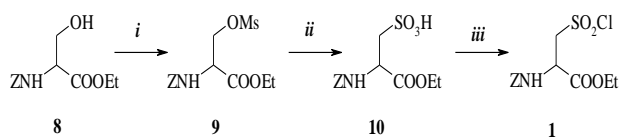


Fig. 3. Synthesis of sulfonylchloride. Reagents and condition: **i**) CH₃SO₂Cl/DIPEA/DMF; **ii**) Na₂SO₃/H₂O; **iii**) SOCl₂/CH₂Cl₂.

The experiments showed that stable cysteine sulfochloride derivatives could be obtained only if both the amino and the carboxy groups are blocked [6]. The synthesis of all compounds **1-7a-e** was accomplished in a similar manner as it is outlined in our initial studies [18]. The parent derivatives **2a-e** were afforded by simple condensation of the starting racemic compound *N*_α- carbobenzoxy-cysteic acid *S*-chloride ethyl ester with the desired aliphatic amine (dimethylamine, methylethylamine, methyl-, ethyl-, or propylamine). In all cases the sulfochloride/amine ratio was kept 1:3, the reaction was held at -5 to 0°C, and was realized by drop wise adding of the solution of sulfochloride in CHCl₃ to the ice-cold stirred solution of the corresponding amine in DMF, previously converted to a free base by treatment with Et₃N. After completion of the condensation monitored by TLC, the obtained crude material was precipitated from DMF/hot water and recrystallized from ethyl acetate/light petroleum. These initial derivatives were obtained in yields ranging from 65 to 88%. Resolutions of the racemates **2a-e** was achieved using alkaline protease from *Bacillus subtilis* *DY* strain, whose applicability to selective hydrolysis of amino acid esters with *L*-configuration was shown in previous studies [19]. As well as the high level of enantiomeric discrimination involved with enzymatic processes, the work-up procedure after the use of protease is usually particularly

straightforward since the unchanged *D*-amino acid derivatives **3a-e** can be extracted from the reaction mixture using a water-immiscible solvent, while the *N*_α-*L*-protected enantiomers **4a-e** – after acidifying the reaction mixture. In our present experiments we achieved good resolution of the racemic derivatives of di-substituted aliphatic amines **2a,b** defer from those of mono-substituted methyl, ethyl- and propylamine **2c-e**, where the yields of *D*-enantiomers **3c-e** were quite low – 20 to 25%.

The *N*_α-benzyloxycarbonyl protected *L*-enantiomers **4a-e**, recrystallized from appropriate alcohol in good yields (65 to 93%), were used for catalytic hydrogenation step in order to obtain the final *L*-cysteic acid *S*-amides **5a-e**. The *Z*-protecting group was removed by hydrogenolysis with 10% palladium on charcoal in methanol using formic acid as a hydrogen donor. Because of the *S*-content the reaction time was taken longer, up to 4 hours, determined by thin layer chromatographic analysis of samples taken at various times. The required *S*-cysteic acid sulfonamides **5a-e**, easily obtained as solids from aqueous ethanol directly were used for further modifications or purified finally by reversed phase MPLC (0-30% *i*-PrOH in 0,2% AcOH).

*N*_α-Boc-protected derivatives **6a-e** were obtained by treatment of the free *L*-enantiomers **5a-e** with (Boc)₂O in mixture of water/isopropanol and pH was adjusted to 7.5 - 8.0 with 5% Na₂CO₃. All of the obtained Boc-derivatives after recrystallization from appropriate alcohol were obtained in high yields (95 to 96%) and purity.

Cleavage of the Boc-protecting group was achieved using ethyl acetate saturated with anhydrous HCl (1.5-4N HCl/EtOAc) or TFA/anisole (9 : 1) in 98% yield. Fmoc-OSu was chosen as the preferable reagent for the synthesis of the Fmoc-derivatives **7a-e** because its use results in reproducibly high yields under mild conditions. The optimum procedure was utilized a 10% excess of corresponding *L*-cysteic acid *S*-amide over Fmoc-OSu, a minimum volume of dioxane to aqueous phase (~ 1:10 by volume) and two fold excess of sodium carbonate over amino acid component. The reaction was most efficient when the reactants were stirred vigorously at room temperature. The preparation of Fmoc-cysteic acid *S*-amides was accomplished without serious side reactions, in 84 to 85% yields.

All newly reported cysteic acid *S*-amides and the corresponding derivatives were obtained chromatographically pure (TLC and HPLC) and

Table 1. Analytical data of analogues 5a-e and derivatives

Comp. №	Yield [%]	M.p. [°C]	[α] _D ²⁰ (C=0.1, EtOH)	Elemental analysis				ESMS
				% C	% H	% N	% S	(m/z)
				Found/ Calc.	Found/ Calc.	Found/ Calc.	Found/ Calc.	Found/ Calc.
2a	81	94-96		50,03 / 50,27	6,11 / 6,19	26,32 / 26,78	9,03 / 8,95	358.2 / 358,419
3a	85	92-93	+ 8,8	50,16 / 50,27	6,01 / 6,19	7,88 / 7,82	8,90 / 8,95	358.6 / 358,419
4a	91	103-104	-18,4	47,12 / 47,26	5,30 / 5,49	8,42 / 8,48	9,80 / 9,71	330.3 / 330,365
5a	95	157-160	-35,3	30,55 / 30,61	6,23 / 6,16	14,35 / 14,28	16,42 / 16,34	195.9 / 196,221
6a	95	147-148	-15,8	40,30 / 40,53	6,72 / 6,80	9,33 / 9,45	10,88 / 10,82	296.4 / 296,348
7a	84	133-134	-12,7	57,09 / 57,40	5,28 / 5,30	6,75 / 6,69	7,44 / 7,66	418.3 / 418,474
2b	88	85-87		51,46 / 51,60	6,37 / 6,50	7,34 / 7,52	8,29 / 8,61	372.4 / 372,446
3b	80	83-84	+ 7,7	51,53 / 51,60	6,38 / 6,50	7,63 / 7,52	8,60 / 8,61	372.5 / 372,446
4b	93	112-113	-20,2	48,41 / 48,83	5,55 / 5,85	8,03 / 8,13	9,17 / 9,31	344.3 / 344,392
5b	95	160-163	-37,1	34,33 / 34,28	6,80 / 6,71	13,43 / 13,32	15,34 / 15,25	210.3 / 210,248
6b	93	140-142	-17,0	42,67 / 42,57	7,21 / 7,14	9,19 / 9,03	10,23 / 10,33	310.4 / 310,375
7b	87	129-131	-14,6	58,43 / 58,46	5,66 / 5,37	6,27 / 6,49	7,19 / 7,43	431.3 / 431,482
2c	65	87-90		48,76 / 48,83	5,81 / 5,85	8,20 / 8,13	9,35 / 9,31	344.3 / 344,382
3c	45	86-88	+ 9,1	48,71 / 48,83	5,87 / 5,85	8,15 / 8,13	9,40 / 9,31	344.4 / 344,382
4c	65	113-115	-20,7	45,60 / 45,56	5,04 / 5,10	8,67 / 8,86	10,30 / 10,14	316.2 / 316,328
5c	88	178-180	-35,6	26,47 / 26,37	5,66 / 5,53	15,33 / 15,38	17,71 / 17,60	182.1 / 182,194
6c	91	149-151	-14,1	38,39 / 38,29	6,48 / 6,43	9,98 / 9,92	11,41 / 11,36	282.4 / 282,311
7c	82	140-142	-16,1	56,52 / 56,57	4,35 / 4,75	6,43 / 6,94	7,05 / 7,95	403.3 / 403,429
2d	54	89-92		49,76 / 50,27	6,71 / 6,19	7,20 / 7,82	8,35 / 8,94	358,42 / 358,408
3d	24	88-91	+8,9	50,71 / 50,27	6,71 / 6,19	7,20 / 7,82	8,35 / 8,94	358,42 / 358,408
4d	67	113-117	-21,7	45,36 / 47,27	5,40 / 5,49	8,17 / 8,48	9,30 / 9,70	330,4 / 330,354
5d	61	181-183	-36,6	29,82 / 30,61	5,74 / 6,16	14,93 / 14,28	16,87 / 16,34	195,0 / 196,221
6d	84	149-151	-14,5	39,33 / 40,52	7,11 / 6,80	9,39 / 9,49	10,42 / 10,81	297,1 / 296,454
7d	76	143-146	-17,1	58,11 / 57,52	4,88 / 5,07	7,06 / 6,74	6,90 / 7,68	416,7 / 417,572
2e	70	90-91		51,33 / 51,60	6,47 / 6,50	7,38 / 7,52	8,43 / 8,61	372.6 / 372,446
3e	51	93-95	+ 9,1	51,33 / 51,60	6,47 / 6,50	7,38 / 7,52	8,43 / 8,61	372.3 / 372,446
4e	78	115-116	-21,8	48,74 / 48,83	5,69 / 5,85	8,17 / 8,13	9,23 / 9,31	344.3 / 344,392
5e	85	183-184	-38,7	34,32 / 34,28	6,85 / 6,71	13,13 / 13,32	15,38 / 15,25	210.3 / 210,248
6e	96	152-153	-14,7	42,66 / 42,57	7,18 / 7,14	9,23 / 9,03	10,02 / 10,33	310.4 / 310,375
7e	85	145-148	-18,6	58,49 / 58,46	5,45 / 5,37	6,38 / 6,49	7,51 / 7,43	431.5 / 431,482

identified by elemental analysis and electron spray mass spectra (ESMS). The chiral purity of the final compounds was verified also. The collected physico-chemical and analytical data of the described compounds are presented in Table 1.

In summary, a set of new chirally pure unusual

amino acids, based on cysteic acid *S*-amide was synthesized. We have reported also, the new approach for synthesis of the lead compound **1**. According to our recent investigations these new members of cysteinsulfonamide family are promising candidates for studies on the

physiological roles of the corresponding natural amino acids – leucine, isoleucine and norleucine, as well as attractive peptide modifiers, useful clues for design of more potent and more selective biologically active compounds.

Acknowledgements: *This work was supported by Bulgarian Ministry of Education and Science, project MY-FS-13/07.*

REFERENCES

- 1 C.W. Mosher, R.M. Silverstein, O. B. Crews, B.R. Baker, *J. Org. Chem.*, **23**, 1257 (1958).
- 2 D. Ross, C. Skinner, W. Shive, *J. Org. Chem.*, **24**, 1372 (1959).
- 3 B.V. Bhide, *J. Org. Chem.*, **36**, 134 (1959).
- 4 H. Baganz, G. Dransch, *Chem Ber.*, **93**, 784 (1960).
- 5 T. Heyman, T. Ginsberg, Z. Gulick, E. Konopka, R. Mayer, *J. Am. Chem. Soc.*, **81**, 5125 (1959).
- 6 B. Aleksiev, S. Stoev, *Die Pharmazie*, **24**, 305 (1969).
- 7 S. Brynes, G. J. Burckart, M. Mokotoff, *J. Med Chem.*, **21**, 45 (1978).
- 8 S. Brynes, V. J. Fiorina, D. A. Cooney, H. A. Milman, *J. Pharm. Sci.*, **67**, 1550 (1978).
- 9 S. Zakhariiev, R. Zakhariieva, W. Gryc, S. Stoev, B. Tomicka, E. Golovinsky, B. Aleksiev, M. Karaivanova, G. Kupryszewski, *Pol. J. Chem.*, **55**, 799 (1981).
- 10 L. Maneva, N. Slavcheva, G. Videnov, I. Mancheva, D. Petkov, S. Stoev, B. Aleksiev, *Compt. Rend Acad. Bulg. Sci.*, **41**, 83 (1988).
- 11 B. Aleksiev, S. Stoev, A. Spassov, L. Maneva, E. Golovinsky, In: *Peptides 1972* (ed. by H.Hanson and H-D. Jakubke), 245 (1973).
- 12 B. Aleksiev, S. Stoev, *Die Pharmazie*, **26**, 469 (1971).
- 13 G. Videnov, B. Aleksiev, M. Stoev, T. Pajpanova, G. Jung, *Liebigs Ann. Chem.*, **941** (1993).
- 14 T. Buchinska, S. Stoev, in: *Peptides 1995* (Proceedings of the 14 American Peptide Symposium, Columbus, OH, USA), 1995, p.100.
- 15 E. Popgeorgieva, K. Miteva, S. Pantcheva, T. Buchinska, N. Stoeva, A. Bocheva, L. Kazakov, S. Stoev, in: *Peptides 1995*, (Abstracts of the 14th American Peptide Symposium, Columbus, OH, USA, 1995, p.112.
- 16 T. Pajpanova, A. Bocheva, E. Golovinsky, *Methods Find. Exp. Clin. Pharmacol.*, **21**, 591 (1999).
- 17 L. Maneva, S. Stoev, B. Aleksiev, E. Golovinsky, *Die Pharmazie*, **34**, 423 (1979).
- 18 S. Pantcheva, E. Popgeorgieva, E. Grueva, T. Brakadanska, S. Stoev, in: *Peptides 1998*, (Proceedings of the 24th European Peptide Symposium, Edinburgh, Scotland), 1998, p.709.
- 19 B. Aleksiev, P. Shamljan, G. Videnov, S. Stoev, E. Golovinsky, *Hoppe-Seyler's Z Physiol. Chem.*, **362**, 1323 (1981).

НОВИ S-АМИДИ НА ЦИСТЕИНОВАТА КИСЕЛИНА, ЗАМЕСТЕНИ В СУЛФОНАМИДНАТА ГРУПА. СИНТЕЗ И МОДИФИКАЦИИ

С.С. Панчева, Р.Х. Калаузка, Е.С. Йовчева, Т.А. Дзимбова, Е.П. Попгеоргиева, Т.И. Пайпанова

Постъпила на 10 юни, 2012 г.; приета на 3 август, 2012 г.

(Резюме)

Институт по молекулярна биология „Акад. Р. Цанев“, БАН, 1113 София

В настоящата работа представяме синтезата на поредица аналози 5a-e на S-амидите на цистеиновата киселина със заместена сулфонамидна група. Напълно защитените S-хлориди на D,L-цистеиновата киселина взаимодействат със съответните алифатни амини, при което се получава серия от нови производни, които могат да се приемат като структурни сулфо-аналози на левцин, изолевцин и норлевцин, съответно. Тук е представен и нов метод за получаване на S-хлориди на D,L-цистеиновата киселина. Успешно са направени модификации с различни Na- и Ca-защитни групи за целите на пептидния синтез. Тези съединения са подходящи за изучаване на връзката структура – активност, тъй като могат лесно да се използват както при твърдофазен, така и при конвенционален синтез на биологично активни пептиди.

A facile synthesis and IR-LD spectral elucidation of *N*-acetyl amino acid derivatives

A.G. Chapkanov^{1*}, T.A. Dzimbova², B.B. Ivanova³

¹Department of Chemistry, Faculty of Mathematics and Natural Sciences, SWU "N. Rilski", 66 "I. Mihailov" Str., 2700 Blagoevgrad, Bulgaria

²Institute of Molecular Biology "R. Tsanev", Bulgarian Academy of Sciences, 21 Acad. G.Bonchev str., 1113 Sofia, Bulgaria

³Faculty of Chemistry, Sofia University, 1 J. Boucher Boulevard, 1164 Sofia, Bulgaria

Received June 10, 2012; Accepted August 3, 2012

Abstract: The synthesis of *N*-acetyl derivatives of α -amino acids (L-Gly, L-Val, L-Phe, L-Ile, L-Pro and L-Cys) using a simple and efficient method for preparation was carried out. The *N*-acetyl derivatives were obtained using acetic anhydride in basic conditions at room temperature. The methyl amides of *N*-acetyl amino acid were synthesized by mixed anhydride procedure using a Piv-Cl as a reagent. The conventional and IR-LD spectral analysis were applied for elucidation and characterization of typical IR-bands of the starting and intermediate compounds. Spectral investigation includes IR-characteristic bands assignment and elucidation of amino acids as zwitterions structures – L-Valine (L-Val), L-Proline (L-Pro) L-Cystein (L-Cys) and their intermediates by linear-dichroic infrared (IR-LD) spectroscopy of oriented solid sample as a nematic liquid crystal suspension. The experimental IR-characteristic bands obtained, were accompanied with spectral elucidation and structural prediction of the investigated compounds.

Key words: α -amino acids, *N*-acetyl-derivatives, IR –LD spectral analysis

INTRODUCTION

The profound significance of biological compounds in our daily lives has prompted a lot of research into their analysis and identification. The determination of peptide and protein structures constitutes one of the pillars of current investigation in molecular biology and biochemistry.

A great interest to *N*-acetyl derivatives of α -amino acids is because of their wide spectrum of actions [1]. There are many examples for *N*-acetylated amino acids in living organisms. *N*-acetyl derivatives of L-proline, L-glutamine and 4-hydroxy-L-proline are particular importance, because of their uses as medicines and biologically active supplements. *N*-Acetyl-4-hydroxy-L-proline has found practical use in producing of the medicines which has anti-inflammatory and analgesic actions [2, 3]. *N*-Acetylaspartic acid is a derivative of aspartic acid, which is the second most concentrated molecule in the brain after the amino acid glutamate. It is synthesized in neurons from the amino acid aspartate and acetyl coenzyme A. *N*-Acetyl-L-glutamine is used in sport medicine as a component for increasing training intensity, muscle growth and strength. *N*-Acetyl cysteine is

derived from cysteine found in food and synthesized in the body. It helps the body to synthesize glutathione, which is used as a mucolytic agent to reduce the viscosity of mucous secretions [4].

The development of an effective synthetic method of *N*-acetyl derivatives of amino acids has a practical importance, as well as the development of fast and simple analytical methods for structure determination. Powder X-ray diffraction is one of the powerful and routine method for determination of solids in pharmaceutical industry. However, the method is relatively expensive, difficult for operation and requiring a preliminary samples treatment.

Infrared (IR-) and Raman spectroscopy are other also wide used in the practice and pharmaceutical industry. However, in many cases the choice of suitable method for analysis often is difficult on account of the typical for crystals effects of Fermi-resonance [5–7]. Linear-polarized IR-spectroscopy of oriented colloids in nematic host could resolve a lot of these problems. The method is unique for experimental assignment of the characteristic bands and local structural elucidation independently of the crystalline or amorphous character of the samples [8–11]. Different *N*-acetyl amino acid derivatives were synthesized, characterized and reported earlier

* To whom all correspondence should be sent:
E-mail: chapkanov@swu.bg

as well as and the corresponding spectral study [12–19].

EXPERIMENTAL

Materials and methods

Amino acids and solvents were purchased from Fluka and used without further purification. Melting points were measured on Büchi (Switzerland) model 535. Optical rotation was determined on Polarimeter 141, Perkin Elmer (USA). For TLC silicagel plates (Merck, 60F₂₅₄) were used and following systems: A) CHCl₃ : MeOH : H₂O (80:30:5); B) CH₃CN : H₂O (4:1).

SYNTHESIS

N-Acetyl amino acids Amino acid (0.1 g) was dissolved in 5N NaOH (3 ml) and acetic anhydride (2 × 0.2 ml) was added over 15 min. period of time. Reaction mixture was stirred at room temperature for 1 hour and the water was evaporated under reduced pressure. The residue obtained was dried and used without further purification in the next reaction stage.

N-Acetyl amino acid methyl amides. To the solution of N-acetyl amino acid (3 mM) in the solvents (2 ml DMF and 2 ml THF) mixture, NMM (0.33 ml, 3 mM) was added and the reaction mixture was chilled to –10°C. The reagent Piv-Cl (0.37 ml, 3 mM) was added dropwise and after 10 minutes solution of methyl amine hydrochloride (1g, 15 mM) and Et₃N (0.415 ml, 15 mM) in water (2 ml) was added. The reaction process completed after 1.5 hour at –10°C and the solvents were evaporated under reduced pressure. The residue was dissolved in CHCl₃ (10 ml) and washed with water (2 × 10 ml). Organic layer was dried over anhydrous Na₂SO₄ and CHCl₃ was evaporated. The pure product was obtained after column purification (silicagel) and eluent: CH₃CN : H₂O (4 : 1, v/v).

METHODS

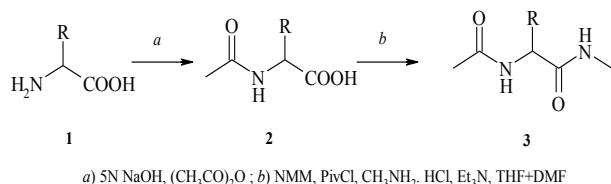
The IR-spectra were measured using a Bomem-Michelson 100 FT-IR-spectrometer (4000 – 400 cm⁻¹, 2 cm⁻¹ resolution, 150 scans) equipped with a Perkin Elmer wire-grid polarizer. Non-polarized solid-state IR spectra were recorded, using the KBr disk technique. The oriented samples were obtained as a colloidal suspension in a nematic 4'-cyano-4'-alkylbicyclohexyl mixture (ZLI-1695, Merck), whose poor IR-spectrum allows the recording of the guest-compound bands in the whole 4000 – 400 cm⁻¹ range. The presence of the isolated nitrile stretching IR-band at about 2230 cm⁻¹ additionally

serves as an orientation indicator. The effective orientation of the solid samples was achieved by the next procedure: the investigated compound (5 mg) was mixed with the liquid crystal substance until obtaining of a slightly viscous suspension. The phase prepared thereby was pressed between two KBr-plates, which in advance were rubbed out in one direction by fine sand-paper. The grinding of the prepared mull in the rubbed direction promotes in addition the sample orientation [20, 21]. For polarized IR-spectra interpretation, the IR-LD spectroscopy use stepwise reduction procedure [22–25]. The IR-LD data interpretations are consisted in subtraction of the perpendicular spectrum (IR_s – a result of the 90° angle between the polarized light beam electric vector and the orientation of the sample) from the parallel spectrum (IR_p) obtained with a co-linear mutual orientation. The recorded difference (IR_p-IR_s) spectrum divides the integrated absorbance into positive and negative bands. Positive bands originate from transition moments which form average angles with the orientation direction (n) between 0° and 54.7° (magic angle) and negative bands corresponding to transition moments, which are directed between 54.7° and 90°. In the reducing-deference procedure, the perpendicular spectrum, multiplied by the variable parameter c, is subtracted from the parallel spectrum and parameter c is varied until at least one band or set of bands is eliminated in the obtained (IR_p – cIR_s) reduced IR-LD spectrum. The simultaneous disappearance of these bands in the reduced spectrum provides information about the mutual disposition of the molecular fragments. This elimination method is carried out graphically using the attached subtracting procedure for processing of IR spectra.

RESULTS AND DISCUSSION

This work is a part of systematic synthetic, spectroscopic and structural investigations on amino acids, their derivatives and small peptides about the possibilities for application as potential medicines [26–28]. The aim was to develop simple and efficient methods for preparation N-acetyl-α-amino acids derivatives using a mixed anhydride procedure – the action of acetic anhydride using water as the reaction medium. The synthesis of the desired N-acetyl amino acid methyl amides was done according to the Scheme 1.

The first step in our scheme is the synthesis of N-acetyl amino acid derivatives using acetic anhydride at basic conditions (5N NaOH) in aqueous solution and room temperature for 1 hour.



Scheme 1. Synthesis of N-acetyl amino acid methyl amides

N-Acetyl amino acids were used on the next step after evaporation of the solvent, drying of the crude product without further purification. N-Acetyl amino acid methyl amides were obtained in mixed anhydride procedure – Piv-Cl was used as a reagent. The reaction was carried out at -10°C in mixture of THF and DMF as solvents. The reaction process continued for 1.5 hour and the desired N-acetyl amino acid methyl amide was obtained after column purification (silicagel, CH₃CN : H₂O, 4:1, v/v). Some physical constants and chemical characteristics of the synthesized compounds are presented in Table 1.

Table 1. Some physical data and characteristics of amino acid derivatives

Amino acid derivatives	Melting point (mp), °C	Optical rotation [α] _D ²⁰	Yield (%)
Ac-Pro	115–117	-86 (C=1, C ₂ H ₅)	77
Ac-Val	124–125	+7,4 (water)	82
Ac-Gly	207–209	–	80
Ac-Cys	109–112	-35 (water)	81
Ac-Phe	168–169	+47 (water)	78
Ac-Ile	oil	+42 (water)	81
Ac-Pro-NH-CH ₃	32	-210 (C=1, water)	25
Ac-Gly-NHCH ₃	oil	–	27
Ac-Cys-NHCH ₃	81	-24 (MeOH)	31
Ac-Phe-NHCH ₃	196	+2.9 (MeOH)	33
Ac-Ile-NHCH ₃	220	-1.5 (MeOH)	26

IR-SPECTRAL ANALYSIS

The spectral results of the investigated compounds are assigned on the basis of known IR-data about similar systems [29-32]. The characteristic IR-bands of the pure amino acids L-Val, L-Pro and L-Cys are listed in Table (2). Using the statement, that pure amino acids stabilize zwitterionic (H₃N⁺-R-COO⁻ (L-Val and L-Cys)) and H₂N⁺-R-COO⁻ (L-Pro) structure with characteristic IR-spectral bands of -NH₃⁺ and -COO⁻ groups, the comparison and assignment of the solid-state IR-spectra (Figs. 2.1) of the systems studied was carried out. The method of polarized IR-spectroscopy is appeared to be unique for the experimental proving of the vibrational bands to corresponding modes. In all cases a preliminary deconvolution and curve-fitting procedure for the

peak positions obtained and corresponding integral absorbance are in the 1750 – 1500 cm⁻¹ region according to [18].

Table 2. IR-characteristic bands of some amino acids in 1700 – 1350 cm⁻¹ region

Assignment v[cm ⁻¹]	L-Val	L-Cys	L-Pro
vNH ₃ ⁺	3200 – 2700	3320–1800	
v ^{as} NH ₃ ⁺		3170	
vNH ₂ ⁺	-		3000 – 2400
δ ^{as} NH ₃ ⁺	1629	1654	
δ ^{as} NH ₃ ⁺	1612	1610	
δ ^s NH ₃ ⁺	1567	1530	
δNH ₂ ⁺			1626, 1612
v ^{as} COO ⁻	1585	1589, 1567, 1552	
v ^s COO ⁻	1508	1397, 1407, 1402	
vSH		2551	
δ ^{as} NH ₃ ⁺ + tNH ₃ ⁺		2068	
vC-N		1349	

*IR-data obtained after applied deconvolution and curve-fitting procedures

The comparative spectral analysis shows the presence of bands in the 3320 – 1800 cm⁻¹ region assigned to the v^{as}NH₃⁺ and v^sNH₃⁺ stretching vibrations of the protonated amino group -NH₃⁺ for amino acid L-Val and L-Cys and vNH₂⁺ stretching vibrations for L-Pro. The band with frequency at 3170 cm⁻¹ belongs namely to v^{as}NH₃⁺ of L-Cys. In the spectra of L-Val and L-Cys are observed two couple of bands at 1629, 1612 cm⁻¹ and at 1654, 1610 cm⁻¹ characterizing asymmetric banding vibrations (δ^{as}NH₃⁺). The corresponding bands for protonated -NH₂ group in L-Pro are at 1626 and 1612 cm⁻¹. (see Table 2). The bands at 1567 cm⁻¹ (L-Val) and at 1530 cm⁻¹ (L-Cys) are assigned to the symmetric banding vibrations (δ^sNH₃⁺). The typical -COO⁻ maxima are in the 1600 – 1400 cm⁻¹ spectral range. The character of the band at 1585 cm⁻¹ and 1508 cm⁻¹ are assigned and belonging to the asymmetric and symmetric stretching modes of COO⁻ fragment (v^{as}COO⁻ and v^sCOO⁻) in the molecule of L-Val. The bands at 1589 and 1397 cm⁻¹ correspond to v^{as}COO⁻ and v^sCOO⁻ stretching vibrations of COO⁻ fragment of L-Cys. For L-Pro are defined two pair of bands corresponding at 1567, 1552 cm⁻¹ (v^{as}COO⁻) and 1407, 1402 cm⁻¹ (v^sCOO⁻) probably as a result of different molecular interactions (see Fig.1). The observed other bands for L-Cys at 2068 cm⁻¹ corresponds to δ^aNH₃⁺ + τ_{NH₃⁺ combination mode, while the intensive band at 2551 cm⁻¹ corresponds to v_{SH} stretching vibration of the SH-group. The band at 1349 cm⁻¹ belongs to v_{C-N} stretching mode.}

Using stepwise reduction procedure of IR-LD method, the obtained reduced spectrum for L-Pro

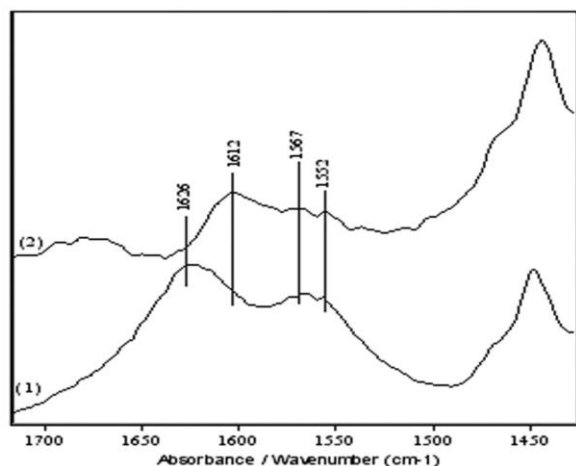


Fig. 1. Non-polarized IR-(1) and reduced IR-LD (2) spectra of L-Pro after elimination of 1626 cm^{-1} peak

illustrated the strong reduction of 1567 cm^{-1} peak with the 1626 cm^{-1} one (see Fig.1.2 and Table 2). Due to the last procedure second pairs of observed maxima at 1612 cm^{-1} and 1552 cm^{-1} probably correspond to $\delta_{\text{NH}_2^+}$ and $\nu^{\text{as}}\text{COO}^-$ modes of other second molecule which is very likely to be oriented differently in the frame unit cell of L-Pro. This assumption is confirmed by single crystal X-ray data of L-Pro [33], where the unit cell contains four molecules which are similarly mutual oriented by pairs. Similar behaviour is observed in L-Val, where the simultaneously elimination of pairs of peaks at 1629 cm^{-1} and 1612 cm^{-1} confirmed their character as $\delta^{\text{as}}_{\text{NH}_3^+}$ and $\delta^{\text{as}}_{\text{NH}_3^+}$ (Tab. 2) due to their possession of the same symmetry class.

It is necessary to underline, that the non-polarized IR- and IR-LD spectra of N-acetyl-L-cysteine (Fig.2) are characterized with significant degree of particles orientation in nematic liquid crystal [10, 11], allowing the precise assignment of corresponding IR-bands. The observed broad absorption band in the 3100 – 1800 cm^{-1} range belongs to ν_{OH} stretching vibration of the intermolecular interaction OH-group of the COOH, typical for carboxylic acid. The obtained maximum with low intensity at 1918 cm^{-1} is typical too for systems with stronger intermolecular hydrogen bonding. The intensive band at 3374 cm^{-1} belongs to ν_{NH} stretching vibration of the amide fragment, while the maximum at 1716 cm^{-1} to $\nu_{\text{C=O}}$ stretching vibration of COOH group (see Fig.2).

The reduction of last band in the difference IR-LD spectrum (Fig.2) indicates, that the transition moment of corresponding C=O vibration is oriented towards the orientation direction (**n**) of the liquid crystal at angle of 54.7° (magic angle). The intensive band about 1575 cm^{-1} belongs to δ_{NH} bending vibration. This maximum is strong reduced

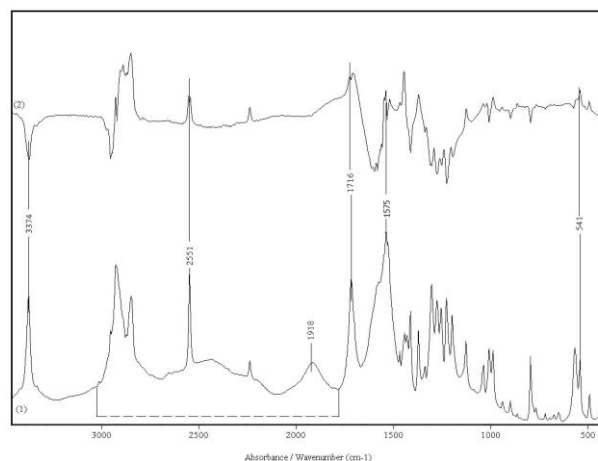


Fig. 2. Non-polarized IR-(1) and difference IR-LD (2) spectra of N-acetyl-L-cysteine

with the elimination of the $\nu_{\text{C=O}}$ band from –COOH group (Fig.2) which is in accordance with the assumption, that both transition moments are approximately equal oriented. The same procedure leads to elimination of the band at 541 cm^{-1} , indicating probably its belonging to bending vibration ($\delta_{\text{C=O}}$) of carbonyl group. On the other hand, the elimination of the $\nu_{\text{C=O}}$ band leads to reduction of the maximum at 2551 cm^{-1} characterizing stretching vibration of ν_{SH} , which shows, that both transition moments are also near to co-linear oriented.

CONCLUSION

The N-acetyl- derivatives of α -amino acids (L-Gly, L-Val, L-Phe, L-Ile, L-Pro and L-Cys) were synthesized by efficient and simple method using acetic anhydride in basic conditions and mixed anhydride procedure following using Piv-Cl as a reagent. The IR - spectral investigation includes determination of the characteristic bands of some strating compounds (as zwitterionic structure) and N-acetyl- derivatives (N-acetyl-L-cysteine). The method of linear polarized vibrational IR-spectroscopy of oriented colloids in nematic host is applied on L-Val and L-Cys, with a view to obtain experimental bands assignment and local structural elucidation in solid-state. The obtained experimental IR-LD results confirm the applicability of the used spectral method for structural determination.

Acknowledgements: This investigation was supported by the project SRP-A8 “Synthesis and spectral characterization of biological-activated substance - amino acids and their N-substituted derivatives”- SWU”N. Rilski”, 2011.

REFERENCES

- 1 A. P. Mihalkin, *Usp. Khimii*, **64**, 275 (1996).
- 2 G. Herrmann, D. Steiger, M. Klasser, *Clin. Rheumatol.*, **19**, 99 (2000).
- 3 M. Parnham, *Biochem. Pharm.*, **58**, 209 (1999).
- 4 D.K.Q. Lauer, C.J. Schreiber, W. Zollinger, M. Gutteck-Amsler, U. Cuenod, M. Holsboer, F. J. Neurochem. **65**, 2652 (1995)
- 5 A. Davydov, Theory of Molecular Excitons, Nauka, Moscow. (1968).
- 6 J. Evans, *Spectrochim. Acta*, **16**, 994 (1960).
- 7 K. Chou, *Biochemical J.* **215**, 465 (1983a).
- 8 B. Ivanova, M. Arnaudov, P. Bontchev, *Spectrochim. Acta, Part A*, **60**, 855 (2004).
- 9 B. Ivanova, D. Tsalev, M. Arnaudov, *Talanta*, **69**, 822 (2006).
- 10 B. Ivanova, V. Simeonov, M. Arnaudov, D. Tsalev, *Spectrochim Acta, Part A*, **67**, 66 (2007).
- 11 B. Koleva, T. Kolev, V. Simeonov, T. Spassov, M. Spiteller, *J. Inclusion Phenom.*, **61**, 319 (2008a).
- 12 W. Harris, S. Tenjarla, J.M. Holbrook, J. Smith, C. Mead, J. Entekin, *J. Pharm. Sci.* **84**, 640 (1995).
- 13 A. Cooke, J. Bennett, E. McDaid, *Tetrahedron Lett.*, **43**, 903 (2002).
- 14 S. Tenjarla, R. Kasina, P. Puranajoti, M. Omar, S. Wayne, T. Harris, *Inter. Jour. Pharmaceutics*, **192**, 147 (1999).
- 15 Z. Kuvaeva, D. Lopatik, T. Nikolaeva, A. Knizhnikova, V. Najdenov, M. Markovich, *Pharmac. Chem. J.*, **44**, 22 (2010).
- 16 I. Nemeč, Z. Micka, *J. Molec. Struct.*, **563/564**, 289 (2001).
- 17 B. Ivanova, M. Arnaudov, P. Bontchev, *Spectrochim. Acta, Part A*, **60**, 855 (2004).
- 18 A. Chapkanov, S. Zareva, *Protein&Peptide Lett.*, **17**, 347 (2010).
- 19 A. Chapkanov, T. Dzimbova, B. Ivanova, Proc. IV-International Conference, FMNS-2011, Blagoevgrad, Bulgaria, 07-09.06.2011.
- 20 B. Ivanova, D. Tsalev, M. Arnaudov, *Talanta*, **69**, 822 (2006).
- 21 B. Ivanova, V. Simeonov, M. Arnaudov, D. Tsalev, *Spectrochim. Acta, Part A*, **67**, 66 (2007).
- 22 E. Thulstrup, M. Eggers, *J. Chem. Phys. Lett.*, **1**, 690 (1968).
- 23 E. Thulstrup, J. Michl, Spectroscopy with Polarized Light, VCH, Wienheim, (1986).
- 24 B. Jordanov, R. Nentchovska, B. Schrader, *J. Mol. Struct.*, **297**, 401 (1993).
- 25 B. Jordanov, B. Schrader, *J. Mol. Struct.*, 347, 389 (1995).
- 26 A. Chapkanov, S. Zareva, *Protein&Peptide Lett.*, **16**, 1277 (2009).
- 27 T. Kolev, M. Spiteller, B. Koleva, *Amino Acids*, **38**, 45 (2010).
- 28 T. Kolev, B. Koleva, I. Stoineva, B. Jakimova, B. Tchorbanov, *Protein&Peptide Lett.*, **16**, 112 (2009).
- 29 S. Pandiarajan, M. Umadevi, R. Rajaram, V. Ramakrishnan, *Spectrochim. Acta, Part A*, **62**, 630 (2005).
- 30 R. Jacob, G. Fischer, *J. Phys. Chem. A*, **107**, 6136 (2003).
- 31 B. Rajkumar, V. Ramakrishnan, *J. Raman Spectrosc.* **31**, 1107 (2000).
- 32 R. Schweitzer-Stenner, F. Eker, A. Perez, K. Griebenow, X. Cao, L. Nafie, *Biopolymers (Peptide Science)*, **71**, 558 (2003).
- 33 Y. Mitsui, M. Tsuboi, Y. Iitaka, *Acta Crystallogr.*, **25B**, 2182 (1969).

СИНТЕЗ И ИЧ-ЛД СПЕКТРАЛНО ОПРЕДЕЛЯНЕ НА N-АЦЕТИЛ АМИНОКИСЕЛИННИ ПРОИЗВОДНИ

А. Г. Чапкънов^{1*}, Т. А. Дзимбова², Б. Б. Иванова³

¹Катедра "Химия", ПМФ, Югозападен университет „Н. Рилски“, 2700 Благоевград

²Институт по молекулярна биология „Акад. Р. Цанев“, БАН, 1113 София

³Химичен факултет, СУ „Св. Климент Охридски“, 1164 София

Постъпила на 10 юни, 2012 г.; одобрена на 3 август, 2012 г.

(Резюме)

В настоящата работа е представен лесен и ефикасен метод за синтез на N-ацетилни производни на α-аминокиселините (L-Gly, L-Val, L-Phe, L-Ile, L-Pro и L-Cys). N-Ацетилните производни са получени с помощта на оцетен анхидрид в алкална среда при стайна температура. Метиламидите на N-ацетил аминокиселините са синтезирани с използването на метода на смесените анхидриди и Piv-Cl като реагент. За определяне на характеристикните ИЧ-ивици на изходните и междинни съединения е приложен конвенционален и ИЧ-ЛД спектрален анализ. Спектралните изследвания включват определяне на характеристикните ИЧ-ивици на аминокиселините като цвитер-йонни структури - L-валин (L-Val), L-пролин (L-Pro) L-цистеин (L-Cys) и техните производни с ИЧ-ЛД спектроскопия в нематичен течен кристал. Експерименталните характеристикни ИЧ-ивици са използвани за спектрално охарактеризиране и предсказване на структурата на изследваните съединения.

Antioxidant capacity of new analogs of octreotide

S. Ts. Staykova^a, B. D. Mihaylova^b, I. G. Goshev^b, D. W. Wesselinova^c, L. T. Vezekov^a, E. D. Naydenova^{a*}

^aDepartment of Organic Chemistry, University of Chemical Technology and Metallurgy, Blvd. 8 Kliment Ohridski, 1756 Sofia, Bulgaria

^bInstitute of Organic Chemistry, Bulgarian Academy of Sciences, Academician Georgi Bonchev Street, Bl. 9, 1113 Sofia, Bulgaria

^cInstitute of Experimental Morphology, Pathology and Anthropology with Muzeum, Bulgarian Academy of Sciences, Academician Georgi Bonchev Street, Bl. 25, 1113 Sofia, Bulgaria

Received June 10, 2012; accepted August 10, 2012

New C-amide analogs of octreotide (SMS 201–995) modified at positions 5 with Orn, Dab (diaminobutanoic acid) and Dap (diaminopropanoic acid) and at positions 6 with the unnatural amino acids Tle (t-leucine) were synthesized. The antioxidant capacity of the compounds was tested by ORAC (Oxygen Radical Antioxidant Capacity) and HORAC (Hydroxyl Radical Averting Capacity) methods. All substances express significantly higher antioxidant capacity by comparison with gallic acid. Compound **1** (D-Phe-c(Cys-Phe-D-Trp-Dab-Tle-Cys)-Thr-NH₂) showed the highest antioxidant effect.

Key words: antioxidant, antiproliferative, somatostatin analogs, SPPS, unnatural amino acids

INTRODUCTION

Oxygen free radicals or, more generally, reactive oxygen species (ROS), as well as reactive nitrogen species (RNS), are products of normal cellular metabolism. ROS and RNS are well recognized for playing a dual role as both deleterious and beneficial species, since they can be either harmful or beneficial to living systems. Beneficial effects of ROS occur at low/moderate concentrations and involve physiological roles in cellular responses to noxia, as for example in defense against infectious agents and in the function of a number of cellular signaling systems. The harmful effect of free radicals (oxidative stress) is observed by the excess of ROS which can damage cellular lipids, proteins, or DNA inhibiting their normal function [1].

Naturally occurring somatostatins have diverse biological effects in many cells and organs throughout the body. They are produced by normal endocrine, gastrointestinal, immune and neuronal cells, as well as by certain tumors. The effects of somatostatins are broadly inhibitory on the secretion of hormones (e. g. growth hormone), as well as on the proliferation and survival of both normal and tumor cells [2]. Native somatostatin (SST) has a very short or transient effect *in vivo* as

it is rapidly inactivated by endo- and exo-peptidases [3, 4]. In recent years, increasing data have supported the hypothesis that different somatostatin analogs with longer half-life can also function as antineoplastic agents capable of inhibiting tumor growth and tumor angiogenesis [5–9].

Octreotide (Sandostatin, SMS 201-995: D-Phe-c(Cys-Phe-D-Trp-Lys-Thr-Cys)-Thr-ol) is the somatostatin analog used in clinical practice that mimics natural hormone somatostatin (SST-14: Ala-Gly-c(Cys-Lys-Asn-Phe-Phe-Trp-Lys-Thr-Phe-Thr-Ser-Cys) pharmacologically, but it is more potent inhibitor of growth hormone, glucagon, and insulin than SST [10]. It is used for the treatment of acromegaly, diarrhea and flushing episodes associated with carcinoid syndrome, in nuclear medicine imaging and peptide receptor radionuclide therapy [11–13].

Previous structure-function studies indicate that the sequence required for biological activity of the shortened SSAs consists of the β -turn fragment Phe-Trp-Lys-Thr corresponding to the residues 7–10 of the somatostatin. A β -turn structure about Trp-Lys (or Orn) in the analogs was a preferred stable conformation [14–17]. The introduction of D-residues increased the half-life and biological activity of the SST analogs. The substitutions of D-Trp decreased significantly or lead to full loss of antitumor activity [18]. The replacement of the C-terminal carboxyl group with amide group led to

* To whom all correspondence should be sent:
E-mail: e_naydenova@abv.bg

molecules with high biological activity [14–19]. RC-102 is the SST analog with GH and insulin-inhibitory activity [18].

Recently new modified C-amide analogs of Octreotide were synthesized substituting ornithine (Orn), diaminobutanoic (Dab) and diaminopropanoic (Dap) acids for lysine (Lys) and with Tle (t-leucine) for the threonine (Thr) based on templates D-Phe-c(Cys-Phe-D-Trp-Lys-Thr-Cys)-Thr-ol (Octreotide, Sandostatin, SMS 201-995). The *in vitro* antiproliferative activity were evaluated against 4 human tumor cell lines (HeLa, Hep G-2, MDA-MB-231, HT-29) and in the non-tumor Lep-3 cell line. The compounds showed different activity depending on the cell line and amount applied. The compound **2** (D-Phe-c(Cys-Phe-D-Trp-Dap-Tle-Cys)-Thr-NH₂) had antiproliferative effects on MDA-MB-231 cells with the IC₅₀ 0.03 mM. The most antiproliferative effect against the HeLa and HepG-2 cells exert the peptides **3** (D-Phe-c(Cys-Phe-D-Trp-Lys-Tle-Cys)-Thr-NH₂), **4** (D-Phe-c(Cys-Phe-D-Trp-Orn-Tle-Cys)-Thr-NH₂) and **5** (RC-102). The peptides were not cytotoxic to the normal Lep-3 cells [20].

Our results demonstrated that these new somatostatin analogs exhibit cytotoxic effect against some tumor cell lines (HeLa, Hep G2, MDA-MB-231 and HT-29) but their antioxidant effect is still unknown.

The aim of present investigation was to study the antioxidant capacity of the previously synthesized modified C-amide analogs of Octreotide: D-Phe-c(Cys-Phe-D-Trp-Dab-Tle-Cys)-Thr-NH₂ (**1**), D-Phe-c(Cys-Phe-D-Trp-Dap-Tle-Cys)-Thr-NH₂ (**2**), D-Phe-c(Cys-Phe-D-Trp-Lys-Tle-Cys)-Thr-NH₂ (**3**), D-Phe-c(Cys-Phe-D-Trp-Orn-Tle-Cys)-Thr-NH₂ (**4**) and D-Phe-c(Cys-Phe-D-Trp-Lys-Thr-Cys)-Thr-NH₂ (**5**) (RC-102) by ORAC (Oxygen Radical Antioxidant Capacity) and HORAC (Hydroxyl Radical Averting Capacity) methods.

EXPERIMENTAL

Synthesis

The protected amino acids and Fmoc-Rink Amide MBHA Resin were purchased from Iris Biotech (Germany). All other reagents and solvents were analytical or HPLC grade and were bought from Merck (Germany). The LC/ MC spectra were recorded on a LTQ XL Orbitrap Discovery instrument, Thermo Corporation, USA. The optical rotation was measured on automatic standard polarimeter Polamat A, Carl Zeis, Jena.

The conventional solid-phase peptide synthesis based on Fmoc (9-fluorenylmethoxycarbonyl)

chemistry was employed to synthesize a series of new analogues of SSAs. Rink-amide MBHA resin and TBTU (2-(1H-benzotriazole-1-yl)-1,1,3,3-tetramethyluronium tetrafluoroborate) were used as solid-phase carrier and condensing reagent. Three-functional amino acids were embedded as N^α-Fmoc-Thr(tBu)-OH, N^α-Fmoc-Cys(Acm)-OH, N^α-Fmoc-Lys(Boc)-OH, N^α-Fmoc-Orn(Boc)-OH, N^α-Fmoc-Dab(Boc)-OH, N^α-Fmoc-Dap(Boc)-OH, N^α-Fmoc-D-Trp(Boc)-OH. The coupling reactions were performed, using for amino acid/TBTU/HOBT/DIEA/resin a molar ratio 3/3/3/9/1. The Fmoc-group was deprotected by a 20% piperidine solution in dimethylformamide. The coupling and deprotection reactions were checked by the Kaiser test. For direct disulphide bond formation on the solid phase Ti(CF₃CO₂)₃ has been employed, using a mixture of 1,2 mmol Ti(CF₃CO₂)₃, 43 mmol anisol and 100 ml DMF at 0°C for 2.5 h. The oxidized peptidyl-resin was dried and next cleaved from the resin. The cleavage of the synthesized peptide from the resin was done, using a mixture of 95% trifluoroacetic acid (TFA), 2.5% triisopropylsilan (TIS) and 2,5 % water. The peptide was obtained as a filtrate in TFA and precipitated with cold dry ether. The precipitate was filtered, dissolved in water and lyophilized to obtain the crude peptide. The disulphide bridges were proved by reduction of the cyclic peptides with TCEP (tris(2-carboxyethyl)phosphine). The peptide purity was monitored on a RP-HPLC XTera C18 3.5 μm (125×2.1mm) (Waters Co.) column, flow 200 μl/min, using a linear binary gradient of phase B from 10% to 90% for 15 min (phase A: 0.1% HCOOH/H₂O; phase B: 0.1% HCOOH/AcCN). The compounds were checked by electrospray ionization massspectrometry and the optical rotation was measured in water.

Cytotoxic effect

Cytotoxicity of the substances was measured *in vitro*, using cultivated human tumor cell lines (American Type Culture Collection ATCC, Rockville, MD, USA). The cytotoxic activity of the tested somatostatin analogs (**1–5**) was evaluated by the MTS-dye reduction assay for cell viability against the Hep G-2 (human hepatocellular carcinoma cell line), MDA-MB-231 (human breast cancer cell line), HT-29 (human colorectal cancer cell line), HeLa (cervical cancer cell line), Lep-3 (normal human diploid cell line, delivered from 3-month embryo) as a control. Cells were cultivated with different amounts of the substances at concentration from 4.10⁻³ – 4.10⁻⁸ M.

The test (Cell Titer 96 Non-Radioactive Cell proliferation assay, Promega Corporation USA) was performed according to protocol of "Promega" and the details are previously described [20–22].

ANTIOXYDANT ACTIVITY

Preparation of the samples

Approximately 2 mg of each sample were dissolved in 2 mL acetone: dist. water: conc. acetic acid = 70:29.5:0.5 at room temperature for 1 hour. This solvent system is widely applied for enhanced extraction of phenolic substances from plant materials, foods etc. [23]. The solutions obtained were applied for determination of the antioxidant capacity immediately.

Determination of antioxidant capacity

AAPH, (2,2'-azobis-2-methyl-propanimidamide, dihydrochloride), a water-soluble free radical (peroxyl radical, ROO[•]) generator was delivered from Cayman Chemical Company. Fluorescein-disodium salt, gallic acid and TROLOX[®] (6-Hydroxy-2,5,7,8-tetramethylchroman-2-carboxylic acid) (a water-soluble analog of Vitamin E) were delivered from Sigma Aldrich. All other chemicals were of reagent grade.

HORAC (Hydroxyl Radical Averting Capacity)

The applied procedure is based on a scheme given by Ou et al. with some modifications [24]. Fluorescein-disodium salt (λ_{ex} 493 nm, λ_{em} 518 nm) was used as indicator for monitoring the generation of hydroxyl radical according to Fenton reaction mechanism and the effect of the tested substance.

ORAC (Oxygen Radical Antioxidant Capacity)

The procedure used is based on the thermal destruction of AAPH, which is accompanied by generation of peroxyl radicals (ROO[•]) as it is described by Yilmaz and Toledo [25], Wada and Ou [26] and Gheldof and Engeseth [27].

The experiments in both cases (HORAC & ORAC) were performed on a Perkin Elmer LS 5 spectrofluorimeter, equipped with thermostated cell holder (working temperature 37°C) in a 10 mm quartz cell. Data were collected for 30 min at a constant step of 0.5 sec.

Processing of data. The data obtained for each sample, the corresponding standard and the blank probe are normalized to the initial value (I_0) and the measuring interval (0.5 sec). Then the Area Under Curve (AUC) value is calculated according to the formula:

$$AUC = I_2/I_0 + I_3/I_0 + \dots + I_{n-1}/I_0$$

The calculation of the antioxidant capacity proceeds according to the equation:

$$\text{Antioxidant capacity} = \frac{AUC_{\text{Sample}} - AUC_{\text{Blank}}}{AUC_{\text{Std}} - AUC_{\text{Blank}}} * \frac{C_{\text{eff}}^{\text{Std}}}{C_{\text{eff}}^{\text{Sample}}}$$

[μM Std Equivalents/g sample]
if the effective concentration of the sample is in g/L.

The effective concentrations of the standard and the sample are their final concentrations in the cuvette. If we introduce in the formula the molecular mass of the tested substance, the result is obtained as μM Std Equivalents/M sample. The data processing can be achieved using the standard Excel software.

RESULTS AND DISCUSSION

In our previously investigation we synthesized some new modified C-amide analogs of Octreotide with the following sequences:

D-Phe-c(Cys-Phe-D-Trp-**Xxx**-**Yyy**-Cys)-Thr-NH₂

where:

Xxx: Dab (compound 1), Dap (compound 2), Lys (compounds 3, 5), Orn (compound 4)

Yyy: Tle (compounds 1- 4), Thr (compound 5)

The synthesis and cytotoxic assays were described [20].

All tested substances express significant antioxidant capacity. In Fig.1 and Fig. 2 are shown the fluorescence decay curves in the HORAC - procedure for tested substances.

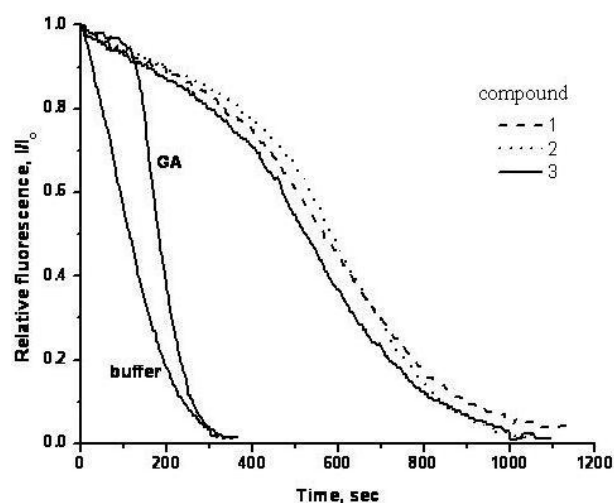


Fig.1. Fluorescence decay curves of compounds 1, 2 and 3 in the determination of HORAC

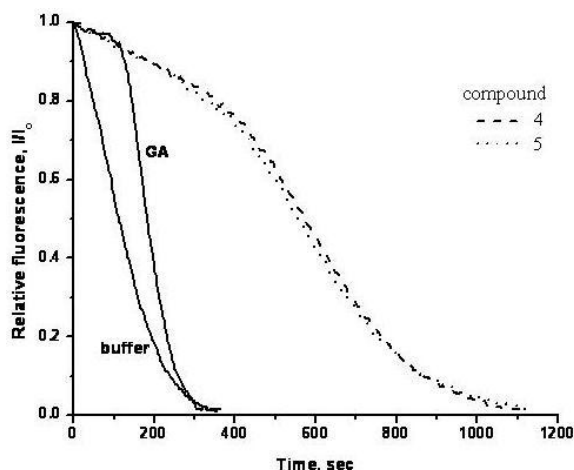


Fig. 2. Fluorescence decay curves of compounds **4** and **5** in the determination of HORAC

It is evident that there is no significant difference in the hydroxyl radical averting capacity of the individual samples, especially in the case of peptide **4** and **5**. The capacity of compound **1** is slightly higher. The lag-phase is not well defined. All tested substances express significantly higher capacity by comparison with gallic acid, i.e. they

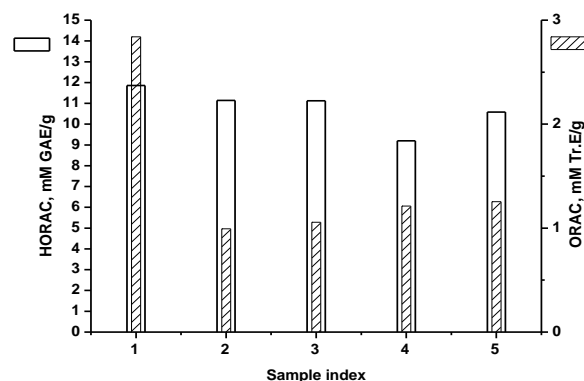


Fig. 3. Comparison of HORAC and ORAC values of the tested substances. GAE – gallic acid equivalents; Tr.E – TROLOX – equivalents.

are good helators of metal ions thus preventing the generation of hydroxyl radicals.

The scavenging effect of the tested substances towards peroxy radical (ORAC) follows the same logics (data not shown). The substance **1** is a stronger free radical scavenger by comparison with the other tested substances (Table 1 and Fig. 3).

Table 1. Summarized data on the antioxidant properties of the tested substances

No	STRUCTURE	MM _{exact}	HORAC M GAE/M	ORAC M Tr.E/M
1	D-Phe-c(Cys-Phe-D-Trp-Dab-Tle-Cys)-Thr-NH ₂	1015.4408	12.030	2.883
2	D-Phe-c(Cys-Phe-D-Trp-Dap-Tle-Cys)-Thr-NH ₂	1001.4252	11.150	0.996
3	D-Phe-c(Cys-Phe-D-Trp-Lys-Tle-Cys)-Thr-NH ₂	1043.4721	10.560	1.104
4	D-Phe-c(Cys-Phe-D-Trp-Orn-Tle-Cys)-Thr-NH ₂	1029.4565	9.470	1.249
5	D-Phe-c(Cys-Phe-D-Trp-Lys-Thr-Cys)-Thr-NH ₂	1031.4357	10.910	1.294

The antioxidant activity of proteins is thought to encompass both free radicals scavenging by amino acid residues and chelation of prooxidative transition metals; however the precise mechanism by which this occurs, remains unclear [28]. In beta-lactoglobulin particularly, Cys was oxidized more easily than Trp. Further, the extent of exposure of a given amino acid residue greatly affects its oxidation kinetics. In our case theoretically the Lys-residue and its analogs (Dap, Dab, Orn) are possible target points. The pKa-value of the epsilon-NH₂-group of Lys is about 10.0 and theoretically it should decrease following the order Dap<Dab<Orn [29]. This means that these amino acid residues are relatively reactive and modifiable under physiological conditions. In other words, the observed antioxidative capacity is a result of the corresponding modifications of lysine residues in the peptide structure. The elucidation of the detailed mechanism requires further investigations.

CONCLUSION

In conclusion we can summarize that the new previously synthesized somatostatin analogs with established *in vitro* anticancer activity express considerable antioxidant activity. Compound **1** has the greatest anti-ROS capacity and moderate anti-proliferative response. To determine the relationship between these activities further investigations are needed.

REFERENCES

- 1 M. Valko, C. J. Rhodes, J. Moncol, M. Izakovic, M. Mazur, *Chem. Biol. Interact.*, **160**, 1 (2006).
- 2 R. D. Murray, K. Kim, S. G. Ren, M. Chelly, Y. Umehara, S. Melmed, *J Clin Invest*, **114**, 349 (2004).
- 3 H. Haberfeld, *Austria-Codex*, 2009/2010 ed.; Österreichischer Apothekerverlag: Vienna, (2009).
- 4 V. Dinnendahl,; U. Fricke, *Arzneistoff-Profil*. 8 (23 ed.); Govi Pharmazeutischer Verlag: Eschborn, Germany (2010).

- 5 J. Strosberg, L. Kvols, *World J Gastroenterol.*, **16**, 2963 (2008).
- 6 W. D. Jia, G.L. Xu, H. C. Sun, L. Wang, J. H. Yu, J. Wang, J. S. Li, Z. M. Zhai, Q. Xue, *J. Cancer Res. Clin. Oncol.*, **129**, 327 (2003).
- 7 M. Appetecchia, R. Baldelli, *J. of Exp. and Clin. Cancer Res.*, **29**, 1(2010).
- 8 M. Pollak, *Yale J. of Biol. and Med.*, **70**, 535 (1997).
- 9 C. Susini, L. Buscail, *Annals of Oncology*, **17**, 1733 (2006).
- 10 W. Bauer, U. Briner, W. Doepfner, R. Haller, R. Huguenin, T. J. Petcher, J. Pless, *Life Sci.*, **31**, 1133 (1982).
- 11 I. Buchmann, M. Henze, S. Engelbrecht, M. Eisenhut, A. Runz, M. Schäfer, T. Schilling, S. Haufe, T. Herrmann, U. Haberkorn, *Eur. J. Nucl. Med. Mol. Imaging.*, **34**, 1617 (2007).
- 12 S. W.J. Lamberts, W. W. deHerder, L. J. Hofland, *Trends Endocrinol. Metab.*, **13**, 451 (2002).
- 13 G. Weckbecker, F. Raulf, B. Stolz, C. Bruns, *Pharmacol. Ther.*, **60**, 245 (1993).
- 14 D. F. Veber, F. W. Holly, R. F. Nutt, S. J. Bergstrand, S. F. Brady, R. Hirschmann, M. S. Glitzer, R. Saperstein, *Nature (London)*, **280**, 512 (1979).
- 15 D. F. Veber, R. M. Freidinger, D. S. Perlow, W. J. Paleveda, F. W. Holly, R. G. Strachan, R. F. Nutt, B. H. Arison, C. Homnick, W. C. Randall, M. S. Glitzer, R. Saperstein, R. Hirschmann, *Nature (London)*, **292**, 55 (1981).
- 16 W. M. Kazmierski, R.D. Ferguson, A. W. Lipkowski, V. J. Huby, *Int. J. Peptide Protein Res.* **46**, 265 (1995).
- 17 S. Prasad, A. Mathur, R. Sharma, N. Gupta, R. Ahuja, M. Jaggi, T. A. Sindh, R. Mukherjee, *Int. J. of Peptide Research and Therapeutics*, **12**, 179 (2006).
- 18 R.-Z. Cai, B. Szoke, R. Lu, D. Fu, T. W. Redding, A. V. Schally, *Proc. Natl. Acad. Sci. USA*, **83**, 1896 (1986).
- 19 W. A. Murphy, M. L. Heiman, V. A. Lance, I. Mezo, & D. H. Coy, *Biochem. Biophys. Res. Commun.*, **132**, 922 (1985).
- 20 S. Staykova, E. Naydenova, D. Wesselinova, A. Kalistratova, L. Vezekov, *Protein&Peptides Lett.*, (in press).
- 21 CellTiter 96 Non-Radioactive Cell proliferation assay, Technical Bulletin #TB112, Promega Corporation USA. Revised 12/99.
- 22 A. Ts. Mavrova, D. Wesselinova, N. Vassilev, J. A. Tsenov, *Eur. J. Med. Chem.*, **46**, 3362 (2011).
- 23 V.L. Singleton, J.A. Jr. Rossi, *Amer. J. Enol. Viticult.*, **16**, 144 (1965).
- 24 B. Ou, M. Hampsch-Woodill, J. Flanagan, E. K. Deemer, R. L. Prior, D. Huang, *J. Agric. Food Chem.*, **50**, 2772 (2002).
- 25 Y. Yilmaz, R. T. Toledo, *J. Agric. Food Chem.*, **52**, 255 (2004).
- 26 L. Wada, B. Ou, *J. Agric. Food Chem.*, **50**, 3495 (2002).
- 27 N. Gheldof, N.J. Engeseth, *J. Agric. Food Chem.*, **50**, 3050 (2002).
- 28 R.J. Elias, D.J. McClements, E.A. Decker, *Agric. Food Chem.*, **53**, 10248 (2005).
- 29 <http://www.cem.msu.edu/~cem252/sp97/ch24/ch24a.html>

АНТИОКСИДАНТЕН КАПАЦИТЕТ НА НОВИ АНАЛОЗИ НА ОКТРЕОТИД

С.Ц. Стайкова^а, Б.Д. Михайлова^б, И.Г. Гошев^б, Д.В. Веселинова^б, Л.Т. Везенков^а, Е.Д. Найденова^{а*}

^аДепартамент по органична химия, Химикотехнологичен и металургичен университет, бул. „Свети Климент Охридски“ № 8, София 1756

^бИнститут по органична химия, Българска академия на науките, София 1113

^сИнститут по експериментална морфология, патология и антропология с музей, Българска академия на науките, София 1113

Получена на 10 юни, 2012 г.; приета на 10 август, 2012 г.

(Резюме)

Ние синтезирахме нови аналози на октреотид (SMS 201-995) под формата на С-крайни амиди. Анализите модифицирахме с некодирани аминокиселини Orn (орнитин), Dab (диаминобутанова киселина) и Dar (диаминопропанова киселина) в позиция 5, както и с аминокиселината Tle (третичен левцин) в позиция 6. Антиоксидантната активност на новосинтезираните пептиди изследвахме с помощта на методите ORAC (Oxygen Radical Antioxidant Capacity) и HORAC (Hydroxyl Radical Averting Capacity). Всички съединения проявяват значително по-висока антиоксидантна активност в сравнение с използвания стандарт галова киселина. Пептид **1** (D-Phe-c(Cys-Phe-D-Trp-Dab-Tle-Cys)-Thr-NH₂) показва най-висок антиоксидантен капацитет.

Synthesis of new hybrid cell penetrating peptides-medical drugs molecules

D.L.Danalev^{a*}, R.N.Raykova^a, D.A.Marinkova^a, L.K.Yotova^a, S.G. Bayryamov^b, B.H.Hristova^a,
V.S. Stoyanova^a

^aUniversity of Chemical Technology and Metallurgy, Biotechnology Department, 1756 Sofia, Bulgaria,

^bRuse University "Angel Kanchev", Department of "Repairing, Reliability and Chemical Technologies", 7017 Ruse, Bulgaria

Received June 10, 2012; accepted August 3, 2012

In 1988 the remarkable ability of a peptide to traverse a cell's plasma membrane independent of a membrane receptor was revealed. They cause changes in the membranes leading to their permeability. This type of peptide molecules is called cell penetrating peptides (CPP). One of these peptides is sweet arrow peptide (SAP). Herein, we report for the synthesis of four analogues of SAP. A new interesting strategy for synthesis of Asn and Gln containing peptides starting from Glu and Asp and using Rink amide resin was applied.

Keywords: cell penetrating peptides, SAP analogues, CPP-medical drug hybrid molecules

INTRODUCTION

As it is well known the main problem with medical drugs absorption in human body is their hydrophilicity. Moreover, cell wall and membrane of the pathogen microorganisms and the membrane of eukaryotic cells and organelles, represent a major barrier to hydrophilic substances to penetrate into the cell.

The process of introducing drugs into cells has always proved a major challenge for research scientists and for the pharmaceutical industry. The cell membrane is selectively permeable and supports no generic mechanism for their uptake. A drug must be either highly lipophilic or very small to stand a chance of cellular internalization. These restrictions mean that the repertoire of possible drug molecules is limited. The existing methods for delivery of macromolecules, such as viral vectors and membrane perturbation techniques, can result in high toxicity, immunogenicity and low delivery yield. However, in 1988 the remarkable ability of a peptide to traverse a cell's plasma membrane independent of a membrane receptor was revealed. They cause changes in the membranes leading to their permeability. This type of peptide molecules is called cell penetrating peptides (CPP) [1].

CPPs have the ability to enter cells independent of a membrane receptor, and they show no cell-type specificity. They are small (10–30 residues in

length), often positively charged sequences of amino acids. CPPs facilitate cellular uptake of various molecular cargo (from small chemical molecules to nanosize particles and large fragments of DNA). The "cargo" is associated with the peptides either through chemical linkage via covalent bonds or through non-covalent interactions. The function of the CPPs are to deliver the cargo into cells, a process that commonly occurs through endocytosis with the cargo delivered to the endosomes of living mammalian cells. CPPs hold great potential as *in vitro* and *in vivo* delivery vectors for use in research and medicine. Remarkable is the extremely low toxicity that these peptides show. Their current application in medical practice is limited due to lack of cell selectivity in delivery of goods and lack of understanding of how their utilization. However, the CPP have found many applications in medicine as suppliers of medicines to treat various diseases including cancer, inhibitors of viruses, as well as in diagnosis, as transporters of contrast agents for cellular "labeling".

Three different mechanism of cellular uptake were revealed [2]:

- direct penetration
- translocation through the formation of a transitory structures
- translocation mediated by the formation of inverted micelles

* To whom all correspondence should be sent:

E-mail: dancho.danalev@gmail.com

But today, it is thought that each CPP expresses its own preferred mechanism of uptake. CPPs typically could be 2 different types:

- with amino acid composition containing a high relative abundance of positively charged amino acids such as lysine or arginine;
- or have sequences that contain an alternating pattern of polar/charged amino acids and non-polar, hydrophobic amino acids.

These two types of structures are referred to as polycationic or amphipathic, respectively.

A well known member of second group peptides, with proven membrane-penetrating properties, is so called "sweet arrow peptide" (SAP) (VRLPPP)₃ described by Fernandez-Carneado et al. in 2004 [3].

Herein, we report on the synthesis of four SAP analogues replacing Leu residue with Asp, Glu, Asn and Gln in order to introduce in the final molecule a specific functions we need to obtain hybrid structures CPP-medical drug.

RESULTS AND DISCUSSION

Our attention was attracted by SAP because it has relatively simple and easily realizable synthetically primary structure consisting of 6 amino acid residues.

We chose to replace Leu residue of SAP with the amino acids Asp, Glu, Asn and Gln and to synthesise the following products:

H-Val-Arg-Asp (drug molecule)-Pro-Pro-Pro-OH;

H-Val-Arg-Glu (drug molecule)-Pro-Pro-Pro-OH;

H-Val-Arg-Asn-Pro-Pro-Pro-drug molecule;

H-Val-Arg-Gln-Pro-Pro-Pro-drug molecule.

These amino acids were chosen because of its adequate structure to provide us the necessary additional functional groups in their side chains for binding of the drug molecules. This decision was also framed by the idea of using two strategies for the synthesis of CPP-drug molecule. For the synthesis of aim CPP we used conventional SPPS (solid phase peptide synthesis) by Fmoc-strategy.

Here drug molecule was previously linked to the carboxyl function of the side chain of Asp or Glu. For this purpose, two acidic amino acids were previously protected on their ^oNH₂-group with Fmoc-group and ^oCOOH group as allyl esters. This type of esters became very useful in recent years due to their specific properties. They are completely stable in acidic and alkaline hydrolysis,

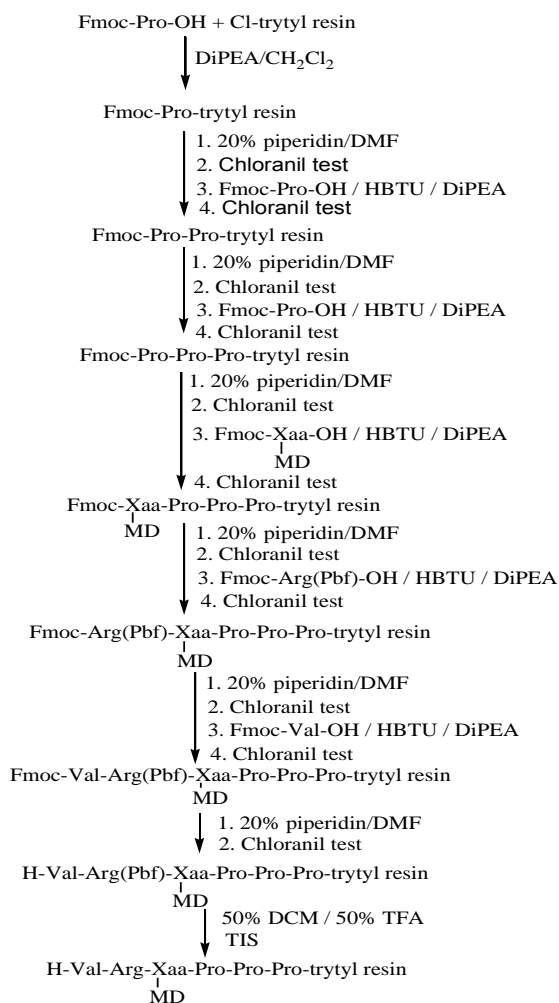
unlike other ester groups such as OMe, OEt, OBzl and OBut. On every stage, this function can be successfully unblocked by treatment with tetrakis / Pd, allowing the extension of the main chain. At the beginning Wang resin was used as solid phase carrier. After connecting the second Pro residue during the reaction of deblocking of Fmoc-function, we found that the obtained dipeptide Pro-Pro is cleaved from the resin. The literature data shown that during the synthesis of difficult sequences to the C-terminal peptides as a Pro-Pro, Val-Pro, Tyr-Pro and others in the process of unblocking of Fmoc-group in alkaline medium using Wang-resin the diketopiperazines are formed [4]. The authors recommend using of chlorotrytyl resin for this type of sequences. That's why we changed our strategy and used cholotrytyl resin for synthesis of target peptides. Thus, we synthesize the first two peptide H-Val-Arg-Asp(drug molecule)-Pro-Pro-Pro-OH and H-Val-Arg-Glu(drug molecule)-Pro-Pro-Pro-OH. Compounds were synthesized according to the following scheme:

Strategy I

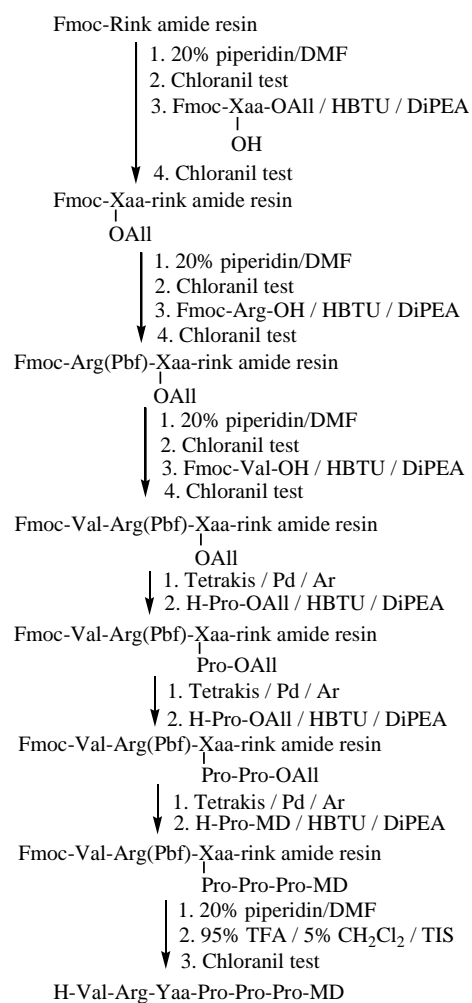
Since in our opinion the incorporation of drug molecule in the middle of the peptide fragment could lead to distortions of secondary and tertiary structure of the peptide, and hence the loss of its membrane penetrating properties, we decided to realize the synthesis of these peptides, but linking drug molecules to their C-terminus. For this purpose, was used strategy II.

Strategy II

Again, we replaced the amino acid Leu in the structure of SAP with Gln and Asn using an original strategy for the synthesis of Gln and Asn – containing peptides previously created by us, assuming adequately protected Glu and Asp and connect them to the Rink amide resin [5]. For this purpose the connection of peptide and resin is made by COOH functions in a side chain of Glu and Asp. Typical of Rink amide resin is that the final peptide unblocking leads to the amides obtaining. Thus using Glu and Asp as starting amino acids, in the final peptides they become to Gln and Asn. Reactions were conducted according to the following scheme 2:



Scheme 1. SPPS of peptides H-Val-Arg-Asp(drug molecule)-Pro-Pro-Pro-OH and H-Val-Arg-Glu(drug molecule)-Pro-Pro-Pro-OH, where Xaa = Asp or Glu and MD = medical drug



Scheme 2. Synthesis of H-Val-Arg-Asn-Pro-Pro-Pro-drug molecule and H-Val-Arg-Gln-Pro-Pro-Pro-drug molecule, where Yaa = Asn or Gln, and MD = medical drug

CONCLUSION

We synthesized 4 new peptides analogues of SAP with potential cell penetrating properties. A new interesting strategy for synthesis of Gln and Asn containing peptides starting from Glu and Asp and using Rink amide resin was applied for the synthesis of two of the target peptides. The biological investigations on the cell penetrating properties of newly synthesized peptides are in the progress.

Acknowledgements: This work is realized by financial support of project 10911 with Scientific Research Centre of UCTM.

REFERENCES:

1. L. Vezekov, M. Maynadier, J.-F. Hernandez, M.-C. Averlant-Petit, O. Fabre, E. Benedetti, M. Garcia, J. Martinez, M. Amblard, *Bioconjugate Chem.* **21**, 1850 (2010)
2. http://en.wikipedia.org/wiki/Cell-penetrating_peptide.
3. J. Fernandez-Carneado, M.J. Kogan, S. Castel, E. Giralt, *Angew. Chem. Int. Ed.* **43**, 1811 (2004).
4. P. M. Fischer, *J. Peptide Sci.*, **9**, 9 (2003).
5. I. Minchev, D. Danalev, L. Vezekov, L. Nikolaeva-Glomb, A. Galabov, *Inter. J. Pept. Res. Therap.*, **16**, 233 (2010)..

СИНТЕЗ НА НОВИ ХИБРИДНИ МОЛЕКУЛИ ВКЛЮЧВАЩИ МЕМБРАННО ПРОНИКВАЩИ ПЕПТИДИ И ЛЕКАРСТВЕНИ МОЛЕКУЛИ

Д.Л. Даналев^{а*}, Р.Н. Райкова^а, Д.А. Маринкова^а, Л.К. Йотова^а, С.Г. Байрямов^б, Б.Х. Христова^а, В.С. Стоянова^а

^а)Химикотехнологичен и металургичен университет, катедра „Биотехнология“, 1756 София

^б)Русенски Университет “Ангел Кънчев”, катедра “Ремонт, надежност и химични технологии”, 7017 Русе

Постъпила на 10 юни, 2012 г.; приета на 3 август, 2012 г.

(Резюме)

През 1988 е отрито забележителното свойство на група пептиди да преминават през клетъчната мембрана, независимо от мембранните рецептори. Те предизвикват промени в мембраната, водещи до поява на пропускливост. Тези молекули са наречени мембранно проникващи пептиди (СРР). Един представител на тази група съединения е т.нар. „sweet agrow” пептид (SAP). В тази работа ние докладваме синтезата на 4 аналога на SAP. Описани са и някои интересни подходи за синтез на пептиди включващи Asp и Gln изхождайки от съответстващите им киселини Glu и Asp, свързани към Rink амиден твърдофазен носител.

Computer modeling of ligand-receptor interactions – enkephalin analogues and delta-opioid receptor

T. Dzimbova*¹, R. Mavrevski², N. Pencheva², T. Pajpanova¹, P. Milanov^{2,3}

¹Institute of Molecular Biology, Bulgarian Academy of Sciences, Bulgaria, 1113 Sofia

²South-West University "Neofit Rilski", Bulgaria, 2700 Blagoevgrad

³Institute of Mathematics and Informatics, Bulgarian Academy of Sciences, Bulgaria, 1113 Sofia

Received June 10, 2012; accepted July 26, 2012

Since, Hughes determined endogenous opioid pentapeptides – enkephalins, large number of synthetic analogues were prepared. Many analogues of enkephalins were synthesized by our group in addition. In our previous study we established a relationship between the replacement in position 2 in endogenous enkephalins and their δ -opioid receptor selectivity.

Computer modeling was used in this study to analyze binding affinity of a series of δ -opioid selective enkephalin analogues to the model of δ -opioid receptor, published in PDB (id: 1OZC). MolDoc SE algorithm implicated in the software program Molegro Virtual Docker was used.

Basing on docking results was established that: 1) all enkephalin analogues have good binding affinity to δ -opioid receptor by forming H-bonds with specific amino acid residue in the receptor pocket; and 2) the rank of the derivatives obtained with this approach is rather different compared with the rank of their biological *in vitro* assay activity. These results reveal further steps for the computer modeling of selective enkephalin analogues such as: 1) development of a novel optimization procedure; and 2) application of a different algorithm and software.

Key words: enkephalins, delta-opioid receptor, computer modeling, docking

INTRODUCTION

It is well established that there are at least three major opioid receptor types in the brain and periphery. These receptors are referred to as μ -, δ -, and κ -opioid receptor and have distinct pharmacological profiles, anatomical distribution, and functions [1–4]. [Met⁵]- and [Leu⁵] – enkephalins have high affinities for δ -opioid receptors. Many analogues of enkephalins were synthesized and their biological activity was evaluated, in order to establish selective ligand to δ -opioid receptor (DOR) [5–8]. This process is time consuming, very expensive and it involves many specialists: chemists, biologists, and medics. Computational approach is innovative and rational method, in which chemical synthesis and biological screening is replaced by virtual screening. It makes possible screening a huge number of compounds in a short period of time in a low cost. Therefore, the target of our work is the DOR.

Here we present a computer assisted modeling of ligand – receptor interactions, in our case δ -opioid selective ligands with DOR. Our aim is to

check the reliability of three dimensional (3D) models of the DOR using the experimental data obtained with *in vitro* assay and the parameters calculated from docking approach.

METHODOLOGICAL APPROACHES

1. Objects/Ligands:

DPDPE ([D-Pen^{2,5}]-enkephalin, selective δ -opioid receptor agonist) [5];

endogenous opioid pentapeptides ([Leu⁵]- and [Met⁵]-enkephalin) and their analogues are presented in Table 1 [5–8].

Table 1. Ligands used in our study.

Ligand	Primary structure
DPDPE	Tyr-D-Pen-Gly-Phe-D-Pen
[Leu ⁵]-enk	Tyr-Gly-Gly-Phe-Leu
[Met ⁵]-enk	Tyr-Gly-Gly-Phe-Met
[Cys(Bzl) ² , Leu ⁵]-enk	Tyr-Cys(Bzl)-Gly-Phe-Leu
[Cys(Bzl) ² , Met ⁵]-enk	Tyr-Cys(Bzl)-Gly-Phe-Met
[Cys(O ₂ NH ₂) ² , Leu ⁵]-enk	Tyr-Cys(O ₂ NH ₂)-Gly-Phe-Leu
[Cys(O ₂ NH ₂) ² , Met ⁵]-enk	Tyr-Cys(O ₂ NH ₂)-Gly-Phe-Met
[DCys(O ₂ NH ₂) ² , Leu ⁵]-enk	Tyr-D-Cys(O ₂ NH ₂)-Gly-Phe-Leu
[DCys(O ₂ NH ₂) ² , Met ⁵]-enk	Tyr-D-Cys(O ₂ NH ₂)-Gly-Phe-Met
[HCys(O ₂ NH ₂) ² , Leu ⁵]-enk	Tyr-HCys(O ₂ NH ₂)-Gly-Phe-Leu
[HCys(O ₂ NH ₂) ² , Met ⁵]-enk	Tyr-HCys(O ₂ NH ₂)-Gly-Phe-Met

Target: human δ -opioid receptor (DOR), published in PDB (id: 1OZC), [9].

* To whom all correspondence should be sent:
E-mail: tania_dzimbova@abv.bg

2. Docking Procedure

To apply the docking procedure we postulated the following assumptions:

Opioid receptors (ORs) belong to “G-Protein Coupled Receptors (GPCRs)” which have structural similarity with the bacteriorhodopsin. Because the receptor is located in the membrane, 3D structures of GPCRs are unknown. In the absence of crystallographic data, indirect methods, which include site-directed mutagenesis, chimeric studies, the substituted cysteine accessibility method, and affinity labeling studies, have been instrumental in locating key contacts for molecular recognition [10]. As a target of our docking procedure we used model of human DOR, published in PDB (id: 1OZC), [9]. It was found that there are several key amino acid residues which are responsible for ligand binding. First very important residue is aspartate in *trans* membrane helix III. It is conserved among all biogenic amine receptor families. The role of this residue is to bind a free amino group of the ligand. Since the structurally similar phenolic group is often essential for opiate and opioid activity [11], it was believed that the formation of a hydrogen bond might be important for the recognition processing of the opioid receptor family as well. Histidine (His) residue in helix V is very important for hydrogen-bond formation with opioid phenol of Tyr residue. In key positions DOR has Trp in helix VI and Leu in Helix VII.

Basing on these assumptions, ligands were evaluated by external electrostatic interactions and external hydrogen-bond formation, during docking procedure. MolDoc SE algorithm [12] was used with 10 runs for each ligand with energy minimization and hydrogen-bond optimization after docking. Five poses for each ligand were generated. Because receptor did not contain any cavity, procedure of docking was made four times with different constrains, in fact they were four different amino acid residues in binding site of receptor – Asp128, Trp274, His278 and Leu300.

3. Computational tools

In this study we used a model of DOR, published in PDB (id: 1OZC, [9]). Docking studies were performed using Molegro Virtual Docker, run on Windows operating system. Visualizations of enkephalins, enkephalin analogues and of docking poses were made and analyzed on Molegro Molecular Viewer, and evaluation function for efficacy of docking of the ligand and receptor is the following:

$$E_{score} = E_{inter} + E_{intra},$$

where E_{score} is a docking scoring function, E_{inter} – ligand-protein interaction energy, and E_{intra} – internal energy of the ligand [12]. Values of the scoring function and its components were presented in Table 2.

4. Correlations

In order to find relationship between sets of data derived from in vitro assay and docking results, we tried to predict it with a help of the Spearman correlation, using GraphPad Prism 3.0. Spearman's rank correlation coefficient is a non-parametric measure of statistical dependence between two variables. It assesses how well the relationship between two variables can be described using a monotonic function. If there are no repeated data values, a perfect Spearman correlation of +1 or –1 occurs when each of the variables is a perfect monotone function of the other. To interpret Spearman, for values of r_s of 0.9 to 1, the correlation is very strong; between 0.7 and 0.89, correlation is strong; between 0.5 and 0.69, correlation is moderate; between 0.3 and 0.49, correlation is moderate to low; between 0.16 and 0.29, correlation is weak to low; and below 0.16, correlation is too low to be meaningful [13]. It can be calculated by the equation:

$$\rho = 1 - \frac{6 \sum d_i^2}{n(n^2 - 1)},$$

where differences $d_i = x_i - y_i$ between the ranks of each observation on the two variables are calculated, and n is the number of the variables in each set.

RESULTS

1. Docking results

Docking program generates five pose for each analogue. Total energy of the ligand-receptor complex was calculated and hydrogen-bond interactions were evaluated.

Analyzing these docking results, we choose the best pose for each ligand with the lowest value of the scoring function. The data are presented in Table 2. The range of the values obtained was between -137.509 to 41.3876 kcal/mol. The lowest potential energy is characteristic for the complex of DOR with [Leu⁵]-enk and the highest for [Cys(O₂NH₂)², Met⁵]-enk.

Table 2. Ligands in ascending order of the scoring function (E_{score}) obtained with docking.

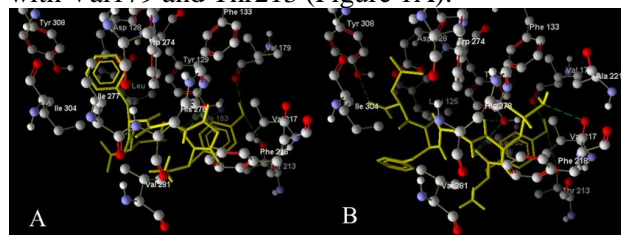
Ligand	E_{score}	E_{inter}	E_{intra} (vdw)
[Leu ⁵]-enk	-137.509	-156.052	82.0781
DPDPE	-127.274	-141.104	71.3263
[Cys(O ₂ NH ₂) ² , Leu ⁵]-enk	-111.597	-157.553	137.362
[DCys(O ₂ NH ₂) ² , Leu ⁵]-enk	-110.925	-161.443	135.278
[DCys(O ₂ NH ₂) ² , Met ⁵]-enk	-109.216	-145.814	87.1034
[Met ⁵]-enk	-107.048	-127.242	85.6935
[Cys(Bzl) ² , Met ⁵]-enk	-90.9322	-171.597	179.634
[Cys(Bzl) ² , Leu ⁵]-enk	-71.2288	-130.887	142.195
[HCys(O ₂ NH ₂) ² , Leu ⁵]-enk	-59.6588	-133.404	303.431
[HCys(O ₂ NH ₂) ² , Met ⁵]-enk	-44.7916	-80.1617	165.299
[Cys(O ₂ NH ₂) ² , Met ⁵]-enk	-41.3876	-104.626	133.122

The data presented in Table 3 concerns the number of hydrogen bonds formed during interaction between DOR and the ligands. DPDPE well-known selective DOR agonist binds to the receptor pocket with four hydrogen bonds: Tyr129 forms 3 H-bonds with 2 NH-groups of peptide backbone and with free NH₂-group of Tyr; and Thr213 with CO group from peptide backbone.

Table 3. H-bonds and interactions between ligand and receptor pocket.

Ligand	Number of hydrogen bonds	Other interactions
DPDPE	4	no
[Leu ⁵]-enk	3	no
[Met ⁵]-enk	2	Salt bridge
[Cys(Bzl) ² , Leu ⁵]-enk	3	π - π Trp274 – Phe
[Cys(Bzl) ² , Met ⁵]-enk	2	π - π Phe218 – Phe
[Cys(O ₂ NH ₂) ² , Leu ⁵]-enk	3	π - π Trp274 – Tyr, SO ₂ NH ₂ – Asp128, Tyr308
[Cys(O ₂ NH ₂) ² , Met ⁵]-enk	4	π - π Phe218 – Tyr, SO ₂ NH ₂ – Thr213, Val179
[DCys(O ₂ NH ₂) ² , Leu ⁵]-enk	6	2SO ₂ NH ₂ – Tyr308
[DCys(O ₂ NH ₂) ² , Met ⁵]-enk	3	SO ₂ NH ₂ – Tyr129
[HCys(O ₂ NH ₂) ² , Leu ⁵]-enk	5	π - π Phe222 – Phe, SO ₂ NH ₂ – Tyr129
[HCys(O ₂ NH ₂) ² , Met ⁵]-enk	3	SO ₂ NH ₂ – His278

In the case of [Leu⁵]-enk there are 3 H-bonds: Tyr129 with CO-group from peptide backbone and Tyr interact with the receptor by forming H-bonds with Val179 and Thr213 (Figure 1A).

**Fig. 1.** Interactions in the binding pocket of DOR with: A) [Leu⁵]-enkephalin and B) [DCys(O₂NH₂)², Leu⁵]-enkephalin

[Met⁵]-enk bind to the receptor pocket by forming two H-bonds: Asp128 with NH₃ of Tyr and His278 with Tyr. Additionally it forms the salt bridge with COO⁻ of Asp128 and NH₃⁺ of Tyr.

In the case of [Cys(Bzl)²] analogues of [Leu⁵] and [Met⁵]-enkephalins, π - π interactions occur: Phe274 with Phe in [Leu⁵], and Phe218 with Phe in [Met⁵]-analogue. [Cys(Bzl)², Leu⁵]-enk forms three H-bonds in DOR pocket – OH group of Tyr forms H-bonds with Val179 and Thr213, and COOH group of Leu with Tyr308. [Cys(Bzl)², Met⁵]-enk binds receptor with two H-bonds – Tyr129 with NH from peptide backbone and Val217 with OH of Tyr.

Complex of [Cys(O₂NH₂)², Leu⁵]-enk with DOR has relatively high total potential energy but it binds very strong to the receptor pocket by three H-bonds (SO₂NH₂ with Asp128, Tyr308 and Tyr129 with NH from peptide backbone) and π - π interaction (Trp274 with Tyr).

[Cys(O₂NH₂)², Met⁵]-enk binds to the receptor with four H-bonds. SO₂NH₂ interact with Thr213, Val179, Tyr129 – with NH group from peptide backbone, and His278 – with OH group of Tyr. Additionally π - π interaction occurs between Phe218 and Tyr rings.

The data with [DCys(O₂NH₂)², Leu⁵]-enk are very different. It forms six H-bonds with the amino acid residues in the receptor pocket. The interactions are as follows: Tyr129 forms two H-bonds with CO groups from peptide backbone, Val179 and Thr213 with OH group of Tyr residue, Val217 with SO₂NH₂, and Tyr308 with COOH group of Leu (Figure 1B).

In the case of [DCys(O₂NH₂)², Met⁵]-enk just three hydrogen bonds are formed: Tyr129 – CO from backbone, Ile304 – OH (Tyr), and Tyr308 – OH (Tyr).

[HCys(O₂NH₂)², Leu⁵]-enk forms five H-bonds with receptor pocket. Tyr128 interacts with OH group of Tyr, Ile304 with free NH₃ group, Tyr308 forms two H-bonds with SO₂NH₂ group and one with NH group from peptide backbone. Between Phe222 and Phe rings π - π interaction is established.

The complex [HCys(O₂NH₂)², Met⁵]-enk – DOR is formed with three H-bonds: OH group of Tyr interact with Val179 and Thr213, and SO₂NH₂ group with His278.

2. Correlations

The Spearman's correlation coefficients for all correlations within data obtained with *in vitro* assay and docking are in the range from -0.1545 to 0.1455 for E_{intra}/K_A correlation and E_{inter}/IC_{50} correlation, respectively. For example, correlation

of IC_{50} and E_{score} is presented on Figure 2. The Spearman's correlation coefficient is 0.1091. This low value shows that the correlation between E_{score} and IC_{50} value is very low.

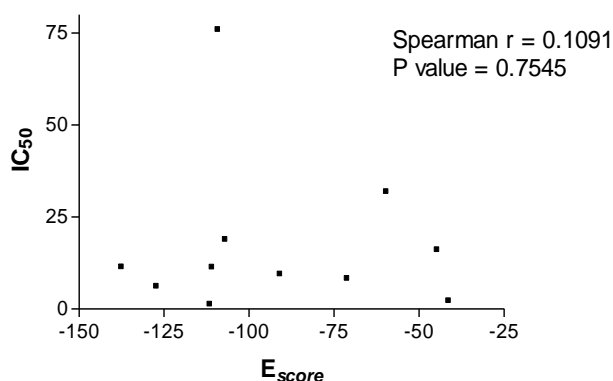


Fig. 2. Figure 2. Spearman correlation for E_{score} and IC_{50} values.

DISCUSSION

The substitution in second position in the enkephalin structures with amino acid containing SO_2NH_2 increases additionally the binding of the respective analogue to DOR.

The incorporation in position 2 in the enkephalin molecules of Cys(Bzl) does not interfere on their ability to bind to DOR. So, additional interaction due to Bzl group does not appear. Total potential energies of their complexes are similar to the endogenous enkephalin complexes with DOR and number of H-bonds formed is the same.

It appears that Tyr129 is very important amino acid residue in receptor pocket, because ligands interact with this residue. It is able to form H-bonds with its OH group and different functional groups of ligands, such as: OH group of Tyr, NH and CO groups of peptide backbone, and SO_2NH_2 group of amino acid analogue in position 2.

Docking data obtained allow characterizing some structural and chemical properties of the investigated analogues. The results of *in vitro* studies of [Leu⁵]- and [Met⁵]-enkephalins and their analogues obtained previously were summarized in Table 4. In this table IC_{50} corresponds to the potency of the ligands, the affinity and efficacy are presented by K_A and e_{rel} , respectively. Calculation of the parameters of *in vitro* experiments did not concern directly 3D structure of the receptors. However, in docking procedure 3D structure is the main tool. In this study we applied 3D model of DOR, published in PDB (id: 1OZC).

The ranking of the compounds based on their *in vitro* assay or docking data are rather different because the correlations between them were not

Table 4. IC_{50} , K_A and e_{rel} obtained *in vitro* [12].

Ligand	Mouse vas deferens IC_{50} (nM)	K_A (nM)	e_{rel}
DPDPE	6.18±1.17	180±35	30.2±10.0
[Leu ⁵]-enk	11.45±2.06	54.9±13.1	5.8±1.0
[Met ⁵]-enk	18.91±2.15	48.4±7.5	3.6±0.3
[Cys(Bzl) ² , Leu ⁵]-enk	8.30±1.40	68.5±29.7	9.3±3.2
[Cys(Bzl) ² , Met ⁵]-enk	9.53±1.20	23.8±3.0	3.5±0.3
[Cys(O ₂ NH ₂) ² , Leu ⁵]-enk	1.29±0.31	36.4±16.4	29.2±9.5
[Cys(O ₂ NH ₂) ² , Met ⁵]-enk	2.22±0.45	14.1±5.4	7.3±2.0
[DCys(O ₂ NH ₂) ² , Leu ⁵]-enk	11.40±2.01	73.4±12.7	7.4±1.9
[DCys(O ₂ NH ₂) ² , Met ⁵]-enk	75.96±11.67	463±161	7.1±1.8
[HCys(O ₂ NH ₂) ² , Leu ⁵]-enk	31.92±5.10	76.4±7.1	3.4±0.2
[HCys(O ₂ NH ₂) ² , Met ⁵]-enk	16.09±1.90	55.7±6.1	4.5±0.3

established, including between E_{score} and IC_{50} . This fact shows that the increasing of the potency (IC_{50}) of the derivatives does not lead to increasing or decreasing of the value of the scoring function, obtained with docking.

Obviously for this kind of investigations on ligand – target interactions a novel optimization procedure has to be initiated in further studies. Since we obtained a set of parameters with docking or with *in vitro* bioassay, probably multi-dimensional vectors have to be introduced, such as two-dimensional vector (K_A , e_{rel}) or three-dimensional vector (IC_{50} , K_A , e_{rel}). In the same way docking results could be presented not only with one but with several scoring functions and the vector would be with the following elements - E_{score} , E_{inter} , E_{intra} .

In these two sets of vectors for *in vitro* and docking studies, respectively, it is possible to introduce a partial order, so that these sets become partially ordered sets. Analysis and comparison of maximal elements in the ordered sets could help to understand better the relationship between *in vitro* biological effects and docking studies and to answer whether the models of the biological macromolecules (in our case δ -opioid receptor) correspond to the real 3D structure.

CONCLUSIONS

Basing on docking results obtained with Molegro Virtual Docker it was established that all enkephalin analogues have good binding affinity to δ -opioid receptor. All of the ligands interact by forming many H-bonds with the receptor. Additional interaction between receptor and ligand appears in the case of analogues substituted with amino acid containing SO_2NH_2 group. This study

could not give a definitive answer if the 3D model of DOR corresponds to the real receptor, because there is no correlation between values obtained *in vitro* and docking results.

ACKNOWLEDGMENTS. This work was supported by NFSR of Bulgaria project DVU 01/197 and COST Action CM0801 project DO 02-135/31.07.2009.

REFERENCES

- 1 P.L. Wood, *Neuropharmacology*, **21**, 487 (1982).
- 2 E.J. Simon, *Med. Res. Rev.*, **11**, 357 (1991).
- 3 R.A. Lutz, H.P. Pfister, *J. Recept. Res.*, **12**, 267 (1992).
- 4 A. Mansour, S.J. Watson, in *Opioid I* (Herz, A., ed) Springer-Verlag, Berlin, pp. 79-106 (1993).
- 5 J.A. Clark, Y. Itzhak, V.J. Hruby, H.I. Yamamura, G.W. Pasternak, *Eur. J. Pharmacol.*, **128**, 303 (1986).
- 6 N. Pencheva, L. Vezekov, E. Naydenova, P. Milanov, T. Pajpanova, S. Malamov, L. Bojkova, *Bulg. Chem. Commun.*, **33**, 47 (2001).
- 7 N. Pencheva, J. Pospíšek, L. Hauzerova, T. Barth, P. Milanov, *Br. J. Pharmacol.*, **128**, 569 (1999).
- 8 N. Pencheva, P. Milanov, L. Vezekov, T. Pajpanova, E. Naydenova, *Eur. J. Pharmacol.*, **498**, 249 (2004).
- 9 F.M. Décaillot, K. Befort, D. Filliol, S. Yue, P. Walker, B.L. Kieffer, *Nat. Struct. Biol.* **10**, 629 (2003).
- 10 B. Kane, B. Svensson, D. Ferguson, *The AAPS Journal* **8**, Article 15 (2006)
- 11 G. Lenz, S. Evans, D. Walters, A. Hopfinger, *Opiates*, Orlando, FL: Academic Press (1986).
- 12 R. Thomsen, M.H. Christensen, *J. Med. Chem.*, **49**, 3315 (2006).
- 13 B. Ratner, *Statistical Modeling and Analysis for Database Marketing: Effective Techniques for Mining Big Data*, Chapman and Hall (2003).

КОМПЮТЪРНО МОДЕЛИРАНЕ НА ВЗАИМОДЕЙСТВИЕТО ЛИГАНД-РЕЦЕПТОР – ЕНКЕФАЛИНОВИ АНАЛОЗИ И ДЕЛТА-ОПИОИДЕН РЕЦЕПТОР

Т. Дзимбова¹, Р. Мавревски², Н. Пенчева², Т. Пайпанова¹, П. Миланов^{2,3}

¹Институт по молекулярна биология „Акад. Р. Цанев“, БАН, 1113 София

²Югозападен университет „Н. Рилски“, 2700 Благоевград

³Институт по математика и информатика, БАН, 1113 София

Постъпила на 10 юни, 2012 г.; приета на 26 юли, 2012 г.

(Резюме)

След определяне на ендогенните опиоидни пептиди – енкефалини от Hughes, са синтезирани голям брой техни синтетични аналози. Нашата група е синтезирала много и различни аналози на енкефалините. В предишно наше изследване е установена връзката между заместванията във втора позиция в ендогенния енкефалин и тяхната селективност по отношение на δ -опиоидния рецептор.

С цел установяване на връзката структура – биологично действие на енкефалинови аналози и δ -опиоидният рецептор е използван докинг. Тъй като липсват кристалографски данни за структурата на δ -опиоидният рецептор, използвахме публикуваният в PBD (id: 1ozc) модел. Използван е MolDoc SE алгоритъм, който лежи в основата на Molegro Virtual Docker. Като лиганди бяха използвани енкефалинови аналози с промяна във втора позиция, за които има данни от *in vitro* изследвания.

В резултат на докинга с получени следните резултати: 1) всички енкефалинови аналози се свързват добре с δ -опиоидния рецептор, като образуват много водородни връзки; 2) подреждането на производните, получено с помощта на докинга, е различно от подреждането им при *in vitro* тестовете. Тези резултати изискват по-нататъшна оптимизация на процедурата за докинг, както и промяна на алгоритъмът и софтуера.

Neuropeptides and urinary bladder ischemia-reperfusion injury

R. Kalfin^{1*}, E. Leventieva-Necheva¹, G. Sgaragli², F. Pessina²

¹Institute of Neurobiology, Bulgarian Academy of Sciences, Acad. G. Bonchev St., Block 23, Sofia 1113, Bulgaria

²Department of Neuroscience, Siena University, Siena, Italy

Received June 10, 2012; accepted July 26, 2012

Urinary bladder decompensation following partial bladder obstruction is directly related to decreased tissue perfusion, resulting in periods of hypoxia and ischemia. Hence, it is important to look for substances which could counteract against the ischemia/reperfusion- induced neuronal damage in detrusor muscle and in such a way to ameliorate the functional disorders of urinary bladder. Many neuropeptides have been found to be synthesized, stored and released in the lower urinary tract. Some of them were reported to reduce ischemia-reperfusion injury. The purpose of this study was to examine the efficacy of vasoactive intestinal peptide (VIP), somatostatin and Sandostatin[®] (Novartis) to counteract the damage suffered by neurons in urinary bladder exposed *in vitro* to experimentally induced ischemia-reperfusion in guinea-pig. We found that VIP (0.3 μ M), somatostatin (300 nM) and sandostatin (1 to 300 nM) improved significantly the response to electrical field stimulation during reperfusion as compared to the control, untreated tissues. The antioxidant activity of VIP, somatostatin and sandostatin, assessed as their capability to scavenge peroxy radicals during linoleic acid oxidation corresponded to 6.4 ± 0.1 , 6.7 ± 0.3 and 7.0 ± 0.6 , respectively. The antioxidant activity of the above mentioned peptides could underlie their neuroprotective action during reperfusion, when a significant amount of free radicals has been formed.

Key words: urinary bladder, vasoactive intestinal peptide, ischemia, somatostatin, sandostatin, injury

INTRODUCTION

Many neuropeptides have been found to be synthesized, stored and released in the lower urinary tract. Some of them are released from the peripheral neural terminals of the autonomic nervous system – vasoactive intestinal peptide (VIP), tachykinins (substance P), neuropeptide Y, calcitonin gene-related peptide, neurokinin A. Others are locally synthesized and act by para-/auto and intracrine mechanisms – for example angiotensin II. The functional role of many of these peptides has not been fully established, however they may have a sensory role, efferent function [1, 2] or serve as NANC neurotransmitters and/or neuromodulators in the bladder ganglia or at the neuromuscular junctions. Their actions have been thought to include mediation of the micturition reflex activation, smooth muscle contraction, potentiation of efferent neurotransmission and changes in vascular tone and permeability [3, 4].

Vasoactive intestinal peptide is expressed in the neural pathways regulating the lower urinary tract. VIP-immunoreactivity is present in afferent and autonomic efferent neurons innervating the bladder

and urethra. In the human urinary bladder neck VIP-containing nerve fibres localized close to noradrenergic and cholinergic intramural neurons have been identified. In both types of nerve, VIP co-localizes with other transmitters, such as calcitonin gene-related peptide, neuropeptide Y, substance P, nitric oxide [5, 6]. Recently, the peptide somatostatin was found to be distributed in the sensory dorsal root ganglia neurons supplying porcine urinary bladder [7]. Sensory nerves, particularly the nociceptive nerves, may send collaterals to the smooth muscle, to the intramural ganglia and to the ganglia of the pelvic plexus [8]. This may be of great importance for the development of the unstable detrusor muscle in the urinary bladder.

Bladder outlet obstruction generally due to prostatic hyperplasia, a common problem in men over 60 years of age, is a major urologic problem that has been the subject of many clinical and experimental studies. The hyperplasia of prostate leads to obstructed micturition, during which occurs periodic bladder ischemia. The latter has been suggested to result in the partial denervation of the detrusor smooth muscle through ischemia and reperfusion injury to the post-ganglionic parasympathetic neurons within the bladder wall [9]. Previous investigations showed that *in vitro*

* To whom all correspondence should be sent:
E-mail: reni_kalfin@abv.bg

ischemia-like conditions were more damaging to the nervous tissue than to the detrusor muscle [10]. Hence, it is important to look for substances which could counteract against the ischemia/reperfusion-induced neuronal damage in detrusor muscle and in such a way to ameliorate the functional disorders of urinary bladder.

It was demonstrated that the urinary bladder neuromodulator vasoactive intestinal peptide possesses the ability to scavenge oxygen free radicals and to reduce the intracellular calcium overloading in ischemic and reperfused heart [11]. Somatostatin-14 and particularly its stable analogue, the cyclic octapeptide Sandostatin[®], are known to exert cytoprotective activities in peripheral tissues and in neuronal cells [12, 13]. The somatostatin peptides were also shown to afford protection against neuronal damage caused by experimentally induced cerebral ischemia in rats [10], to limit intestinal ischemia-reperfusion injury in macaques via suppression of NF-kappaB cytokine pathway [14], and to ameliorate ischemia-reperfusion injury through the early induction of heme oxygenase [15].

The purpose of this study, therefore, was to examine the efficacy of VIP, somatostatin and sandostatin, to counteract the damage suffered by neurons in urinary bladder exposed in vitro to experimentally induced ischemia-reperfusion injury.

EXPERIMENTAL METHODS

Male guinea-pigs (300–500 g, Charles River) were anaesthetised with Ketavet and sacrificed by cervical dislocation. The animals were treated in accordance with European Commission standards concerning the care and use of laboratory animals. The urinary bladders and part of the urethra were removed and placed in oxygenated (95% O₂ and 5% CO₂) cold Krebs solution. The ureters were tied off using silk ligatures. The prostate gland was excised to expose the urethra and the bladder emptied. The urethra was secured to a stainless-steel tube (8 mm long, 2.5 mm diameter) sealed to a glass J-shaped tube that was connected by a three-way valve to a compensated pressure transducer. The organ was filled with 2 ml oxygenated glucose-free Krebs solution at 37°C and suspended in an insulated, 100-ml isolated organ bath containing Krebs solution maintained at 37°C and equilibrated with 95% O₂ and 5% CO₂. Silver plate electrodes on either side of the bladder connected to a Grass S48 stimulator enabled electrical field stimulation (EFS) of intrinsic nerves. Isometric contractions

were evoked by EFS using 5-s trains of square pulses (20 Hz, 1 ms pulse width, 70 V) delivered at 10-min intervals. After a minimum equilibration period of 40 min the bladder was exposed to 10 μM carbachol for about 5 s to test the contractile ability of the tissue. After 30 min recovery from carbachol exposure, the intrinsic nerves were stimulated selectively every 10 min (as described above) until the response was reproducible. Ischemia-like conditions (1 h) were achieved by replacing the gas mixture with 95% N₂ and 5% CO₂ (anoxia) and the organ bath solution with glucose-free Krebs solution (glucopenia). Recovery in normal Krebs solution was then allowed for 2 h. EFS was applied every 10 min during both anoxia-glucopenia and recovery. During the recovery period the Krebs solution was changed every 30 min. Carbachol (10 μM) was applied again at the end of the experiment.

All tested compounds at different final concentrations were added to the Krebs solution during the entire period of ischemia and the first 30 min of reperfusion. The EFS responses obtained in the presence of the tested compounds were compared with those in their absence (control). Control experiments (25% of all experiments) were performed in a randomised manner during the study.

Results are given as means ± SEM. The significance of differences between means was assessed by one-way analysis of variance (ANOVA) followed by Dunnett's test for multiple comparisons, $P < 0.05$ was considered significant. Areas under the curve (AUC) relating muscle contraction to time were calculated for ischemia and re-perfusion conditions separately, using appropriate software (Prism v. 3.03, GraphPad, San Diego, California, USA).

RESULTS AND DISCUSSION

The response to electrical field stimulation (EFS) declined rapidly in the combined absence of oxygen and substrate (ischemia-like condition), and was abolished within an hour (Fig. 1 and Fig. 2). After reintroduction of normal conditions, the recovery of the response to electrical field stimulation (neurogenic response) in control bladders was poor, reaching in 2 hours a maximum of about 25 % of the initial response (Fig. 1 and Fig. 2). At this time, however, the response of the muscle to carbachol had fully recovered (data not shown). To see if somatostatin and Sandostatin[®] could partially reduce the nerve damage described above, the peptides have been perfused during

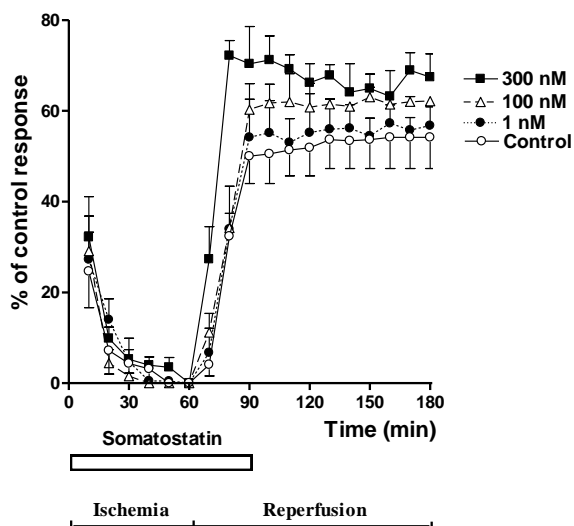


Fig. 1. Electrical field stimulation-induced contractile responses of guinea-pig whole urinary bladder subjected to 60 min of ischemia and subsequent 120 min of reperfusion. Experiments were carried out in the absence or presence of the peptide somatostatin, applied for the first 90 min. Results are expressed as mean \pm SEM of six urinary bladders ($n = 6$).

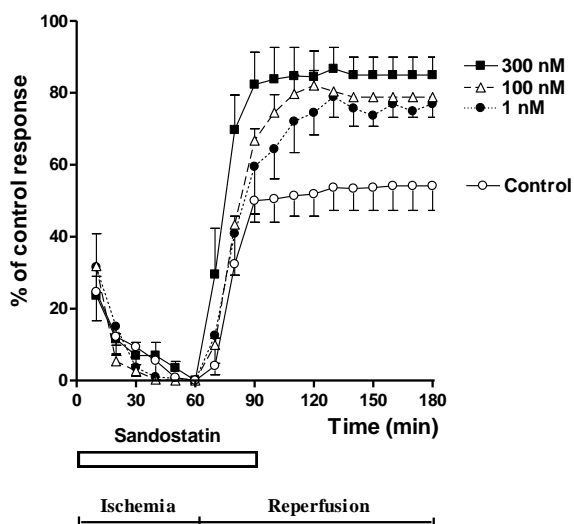


Fig. 2. Electrical field stimulation-induced contractile responses of guinea-pig whole urinary bladder subjected to 60 min of ischemia and subsequent 120 min of reperfusion. Experiments were carried out in the absence or presence of the peptide Sandostatin®, applied for the first 90 min. Results are expressed as mean \pm SEM of six urinary bladders ($n = 6$).

ischemia and the first 30 min of reperfusion, as it is supposed that the major damage to the tissue develops not only during ischemia, but also at the beginning of reperfusion when free radicals are being formed intensively. Sandostatin® at 1, 100 and 300 nM improved significantly the EFS-induced contractile response in reperfusion phase as compared to untreated control bladders ($n = 6$, $P < 0.01$) (Fig. 3B).

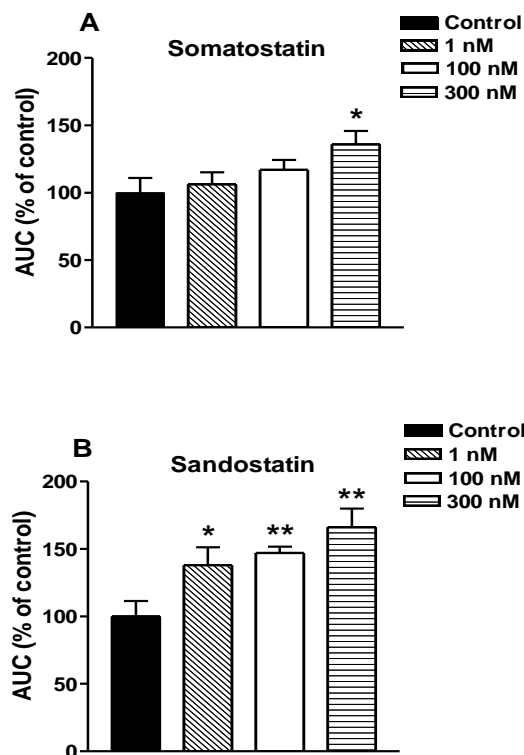


Fig. 3. Electrical field stimulation-induced contractile responses of guinea-pig whole urinary bladder subjected to 60 min of ischemia and subsequent 120 min of reperfusion. Experiments were carried out in the absence or presence of peptides somatostatin (A) or Sandostatin® (B), applied for the first 90 min. Results are expressed as mean of area under curve (AUC) \pm SEM of six experiments in each group. Differences were evaluated by one-way ANOVA followed by Dunnett's *post hoc* comparison test (* $P < 0.05$ and ** $P < 0.01$ versus control; $n = 6$).

Somatostatin at concentrations of 1 and 100 nM did not exert significant effect as compared to the control (Fig. 1, Fig. 3A) while at 300 nM it increased the recovery of contractile response during reperfusion ($n = 6$, $P < 0.05$) (Fig. 3A).

The antioxidant activity of the peptides was assessed for their capability to prevent linoleic acid peroxidation. Both vasoactive intestinal peptide, somatostatin and Sandostatin® exhibited remarkable antiperoxidant activity with a pIC_{50} M values of 6.4 ± 0.1 ; 6.7 ± 0.3 and 7.0 ± 0.6 , respectively (Table 1).

Ischemia, reperfusion, and subsequent free radical damage have been implicated in many voiding disorders. The structure and function of detrusor smooth muscle may be altered by a series of noxae including hypoxia, over distension,

Table 1 Inhibition of lipid peroxidation

Antioxidant	IC ₅₀ (mM) ± SEM	pIC ₅₀ (mM) ± SEM
DTBHA	0.088 ± 0.006	7.1 ± 0.5
Sandostatin®	0.097 ± 0.011	7.0 ± 0.6
Somatostatin	0.164 ± 0.019	6.7 ± 0.3
Vasoactive intestinal peptide	0.380 ± 0.008	6.4 ± 0.1
BHA	0.428 ± 0.005	6.3 ± 0.4
β-TAG	1.040 ± 0.330	6.0 ± 0.4
Propofol	3.100 ± 0.380	5.5 ± 0.3
β-GLU	9.910 ± 2.480	5.0 ± 0.4

diabetes, and ischemia. It was shown that both experimental ischemia and partial outlet obstruction of the urinary bladder induce similar dysfunction with regard to the contractile responses to electrical field stimulation [16]. Previous investigations demonstrated that the response to nerve-mediated stimulation declined rapidly as O₂ and glucose were withdrawn, and recovered only to a limited extent when perfusion with O₂ and glucose started again [17, 16]. We reported that VIP improved this recovery by protecting nervous tissues against anoxia/glucopenia damage [18]. To elicit neuroprotection, however, we incubated the guinea-pig detrusor strips with VIP during the anoxia/glucopenia (i.e. experimental ischemia) phase and the first 30 min of reperfusion. In the last years, increasing evidence has been accumulating that reactive oxygen species (ROS), i.e. hydrogen peroxide (H₂O₂) as well as superoxide anion (O₂⁻) and hydroxyl radical (·OH) generated in greater amounts after reperfusion of the ischemic tissue [19, 20] are important mediators of tissue injury during reperfusion following an ischemic insult. Reactive oxygen species, including the singlet molecular oxygen (¹O₂), by promoting lipid peroxidation can damage cell membranes, causing severe dysfunction with impairment of intracellular Ca²⁺ homeostasis. In turn, increases of intracellular Ca²⁺ concentration during reperfusion following ischemia, may activate a cascade of events, which leads to neuronal cell death [11]. Indeed, it was confirmed that reperfusion results in greater injury than 2 h of ischemia in the rabbit bladder, and that the mechanisms of this injury involve mitochondrial and neuronal damage [21]. The reactive oxygen species burst at the beginning of reperfusion and cytosolic Ca²⁺ overload are two proposed mechanisms to explain cell injury. It is difficult to separate cause-and-effect relationship between these variables, since ROS by activating kinases upstream may induce Ca²⁺ overload, and both ROS and Ca²⁺ are known to be mediators in

the regulation of mitochondrial permeability transition pore formation [22], a key step in the process of reperfusion injury.

In the present study, a remarkable antioxidant activity of Sandostatin®, somatostatin and vasoactive intestinal peptide has been found, which could underlie their neuroprotective action during reperfusion, when a significant amount of free radicals has been formed. The exact mechanism by which the above mentioned peptides protect the detrusor muscle nerves from reperfusion injury is only a matter of speculation, though a loss of VIP and somatostatin among other sensory neuropeptides in the obstructed human bladder has been previously described [23]. Probably activation of some peptide receptor/receptors is involved in their protective action. Indeed, it was recently reported that activation of somatostatin receptor (sst 5) protects rat retina from neurotoxicity [24], and that changes in VIP and associated receptor transcripts and protein expression in micturition pathways resemble some, but not all, changes observed after induction of urinary bladder inflammation [25]. In summary, the pharmacological action of drug Sandostatin® (Novartis), outlined in the present study, may represent a new therapeutic option for the control of functional disorders of the urinary bladder.

Acknowledgements: This study was supported by Grant DDVU-02-24 from the National Science Fund, Sofia, Bulgaria.

REFERENCES

- 1 G. Burnstock, In: Neurobiology of Incontinence: Innervation of bladder and bowel. Ciba Foundation Symposium vol. 151, 2-26, Chichester, Wiley, 1990.
- 2 A.C. Maggi, *Gen. Pharmacol.*, **22**, 1 (1991).
- 3 A.C. Maggi, *Prog. Neurobiol.*, **45**, 1 (1995).
- 4 M. Hernandez, M.V. Barahona, P. Recio, S. Benedito, A.C. Martinez, L. Rivera, A. Garcia-Sacristan, D. Prieto, L.M. Orensanz, *Br. J. Pharmacol.*, **149**, 100 (2006).
- 5 J.S. Dixon, P.Y. Jen, J.A. Gosling, *J. Anat.*, **190**, 125 (1997).
- 6 S. Arrighi, G. Bosi, F. Cremonesi, C. Domeneghini, *Vet. Res. Commun.*, **32**, 291 (2008).
- 7 A. Bossowska, R. Crayton, P. Radziszewski, Z. Kmiec, M. Majewski. *J. Physiol. Pharmacol.*, **60**, 77 (2009)
- 8 J. Nordling, *Exp. Gerontol.*, **37**, 991 (2002).
- 9 A.F. Brading, *Scand. J. Urol.*, **184**, 51 (1997).
- 10 C. Rauca, K. Schafer, V. Holtt. *Naunyn Schmiedebergs Arch. Pharmacol.*, **360**, 633 (1999).

- 11 R. Kalfin, N. Maulik, R.M. Engelman, G.A. Cordis, K. Milenov, L. Kasakov, D.K. Das, *J. Pharmacol. Exp. Ther.*, **268**, 952 (1994).
- 12 T.F. Hoffmann, E. Uhl, K. Messmer, *Pancreas*, **12**, 286 (1996).
- 13 J.B. Morris, N.H. Guerrero, E.E. Furth, T.A. Stellato. *Am. J. Surg.*, **165**, 676 (1993).
- 14 H. Wu, L. Liu, Q. Tan, C. Wang, M. Guo, Y. Xie, C. Tang, *J. Gastrointest. Surg.*, **13**, 983 (2009).
- 15 T. Takano, Y. Yonemitsu, S. Saito, H. Itoh, T. Onohara, A. Fukuda, M. Takai, Y. Maehara. *J. Surg. Res., Apr.* **19** (2011).
- 16 Y. Zhao, S.S. Levin, A.J. Wein, R.M. Levin, *Urology*, **49**, 293 (1997).
- 17 F. Pessina, G. McMurray, A. Wiggin, A. F. Brading, *J. Urol.*, **157**, 2375 (1997).
- 18 F. Pessina, R. Kalfin, G. Sgaragli, *Eur. J. Pharmacol.*, **423**, 229 (2001).
- 19 C.D. Garcarena, J.C. Fantinelli, C.I. Caldiz, G.C. de Cingolani, I. L. Ennis, N. G. Perez, H. E. Cingolani, S.M. Mosca, *Cell Physiol. Biopchem.* **27**, 13 (2011).
- 20 T. Kunimatsu, K. Kobayashi, A. Yamashita, T. Yamamoto, M.C. Lee, *J. Clin. Neurosci.*, **18**, 545 (2011).
- 21 Y.S. Juan, S.M. Chuang, B.A. Kogan, A. Mannikarottu, C.H. Huang, R.E. Leggett, C. Schuler, R.M. Levin, *Int. Urol. Nephrol.*, **41**, 513 (2009).
- 22 S. Javadov, M. Karmazyn, *Cell Physiol. Biochem.* **20**, 1 (2007).
- 23 C.R. Chapple, P. Milner, H.E. Moss, G. Burnstock, *Br. J. Urol.*, **70**, 373 (1992).
- 24 F. Kiagiadaki, M. Savvaki, K. Thermos, *Neuropharmacology*, **58**, 297 (2010).
- 25 B. Girard, S. Malley, K. Braas, V. May, M. Vizzard, *J. Mol. Neurosci.*, **42**, 378 (2010).

НЕВРОПЕПТИДИ И УВРЕЖДАНЕ НА ПИКОЧНИЯ МЕХУР ВСЛЕДСТВИЕ ИСХЕМИЯ И РЕПЕРФУЗИЯ

Р. Калфин^{1*}, Е. Левентиева-Нечева¹, Дж. Сгарали², Ф. Песина²

¹Институт по невробиология, Българска академия на науките, София 1113

²Катедра по невронауки, Университет в Сиена, Италия

Постъпила на 10 юни, 2012 г.; приета на 26 юли, 2012 г.

Декомпенсацията на пикочния мехур, следваща частичната обструкция, е директно свързана с намаляване на тъканната перфузия, което води до поява на хипоксия и исхемия. Следователно е важно да се търсят субстанции, които намаляват предизвиканото от исхемията и реперфузията увреждане на невроните в детрусорния мускул и по такъв начин да подобрят функцията на пикочния мехур. Установено е, че много неuropeптиди се синтезират, съхраняват и освобождават в долната част на пикочните пътища. Показано е, че някои от тях намаляват увреждането, предизвиканото от исхемия и реперфузия. Целта на настоящата работа беше да се изследва способността на вазоактивния интестинален пептид (ВИП), соматостатина и Сандостатин® (Novartis) да намалят увреждането на невроните при експериментална исхемия и реперфузия в изолиран пикочен мехур от морско свинче при условия ин витро. Установихме, че ВИП (0.3 μ M), соматостатин (300 nM) и сандостатин (1 до 300 nM) подобряват значително електрически-предизвикания съкратителен отговор на пикочния мехур по време на реперфузията в сравнение с този в контролните пикочни мехури. Антиоксидантната активност на ВИП, соматостатин и сандостатин, определяна съобразно тяхната способност да предотвратят пероксидацията на линолеовата киселина, беше съответно 6.4 ± 0.1 , 6.7 ± 0.3 и 7.0 ± 0.6 . Антиоксидантната активност на изследваните пептиди вероятно е в основата на невропротективното им действие по време на реперфузията, когато се образува значително количество свободни радикали.

Angiotensin II and Vasopressin effects on motor activity of rat isolated tissue strips from urinary bladder and rectum

P.V. Hadzhibozheva^{1*}, T.K. Georgiev¹, R.E. Kalfin², A.N. Tolekova¹

¹ Department of Physiology, Pathophysiology and Pharmacology, Medical Faculty, Trakia University, Stara Zagora, Bulgaria

² Institute of Neurobiology, Bulgarian Academy of Sciences, 1113 Sofia, Bulgaria

Received June 10, 2012; accepted July 26, 2012

The purpose of this study was to analyze and compare the force and time-parameters of Angiotensin II (Ang II) and Arginine-Vasopressin (AVP)-provoked contractions on muscle strips from rat urinary bladder and rectum in experiments in vitro. Mature Wistar rats, weighting 250–300g, were used. Longitudinal strips from urinary bladder and rectum were prepared and influenced by Ang II and AVP in a dose of 10^{-6} M. The recorded force-vs.-time curves were analyzed including calculation of amplitudes, area under the curve (AUC) of the smooth muscle contraction, as well as defining of different time-parameters. Ang II and AVP caused urinary bladder tonic contractions with similar amplitudes (1.74 ± 0.27 g and 1.55 ± 0.16 g, respectively) and different AUC. Marked difference was observed in the application of both peptides on strips from rectum. Ang II caused tonic reactions with amplitude of 4.60 ± 0.42 g, while AVP do not change significantly phasic contractions. The time-parameters analysis established an analogy in the developed response to Ang II of both organs. In urinary bladder, the action of Ang II derivatives and the interactions of the two peptides with the ion channels of the plasmalemma might be the reason for the observed differences in the contraction parameters. The similarity in the time-parameters of Ang II-mediated contractions of the bladder and the rectum indicates an analogical mechanism of the development of the contraction. The lack of a rectal tonic response when AVP was applied is probably due to different type of the receptors or modifications in the transductional signal pathway.

Key words: Angiotensin II, Vasopressin, rectum, urinary bladder, time-parameters

INTRODUCTION

The growing incidence of micturition disorders and faecal incontinence focuses attention of many researchers on the study of motor activity of the urinary bladder and the recto-anal segment of gastro-intestinal tract. These two organs have mainly a reservoir and evaquatory functions. The maintenance of their adequate tone is essential for a normal quality of life. The precisely coordinated and complex smooth muscle activity of bladder and rectum is regulated by interplay between neural (somatic and autonomic) and endocrine control mechanisms.

The neuropeptides Angiotensin II (Ang II) and Arginine-Vasopressin (AVP) are important factors in the regulation of the blood vessels tone. Furthermore, there is growing evidence for the involvement of these two peptides in the regulation of the smooth muscle activity outside the vascular system, such as urinary bladder and distal segments of the gastrointestinal tract [1–5].

The physiological role of Ang II for the function of the urinary bladder and the exact mechanism mediating its effects has not been fully revealed. According to experimental data of Anderson and co-workers [6], Ang II has a possible role in the micturition. It is proven that Ang II and its precursor Ang I cause dose-dependent contractions of muscle strips from rat urinary bladder [7], and probably act as modulators in neurotransmission in this organ [1]. There are evidences that Ang II accomplish its physiological effects by binding to AT1 receptors [8], whose number in the membrane of the detrusor smooth muscle cells can vary significantly [9, 10]. AT1 receptors activate phospholipase C (PLC), dihydropyridine-sensitive Ca^{2+} -channels and inhibit adenylyl cyclase, reducing intracellular cAMP [11].

Except the well-known constriction of the vessels, AVP affects the contractility of the urogenital smooth muscle, manifested in experiments with rats [1]. It is proven the presence of V1-receptors in smooth muscle of the urinary bladder, whose binding to AVP also leads to activation of the IP_3 pathway, similarly to binding

* To whom all correspondence should be sent:

E-mail: petia_hadjibojeva@abv.bg

of Ang II to AT1 [12, 13].

There is not enough information in the literature, regarding the exact effects of Ang II and AVP on the recto-anal segment of GIT. Local renin-angiotensin system or parts of it had been found in rat rectum [14]. The role of Ang II had been confirmed in the development of diseases such as internal anal sphincter incontinence [4, 5]. In recent years the significance of AVP as an important regulator of the gastro-intestinal smooth muscle activity is growing [15, 16]. Regarding the tone of the rectal musculature this question remains still opened.

The purpose of this study was to analyze and compare in details the registered Ang II and AVP-provoked contractions in experiments in vitro on muscle strips from rat urinary bladder and rectum.

EXPERIMENTAL METHODS

Sample Preparation

The experiments were performed in the urinary bladder and rectal smooth muscles isolated from adult Wistar rats, weighing 250–300 g. The animals were anesthetized with Nembutal 50mg/kg i.p. and exsanguinated. The experiments were carried out in accordance with the national regulations and the Directive 2010/63/EU of the European parliament and of the Council (22 September, 2010) concerning the protection of animals used for scientific purposes.

Abdominal and pelvic cavity were opened and the urinary bladder and rectum were dissected out and immediately placed in cold Krebs solution (3 °C), containing the following composition (in mmol): NaCl 118.0, KCl 4.74, NaHCO₃ 25.0, MgSO₄ 1.2, CaCl₂ 2.0, KH₂PO₄ 1.2, and glucose 11.0. The surrounding tissue was dissected and longitudinal sections from both organs (approximately 8-10 mm long) were prepared.

The two ends of each preparation were tied with ligatures. The distal end was connected to the organ holder; the proximal end was stretched and attached to a mechano-electrical transducer FSG-01 (Experimetria Ltd., Hungary) via a hook. The preparations were placed in organ baths TSZ-04/01, containing Krebs solution, pH 7.4, continuously bubbled with Carbogen (95% O₂, 5% CO₂). The organ baths were mounted in parallel above an enclosed water bath, maintaining the solution temperature at 37 °C. Preparations were placed under an initial tension (preload) of 1 g and allowed to equilibrate for at least 75 min (three periods: 15 min, 45 min and 15 min and two washes with Krebs solution between them). After

the equilibration period, preparations were influenced by Ang II and AVP in a dose of 1 μmol (10⁻⁶ M), applied separately.

Recording of mechanical activity

Mechanical activity was digitized and recorded by using S.P.E.L. ISOSYS Advanced Software (Experimetria Ltd., Hungary). The conversion of the data for later analysis was performed with KORELIA-Processing and the analysis and graphic processing—with KORELIA-Dynamics computer programs [17, 18].

Chemicals and drugs

Ang II (Sigma-Aldrich) and AVP (Sigma-Aldrich) were solubilized in bidistilled water. All reagents for the preparation of Krebs solution were purchased from Sigma-Aldrich.

Data analysis and statistical processing

The recorded force-vs.-time curves were analyzed including calculation of amplitudes, integral force of tonic contraction, presented as area under the curve (AUC), as well as determination of time-parameters. The different phases of the peptide - induced tonic contractions, were clarified and analyzed by application of a time -parameter analysis, similarly to that made in the study of the skeletal muscle contraction [19].

The following time-parameters were defined (Fig. 1.): 1st half-contraction time (T_{hc}), 2nd half-contraction time (T_c-T_{hc}), contraction time (T_c), half-relaxation time (T_{hr}), contraction plus half-relaxation time (T_{chr}).

The duration of the interval for analysis of tonic contraction was defined from the beginning of the contraction, until the amplitude fell to 50% (Fig.1).

For a better analysis and understanding of the different phases of the induced SMC, a normalization of time-intervals was performed. All of the normalized time-intervals were calculated as a relative part from T_{chr}.

Data obtained were processed by the statistical program Statistica 6.1, StaSoft, Inc. and presented as mean ± standard error. A P-value less than or equal to 0.05 was considered to be statistically significant.

RESULTS

Amplitude and AUC urinary bladder

After an equilibration period, the isolated strips from urinary bladder displayed spontaneous activity with an amplitude of 0.30 ± 0.06 g (n=19). Time-parameters of peptide-induced tonic contraction are presented on Fig. 1.

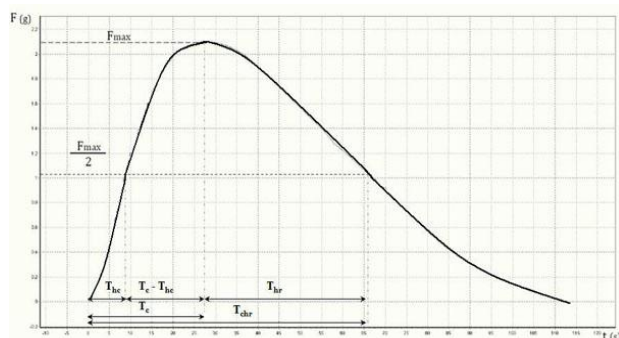


Fig. 1. Time-parameters of peptide-induced tonic contraction: F_{max} – maximal force of the smooth muscle contraction (SMC); $F_{max}/2$ – half of maximal force of the SMC; T_{hc} – 1st half-contraction time: the time interval between the start of the SMC and $F_{max}/2$; $T_c - T_{hc}$ – 2nd half-contraction time: the time interval between 1st half-contraction time and F_{max} ; T_c – time interval between the start of the SMC and F_{max} ; T_{hr} – time interval between F_{max} and $F_{max}/2$; T_{chr} – time between the beginning of the SMC until the amplitude fell to $F_{max}/2$.

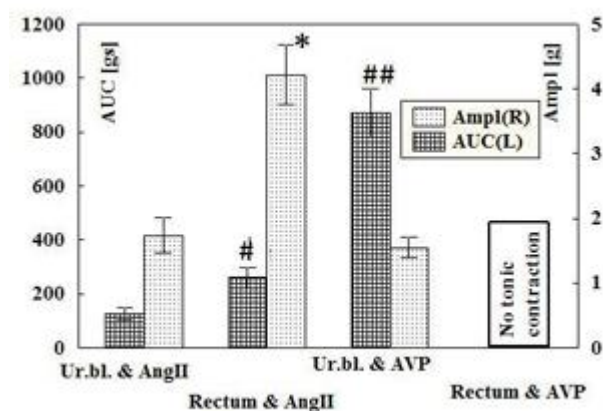


Fig. 2. Amplitudes and integral forces (presented as AUC) of Ang II- and AVP- induced tonic contractions from rat urinary bladder and rectum.

Ang II at a concentration 1 μmol induced tonic contraction with an amplitude of 1.74 ± 0.75 g ($n=10$) (Fig. 2, Fig. 3) and an integral force of muscle contraction of 126.6 ± 67.8 gs (Fig. 2).

AVP at the same concentration (1 μmol) induced tonic contractions with an amplitude of 1.55 ± 0.5 g ($n=18$) (Fig.2, Fig. 3). The integral force of AVP-induced contraction - 871.5 ± 287.8 gs was significantly greater than Ang II-provoked (Fig. 2).

Rectum

After a period of equilibration, the isolated longitudinal strips from rectum displayed spontaneous activity with an amplitude of 1.03 ± 0.5 g ($n=8$), which was significantly higher than the urinary bladder spontaneous activity. Ang II (1

μmol) led to significantly increased ($P < 0.05$) amplitude and integral muscle force of tonic contraction (4.22 ± 1.12 g, 260 ± 92.7 gs) in comparison to bladder contraction (Fig. 2 and Fig.3). The application of AVP in a concentration of 1 μmol did not cause onset of tonic contraction, but there was observed a noticeable increase in the frequency and the amplitude of the rectal phasic activity (Fig.3).

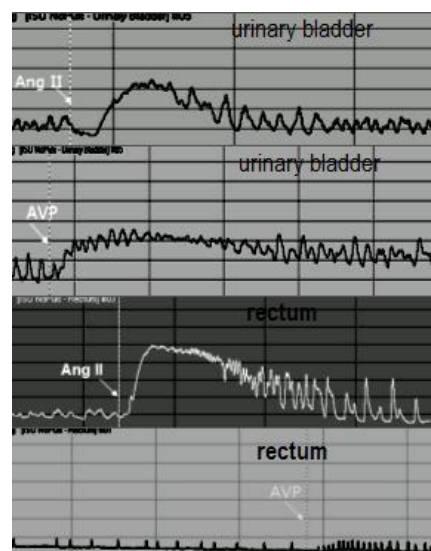


Fig. 3. Original recordings from S.P.E.L. ISOSYS Advanced Software (Experimetria Ltd., Hungary).

Time-parameter analysis

Regardless the reported differences in the amplitude and AUC of Ang II – induced rectal and urinary bladder contractions, such were not observed when time-parameter analysis was applied (Table 1). The initial time - parameter (T_{hc}) was significantly shorter in comparison to the subsequent interval ($T_c - T_{hc}$) and the parameter characterizing the process of relaxation (T_{hr}). In both of the Ang II – induced responses the interval for the second part of the development of contraction was bigger. Statistically significant differences between the absolute time-parameters of the Ang II- provoked contractions from the two preparations were observed only in the second half-contraction time (bladder - 19.5 ± 2.3 s and rectum - 29.5 ± 2.6 s). AVP-induced contraction was characterized by a significantly longer duration of all time-parameters compared to those induced by Ang II.

Table 1. Calculated time – parameters of Ang II – induced rectal and urinary bladder tonic contractions, as well as AVP – induced urinary bladder response. The application of 1µmol AVP did not led to appearance of rectal tonic contraction

Organ	Peptide	T _{hc} [s]	T _c -T _{hc} [s]	T _c [s]	T _{hr} [s]	T _{chr} [s]
Urinary bladder	Ang II	12.8±1.6	19.5±2.3	32.2±3.3	61.5±13.6	93.8±13.3
Rectum	Ang II	11.2±1.4	29.5±2.6	40.7±2.6	57.9±8.5	98.6±9.1
Urinary bladder	AVP	28.0±4.1	99.4±16.8	127.4±18.0	255.3±35.1	382.7±43.1

Normalized time - parameters

After the normalization of the time - parameters, the differences between AVP and Ang II - induced urinary bladder contractions disappeared. The normalized T_{hc} of AVP-induced bladder contraction was significantly less than that of Ang II-induced and represented 0.08 ± 0.01 and 0.16 ± 0.03, respectively (Fig. 4). The comparison of Ang II – provoked bladder and rectal responses revealed differences only in the second part of the contraction (0.23 ± 0.03 and 0.31 ± 0.03, respectively).

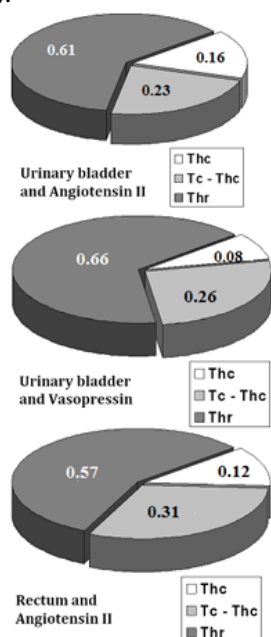


Fig. 4. Normalized time-parameters. All of the normalized time-intervals were calculated as a relative part from T_{chr}.

DISCUSSION

Ang II – and AVP- induced urinary bladder contractions: a detailed view and some assumptions

Ang II receptors have been discovered in detrusor of many species, including human and there is wide variation in the response to this peptide [1]. The application of Ang II and AVP in our experiments at a concentration of 1µmol led to

development of tonic contractions, which confirms our previous investigations and available literature data for the effect of these peptides on urinary bladder contractile activity [2, 12, 13, 20, 21].

The comparison of the results from the independent influence of Ang II and AVP on bladder activity demonstrates that the observed contractions were with approximately equal amplitude, but the developed integrated muscle force was significantly increased after the application of AVP. Time – parameter analysis indicates that Ang II causes contractions for a shorter period of time: the first and the second half – contraction time as well as half – relaxation time were significantly brief. AVP - induced response, which reached a noticeable maximal integrated force, is due to a prolonged achievement of the maxim and the subsequent much slower relaxation. The absence of significant differences in the normalized time - parameters, excluding the initial period of contraction, indicates that the bladder contractile responses to Ang II and AVP generally follow an identical pattern. This is precisely due to the activation of same signal transductional pathway by both peptides. Then what are the differences between the mechanisms of action of the two peptides that alter the muscle force and the absolute time – parameters? A possible explanation is that Ang II is metabolized and its derivatives are biologically active. Their effect, however, is opposite to that manifested by Ang II [22].

Also we can express the assumption that the probable reason for this difference is a consequence of the interaction of these two peptides with the ion channels of the plasmalemma. There is data for the impact of AVP over potassium channels of brain cells after fluid percussive brain injury indicating that AVP blunted K_{ATP} and K_{Ca} channels [23]. It is known that smooth-muscle cells of the bladder have a number of potassium channels, including ATP-dependent K channels and Ca-dependent K channels [2]. Such data could be a possible explanation for the prolonged effect of AVP on SMC.

Ang II stimulates the activity of T-type voltage dependent calcium channels in vascular smooth muscle cells [24]. We can assume that in the smooth muscle cells of the rat bladder is realized the similar effect.

Ang II – provoked rectal response. Comparison with the urinary bladder response

The application of Ang II on the rectal preparation caused a development of expressed tonic contraction, which amplitude and integral muscle force were significantly greater than those of the bladder. The higher amplitude is achieved at the expense of the second half of the contraction. The higher values of the absolute and normalized time – parameters for this interval are the evidence. The difference in the total muscle mass of the preparations significantly contributes for these distinctive force parameters. It is worth noted, that the time-parameters (absolute and normalized) of Ang II – mediated bladder and rectal SMC, with the exception of T_c – T_{hc} parameter, do not indicate significant differences. This proves the suggestion that in the urinary bladder and rectum the Ang II - mediated contractions are developed by similar mechanisms. Moreover, this assumption is an indirect evidence for an approximately equal density of Ang II receptors in these two organs. The uniformity of response to Ang II is supported by the fact that in the rectum a local renin-angiotensin system has also been established [14]. It could be considered again that the locally generated metabolites of Ang II contribute for this pattern of the contraction process.

Does AVP have an importance for the motility of the rectum?

Dose-dependent effects of AVP on gastro-intestinal tract from different species were observed, but regarding the rectal musculature the information is insufficient and controversial [25]. AVP has been shown to increase the gastric and duodenal motility in humans and rabbits [15, 16], as well as colonic peristalsis [16], but the expression of the exact AVP receptors in intestine has not been examined yet [16]. Some authors have demonstrated that AVP increase the gastro-intestinal motility via the oxytocin OT1 receptors, but the experiment is only for stomach and duodenum from rabbits [15].

In our study, the application of AVP does not significantly alter the characteristics of the spontaneous phasic contractile activity of the rectum. This could be explained with the absence of

AVP receptors type V1, which are present in the urinary bladder. In rectal musculature V2 receptors could be presented – in such a case, the rectum as a terminal department of gastro-intestinal tract shows analogy with the distal and the collecting tubules of the kidneys. This is still an assumption that remains to be investigated.

Acknowledgements: This study was supported by Grant 1/2010 from Trakia University, Stara Zagora, Bulgaria.

REFERENCES:

1. K. Andersson, A. Arner, *Physiol. Rev.*, **84**, 935 (2004).
2. B. Uvelius, S. Lundin, K. Andersson, *Eur. J. Pharmacol.*, **182**, 549 (1990).
3. Y.P. Fan, R. N. Puri, S. Rattan, *Am. J. Physiol. Gastrointest. Liver. Physiol.*, **282**, 461 (2002).
4. M. De Godoy, S. Rattan, *J. Pharmacol. Exp. Ther.*, **318**, 725 (2006).
5. W. Park, D. Regoli, F. Rioux, *Br. J. Pharmacol.*, **48**, 288 (1973).
6. G.F. Anderson, R.A. Barraco, H.J. Normile, T.N. Rosen, *Can. J. Physiol. Pharmacol.*, **62**, 390 (1984).
7. K. Andersson, H. Hedlund, M. Stahl, *Acta Physiol. Scand.*, **145**, 253 (1992).
8. N. Tanabe, A. Ueno, G. Tsujimoto, *J. Urol.*, **150**, 1056 (1993).
9. D. Weaver-Osterholtz, G. Reams, Z. Wu, J. Knaus, F. Campbell, J. Bauer, *Am. J. Kidney Dis.*, **28**, 603 (1996).
10. G. Szigeti, G. Somogyi, L. Csernoch, E. Széll, *J. Muscle Res. Cell Motil.*, **26**, 23 (2005).
11. A.T. Chiu, R. D. Smith, P. B. Timmermans, in: *Angiotensin Receptors*, J.M. Saavedra, P.B. Timmermans (eds.), 1st edition, Springer-Verlag, New York, 1994, p. 49.
12. D. J. Crankshaw, *Eur. J. Pharmacol.*, **173**, 183 (1989).
13. A. R. Dehpour, G. R. T. Kivaj, A. Delfan, M. Shahrokhi, *Gen. Pharmacol.*, **28**, 777 (1997).
14. M. De Godoy, S. Rattan, *J. Pharmacol. Exp. Ther.*, **319**, 1088 (2006).
15. Li, X. Kong, H. Liu, C. Liu, *Neurogastroenterol. Motil.*, **19**, 839 (2007).
16. B. Ohlsson, O. Bjorgell, O. Ekberg, G. Darwiche, *Gastroenterology*, **6**, 11 (2006).
17. K. Yankov, *Trakia J. Sci.*, **8**, 41 (2010).
18. K. Yankov, in: *Proceedings of the International Conference on Information Technologies (InfoTech-2011)*, R. Romanski (eds.), Technical University, Sofia, 2011, p. 225.
19. R. Raikova, H. Aladjov, *J. Electromyogr. Kinesiol.*, **14**, 227 (2004).
20. G. Ilieva, A. Tolekova, R. Sandeva, K. Trifonova, Z. Tsokeva, M. Ganeva, *Trakia J. Sci.*, **6**(2) supp. 1, 77 (2008).

21. P. Hadzhibozheva, R. Iliev, A. Tolekova, G. Ilieva, K. Trifonova, R. Sandeva, Z. Tsokeva, R. Kalfin, *Bulg. J. Vet. Med.*, **12**, 67 (2009).
22. R. Ardailou, D. Chansel, *Kidney Int.*, **52**, 1458 (1997).
23. W. Armstead, *Stroke*, **32**, 1408 (2001).
24. H. Lu, R. Fern, D. Luthin, J. Linden, L. Liu, C. Cohen, P. Barrett, *Am. J. Physiol.*, **271** (4 pt 1), 1340 (1996).
25. N. J. Gilmore, J. R. Vane, *Br. J. Pharmac.*, **38**, 633 (1970).

ЕФЕКТИ НА АНГИОТЕНЗИН II И ВАЗОПРЕСИН ВЪРХУ СЪКРАТИТЕЛНАТА АКТИВНОСТ НА ИЗОЛИРАНИ ТЪКАННИ ИВИЦИ ОТ ПИКОЧЕН МЕХУР И РЕКТУМ НА ПЛЪХ

П.В. Хаджибожева^{1*}, Ц.К. Георгиев¹, Р.Е. Калфин², А.Н. Толева¹

¹*Катедра по физиология, патофизиология и фармакология, Медицински факултет, Тракийски университет, Стара Загора, България*

²*Институт по невробиология, Българска академия на науките, София, България*

Постъпила на 10 юни, 2012 г.; приета на 26 юли, 2012 г.

(Резюме)

Целта на настоящото изследване е да се анализират и сравнят силата и времевите характеристики на Ангиотензин II (Анг II) и Аргинин-вазопресин (АВП) – предизвикани контракции на мускулни ивици от пикочен мехур и ректум на плъх, при проведени *in vitro* експерименти. Използвани са мъжки плъхове - линия Wistar, с тегло 250–300g. От пикочния мехур и ректума са приготвени лонгитудинални препарати, на които е въздействано самостоятелно с Анг II или АВП, в дози по 10^{-6} M. Записаните криви сила-време са анализирани посредством изчисляване на амплитуда на съкращението, площ под кривата (AUC), както и чрез определяне на някои времеви параметри. Анг II и АВП предизвикаха тонични контракции на пикочния мехур, със сходна амплитуда (съответно 1.74 ± 0.27 g и 1.55 ± 0.16 g), но с различни AUC. Отчетливи разлики се наблюдаваха при приложението на двата пептида върху гладко-мускулните препарати от ректум: Анг II предизвика тоничен отговор с амплитуда от 4.60 ± 0.42 g, докато АВП не промени съществено фазичната спонтанна активност на препаратите. Анализът по времеви параметри установи аналогично развитие на отговорите към Анг II и при двата вида органи. При пикочния мехур, наблюдаваните различия в Анг II – и АВП – медираните контракции биха могли да се дължат на допълнително действие на Анг II – деривати и/или на взаимодействието на двата пептида с йонните каналчета на плазмалемата. Сходството във времевите параметри на Анг II – предизвиканите съкращения на пикочния мехур и ректума насочва към вероятен сходен механизъм на развитие на контракцията при двата органа. Липсата на тоничен отговор при ректума, след въздействие с АВП, навярно се дължи на различен тип рецептори или модификации на трансдукционната сигнална верига.

Myocardial preconditioning by short ischemia-reperfusion cycles and levels of the peptide interleukin-8

R. Kalfin^{1*}, R. Alexandrova²

¹*Institute of Neurobiology, Bulgarian Academy of Sciences, Acad. G. Bonchev St., Block 23, Sofia 1113, Bulgaria*

²*Institute of Experimental Morphology, Pathology and Anthropology with Museum, Bulgarian Academy of Sciences, Acad. G. Bonchev St., Block 25, Sofia 1113, Bulgaria*

Received June 10, 2012; Accepted July 26, 2012

Coronary angiogenesis and collateral growth are chronic adaptations to myocardial ischemia. In human coronary atherectomy tissue significant expression and angiogenic activity of the pro-inflammatory chemoattractant peptide interleukin-8 (IL-8) was observed. The aim of the present study was to introduce a method for measuring the IL-8 levels in rat heart tissue and to study whether ischemic preconditioning enhances IL-8 level in the infarcted heart. We stimulated myocardial angiogenesis in Sprague Dawley rats through ischemic preconditioning in the form of *in vivo* 4 short repetitive cycles of coronary artery occlusion (5 min) each followed by reperfusion (10 min). Rats were randomly divided into 5 groups: baseline control; normoxia + sham surgery; ischemic preconditioning + sham surgery; normoxia + myocardial infarction; ischemic preconditioning + myocardial infarction. Tissue samples from left ventricle were homogenized and sonicated. Aliquots of homogenate supernatants were obtained and frozen at -70° C until thawed for assay by specific IL-8 ELISA. Samples were assessed in duplicate using cellular communication assay kit for rat IL-8 (GRO/CINC-1). Arteriolar and capillary density was evaluated by the standard deparaffinization protocol. We found that concentrations of IL-8 in the left ventricle were significantly elevated after 2, 4, 7, 14 and 28 days of left coronary artery occlusion in the ischemic preconditioning + myocardial infarction group as compared to the normoxia + myocardial infarction and/or baseline control. The nonparametric correlation showed that IL-8 concentration correlates significantly ($P < 0.05$) and negatively with arteriolar and capillary density. Therefore, IL-8 could be one of the angiogenesis “promoters” in the infarcted heart.

Key words: peptide, interleukin-8, myocardium, ischemia, heart

INTRODUCTION

The peptide Interleukin-8 (IL-8) is a chemoattractant cytokine for neutrophils [1], lymphocytes [2], and fibroblasts [3]. It is a representative of α -chemokines, and was also shown to induce migration and proliferation of endothelial cells [4, 5] and smooth muscle cells [6]. IL-8 is produced by monocytes, endothelial cells, fibroblasts, lymphocytes, neutrophils, keratinocytes, epithelial cells, hepatocytes, and lung macrophages. IL-8 is a potent cytokine involved in mitogenesis [6] and angiogenesis [5]. It was shown that at physiological concentrations human IL-8 induces transient neovascularization in a rabbit corneal pouch model, accompanied by a modest lymphocytic infiltrate [7]. In addition, IL-8 was reported to take part in neovascularization in a variety of tumors [8, 9].

On the other hand, coronary angiogenesis and

collateral growth are chronic adaptations to myocardial ischemia. Simonini *et al.* [10] observed significant expression and angiogenic activity of IL-8 in human coronary atherectomy tissue. Yang *et al.* [11] demonstrated that IL-8 promotes a pro-angiogenic response in endothelial cells. Evidence suggests that like other angiogenic factors, IL-8 may be down-regulated by the hypoxia cascade. Recently, an increase of plasma IL-8 level in patients with chronic heart failure was reported [12]. Having in mind all these facts, we examined a novel method of stimulating myocardial angiogenesis through short cycles of ischemic preconditioning followed by reperfusion.

EXPERIMENTAL METHODS

All animals used in this study received humane care in compliance with the principles of laboratory animal care formulated by the National Society for Medical Research and Guide for the Care and Use of Laboratory Animals published by NIH. The experimental protocol was performed after

* To whom all correspondence should be sent:
E-mail: reni_kalfin@abv.bg

receiving approval from the institutional Animal Care Committee.

Surgical procedures

Male Sprague Dawley rats weighting between 250 and 300 g were anesthetized with ketamine (100 mg/kg i.p.) and xylazine (10 mg/kg i.p.). As preoperative antibiotic cover we administered cefazolin (25 mg/kg i.p.). Rats were randomly divided into 5 groups: baseline control; normoxia + sham surgery; ischemic preconditioning + sham surgery; normoxia + myocardial infarction; ischemic preconditioning + myocardial infarction. After tracheotomy and initiation of ventilation, the heart was exposed through a left lateral thoracotomy. Non-traumatic occluder was applied on the left anterior descending coronary artery (LAD). The myocardium was preconditioned by carrying out a short duration of temporary regional ischemia (5 min) followed by a period of reperfusion (10 min), repeated 4 times. Myocardial infarction was produced by permanent LAD occlusion. The rats in the sham group underwent the same procedure except for the LAD ligation. After completion of all surgical procedures the chest wall was re-closed, rats received buprenorphine (0.1 mg/kg s.c.) and were placed on a heating pad while recovering from anesthesia.

IL-8 enzyme-linked immunosorbent assay (ELISA)

Tissue samples from left ventricle were homogenized and sonicated in 1 ml antiprotease buffer consisted of 1 x PBS with 2 mM phenylmethylsulfonyl fluoride, and 1 µg/ml each of leupeptin and pepstatin A. Total protein concentrations were determined using bicinchoninic acid protein assay kit (Pierce Chemical Company, Rockford, IL, USA). Aliquots of homogenate supernatants were obtained after centrifugation at 10 000 x g for 10 min and frozen at -70° C until thawed for assay by specific IL-8 ELISA. Samples were assessed in duplicate using commercially available cellular communication assay kit for rat IL-8 (GRO/CINC-1) from Amersham Pharmacia Biotech Inc., NJ, USA. The sensitivity of the assay was 0.49 pg/ml. Absorbency was measured by a plate reader at 450 nm. In the heart tissue IL-8 levels were scalar (amount per milligram protein).

Arteriolar and capillary density

The standard deparaffinization protocol was used. Endothelial cells were labeled using mouse monoclonal anti-CD31/PECAM-1 (1:100,

Pharmingen, San Diego, CA, USA) followed by a biotinylated horse anti-mouse secondary antibody (1:200 dilution). The reaction product (brown) was visualized with DAB substrate using the Vector ABC Vectastatin Elite Kit (Vectorlabs, Burlingame, CA, USA) and was counterstained with methyl green (Vectorlabs). On separate slides, vascular smooth muscle cells were labeled using mouse monoclonal anti-smooth muscle actin (1:50, Biogenex, San Ramon, CA, USA) followed by a biotinylated rat-adsorbed horse anti-mouse secondary antibody (1:200 dilution). The reaction product (violet) was visualized with VIP substrate using the Vector ABC Vectastatin Elite Kit (Vectorlabs). Images were captured and stored in digital ".tiff" format for later image analysis. Counts of arteriolar and capillary density per mm² were obtained after superimposing a calibrated morphometric grid on each digital image using Adobe Photoshop Software (Adobe Systems Inc., San Jose, CA, USA).

Statistical analysis

Data are presented as mean ± standard error of the mean (SEM). Differences between groups were tested by one-way ANOVA followed by Newman-Keuls post hoc multiple comparison test. Correlation of arteriolar or capillary density vs. IL-8 concentration in IPMI-group was performed according to the non-parametric statistical method of Spearman. Differences were considered significant when $P < 0.05$. All statistical analyses were performed using GraphPad Prism 3.03 (GraphPad Software Inc., San Diego, CA, USA).

RESULTS AND DISCUSSION

Concentrations of IL-8 in the left ventricle were significantly elevated after 2, 4, 7, 14 and 28 days of left coronary artery occlusion in the ischemic preconditioning + myocardial infarction group as compared to the normoxia + myocardial infarction and/or baseline control or sham groups, which we found to decrease gradually with time (Fig. 1).

Ischemic preconditioning increased capillary and arteriolar density in our experiments. The nonparametric correlation found by plotting of IL-8 levels vs. arteriolar or capillary density is shown in Figures 2 and 3, respectively. In both cases IL-8 concentration correlated with arteriolar and capillary density.

Significant experimental and clinical research has focused on protection of ischemic myocardium.

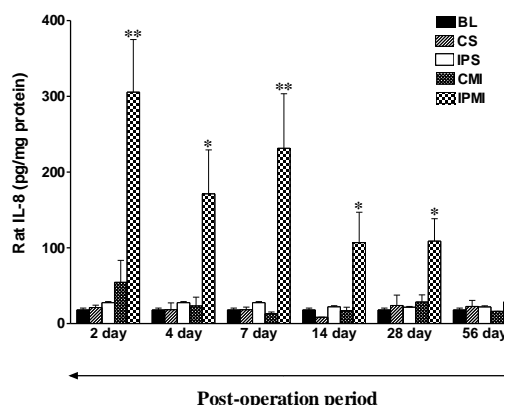


Fig. 1. Concentration of the peptide interleukin-8 (IL-8) in left ventricle of rats, randomly divided into five groups: baseline control (BS); normoxia + sham surgery (CS); ischemic preconditioning + sham surgery (IPS); normoxia + myocardial infarction (CMI); ischemic preconditioning + myocardial infarction (IPMI). Results are expressed as mean \pm S.E.M. of five hearts per group. Significant differences from the CMI group are indicated: * $P < 0.05$; ** $P < 0.01$.

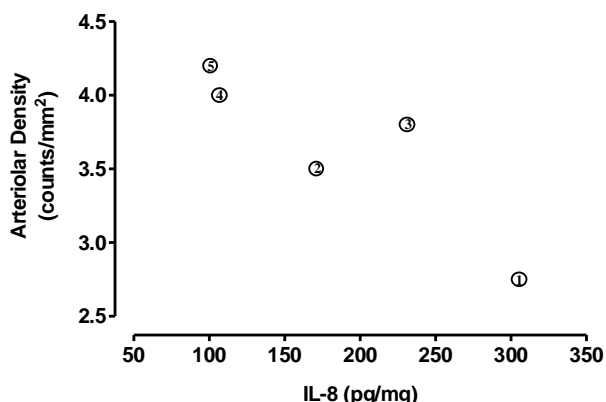


Fig. 2. Non-parametric Spearman correlation of the arteriolar density vs. interleukin-8 concentration in the left ventricle of IPMI (ischemic preconditioning followed by myocardial infarction) group: $P < 0.05$, $r = -0.91$.

Successful protection strategies are diverse and have included sublethal ischemia and certain pharmacological approaches. The biological process now recognized as "preconditioning" enhances endogenous cellular mechanisms within the myocardium, and results in protection against postischemic injury. Angiogenesis, i.e. the growth of new blood vessels from pre-existing vessels, is induced when the metabolic requirements of the tissue exceed the perfusion capability of existing vessels. It is a sequence of events and appears to be a tightly regulated process, for example by various

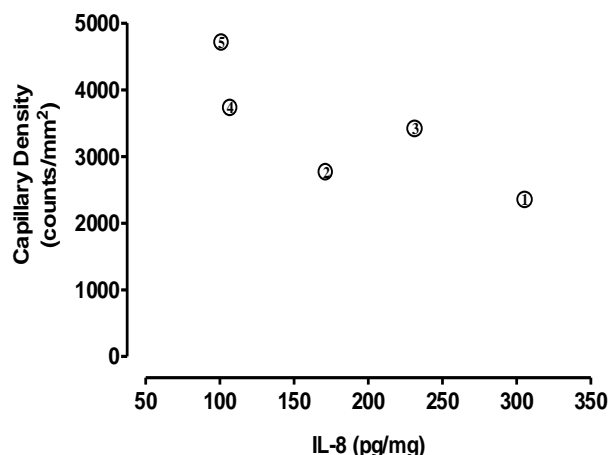


Fig. 3. Non-parametric Spearman correlation of the capillary density vs. interleukin-8 concentration in the left ventricle of IPMI (ischemic preconditioning followed by myocardial infarction) group: $P < 0.05$, $r = -0.90$. growth factors and cytokines. However, the initiation of angiogenesis still remains unclear. Among the various triggers of angiogenesis, tissue hypoxia has been identified as being a particularly important stimulus for the induction of new vessel growth [13, 14]. For example, for a large series of angiogenesis factors it has been shown that these were strongly induced by tissue hypoxia. Based on currently available data, hypoxia inducible angiogenesis factors are VEGF, IL-8, angiogenin, FGF and PDGF [15].

The cytokine interleukin-8 is considered to be involved in angiogenesis, since a structural amino acid ELR motif (Glu-Leu-Arg), present in CXC chemokines as IL-8, is suggested to be associated with stimulation of new blood vessels formation: chemokines that lack this motif, such as IL-10, appeared to be angiostatic [16, 17]. Our findings, described in the present study reveal that in the ischemic preconditioned infarcted heart increased IL-8 levels correlate significantly and negatively with arteriolar and capillary density, hence IL-8 could play a role of angiogenesis "promoter".

Acknowledgements: These studies were supported by NATO Grant LST.CLG.979224 between the University of Connecticut Health Center (UCONN), Farmington, CT, USA and the Institute of Neurobiology at Bulgarian Academy of Sciences. The Bulgarian partners are grateful to Prof. Nilanjana Maulik from the Department of Surgery at UCONN, USA, for the opportunity to carry out research in her laboratory.

REFERENCES

- 1 T. Yoshimura, K. Matsushima, I.J. Oppenheim, E.J. Leonard, *J. Immunol.* **139**, 788 (1987).
- 2 C.G. Larsen, A.O. Anderson, E. Appella, J.J. Oppenheim, K. Matsushima, *Science*, **243**, 1464 (1989).
- 3 J.R. Dunlevy, J.R. Couchman, *J. Cell. Sci.*, **108**, 311 (1995).
- 4 Z. Szekanecz, M.R. Shah, L.A. Harlow, W.H. Pearce, A.E. Koch, *Pathobiology*, **62**, 134 (1994).
- 5 A.E. Koch, P.J. Polverini, S.L. Kunkel, L.A. Harlow, L.A. DiPietro, V.M. Elner, S.G. Elner, R.M. Strieter, *Science*, **258**, 1798 (1992).
- 6 T. Yue, X. Wang, C. Sung, B. Olson, P.J. McKenna, J.L. Gu, G.Z. Feuerstein, *Circ. Res.*, **75**, 1 (1994).
- 7 Strieter R.M., Kunkel S.L., Elner V.M., C.L. Martonyi, A.E. Koch, P.J. Polverini, S.G. Elner, Interleukin-8, a corneal factor that induces neovascularization, *Am. J. Pathol.*, **141**, 1279 (1992).
- 8 E. Barcz, R.E. Skolinska, P. Kaminski, U. Demkow, K. Bobrowska, L. Marianowski, *Int. J. Gynaecol. Obstet.*, **79**, 229 (2002).
- 9 A. Yuan, C.J. Yu, K.T. Luh, S.H. Kuo, Y.C. Lee, P.C. Yang, *J. Clin. Oncol.*, **20**, 883 (2002).
- 10 A. Simonini, M. Moscucci, D.W.M. Muller, E.R. Bates, F.D. Pagani, M.D. Burdick, R.M. Strieter, *Circulation*, **101**, 1519 (2000).
- 11 Y.H. Yang, H. Zhou, N.O. Binmadi, P. Proia, J.R. Basile. *PLoS One*, 6(10):e25826, (2011).
- 12 C. Cappuzzello, L. di Vito, R. Melchionna, G. Melillo, L. Silvestri, E. Cesareo, F. Crea, G. Liuzzo, A. Facchiano, M.C. Capogrossi, M. Napolitano. *J. Transl. Med.*, **9**, 28 (2011).
- 13 O. Hudlicka, M. Brown, S. Egginton. *Physiol. Rev.*, **72**, 369 (1992).
- 14 A. Rivard, J. M. Isner, *Mol. Med.*, **4**, 429 (1998).
- 15 M. Kunz, S. M. Ibrahim, *Mol. Cancer*, **2**, 23 (2003).
- 16 R.M. Strieter, P.J. Polverini, S.L. Kunkel, D.A. Arenberg, M.D. Burdick, Kasper J., Dzuiba J., Van Damme J., Walz A., Marriott D, *J. Biol. Chem.*, **270**, 27348 (1995).
- 17 J.A. Belperio, M.P. Keane, D.A. Arenberg, C.L. Addison, J.E. Ehlert, M.D. Burdick, R.M. Strieter. *J. Leukoc. Biol.*, **68**, 1 (2000).

НИВА НА ПЕПТИДА ИНТЕРЛЕВКИН-8 ПРИ ПРЕКОНДИЦИЯ НА МИОКАРДА ПОСРЕДСТВОМ КРАТКИ ЦИКЛИ НА ИСХЕМИЯ-РЕПЕРФУЗИЯ

Р. Калфин^{1*}, Р. Александрова²

¹Институт по невробиология, Българска академия на науките, ул. «Акад. Г. Бончев», блок 23, София 1113, България

²Институт по експериментална морфология, патология и антропология с музей, Българска академия на науките, ул. «Акад. Г. Бончев», блок 25, София 1113, България

Постъпила на 10 юни, 2012 г.; приета на 26 юли 2012 г.

(Резюме)

Миокардът се приспособява към хроничната исхемия посредством растеж на малките кръвоносни съдове. Наблюдавано е, че коронарната атеректомия при човек значително увеличава експресията и ангиогенната активност на про-възпалителния хемоатрактантен пептид интерлевкин-8 (IL-8). Целта на настоящата работа беше да се въведе метод за измерване нивата на IL-8 в сърце на плъх и да се изследва дали исхемичната прекондиция повишава концентрацията на IL-8 при инфаркт на миокарда. Ние стимулирахме ангиогенезата в миокарда на плъхове от породата Sprague Dawley посредством исхемична прекондиция ин vivo под формата на 4 къси повтарящи се цикъла на коронарна артериална оклузия (5 мин) следвана от реперфузия (10 мин). Плъховете бяха разделени на 5 групи: контролна; нормоксия + отваряне на гръдния кош; исхемична прекондиция + отваряне на гръдния кош; нормоксия + инфаркт на миокарда; исхемична прекондиция + инфаркт на миокарда. Тъканните проби взети от лявата камера бяха хомогенизирани и соникирани с ултразвук. Течността от супернатантата беше разпределена в епендорфки и съхранявана при -70° С до провеждането на IL-8 специфичния ензим-свързан имunosорбентен анализ. Пробите бяха изследвани в дупликат чрез специфичен кит за определяне на плъши IL-8 (GRO/CINC-1). Плътността на артериолите и капилярите беше определяна посредством стандартен депарафиниционен метод. Установихме, че концентрацията на IL-8 в лявата камера е значително повишена на 2, 4, 7, 14 и 28 ден след оклузията на лявата коронарна артерия в групата с исхемична прекондиция + инфаркт на миокарда в сравнение с групата нормоксия + инфаркт на миокарда или контролната група. Непараметричният корелационен анализ показва значителна ($P < 0.05$) негативна корелация между концентрацията на IL-8 и плътността на артериолите и капилярите. Следователно, IL-8 може да бъде един от „промоторите“ на ангиогенезата при сърце в състояние на инфаркт.

New L- valine peptide mimetics as potential neuropharmacological agents

L. P. Tancheva¹, E. N. Encheva^{2*}, D. S. Tsekova³, L. G. Alova⁴, S. L. Stancheva⁴, V. V. Petkov¹,
M. T. Novoselski², R. Klisurov²

¹Behavior Neurobiology, Institute of Neurobiology, Bulgarian Academy of Sciences, Acad. G. Bonchev St., Block 23, 1113 Sofia, Bulgaria

²Department of Physiology, Medical Faculty, Medical University of Sofia, 1 Georgi Sofijski Str., 1431 Sofia, Bulgaria.

³Department of Organic Chemistry, University of Chemical Technology and Metallurgy, 8 Kliment Ohridsky Blvd., 1756 Sofia, Bulgaria

⁴Radioisotopic Laboratory, Institute of Neurobiology, Bulgarian Academy of Sciences, 1113 Sofia, Bulgaria

Received June 10, 2012; Accepted August 7, 2012

Aim of the present study was to evaluate the effect of four recently synthesized peptide mimetics, derivatives of L-Valine, containing moieties of nicotinic/isonicotinic acids and hydrophobic spacers with two different lengths, on the cognitive functions of rodents. Male Albino mice were treated with these compounds in daily doses 125 and 250 mg/kg b. wt. for 3 consecutive days. Their learning and memory were evaluated with Step-through test, their exploratory activity with Hole-board test and their muscular coordination - with Rota-rod test. The ability of the used substances to affect metabolism of biogenic amines in hippocampus was studied in *Wistar* rats, 1 hour after single treatment (250 mg/kg i.p.). Our results revealed a significant dose-dependent effect of two of the compounds, which appear as positional isomers and contain longer hydrophobic spacer. Their effect on the parameters of learning and memory, exploratory activity and muscular coordination, was well pronounced. The levels of neuromediators in hippocampus were significantly changed after a single treatment. Serotonin (5-HT) levels were increased significantly by both compounds, one of which increased also noradrenaline levels. The improving effect on cognitive functions of rodents is most probably related to the presence of L-Valine, as well as nicotinic or isonicotinic residue. The much stronger influence of the pair with a longer hydrophobic spacer is due to the better lipid solubility and the possible blood-brain barrier transport related to it, so as to modulate biogenic neuromediators' levels in rat hippocampus.

Key words: peptide mimetics, L-valine, nicotinic acid derivatives, cognitive functions, neuromediators, neuropharmacological effect

INTRODUCTION

Four newly synthesized peptide mimetics, derivatives of L-Valine bound to nicotinic or isonicotinic acids from one side and to alkyl hydrophobic spacer from the other side, have been synthesized by Tsekova et al. [1]. Their synthesis and self-assembly behavior have been published earlier [1-3] and some data for their biological properties have been recorded [4,5], although investigations on their biological activities are still in progress. In our previous publications these compounds were introduced as M3, P3, M6 and P6, where the sign M means derivatives of m-pyridinic (nicotinic) acid and P means derivative of p-pyridinic (isonicotinic) acid, while 3 and 6 point the number of methylene groups building the hydrophobic spacer in the molecule. All of them possess a very high ability to form intermolecular

H-bonds, and to self-assemble into supra-molecular complexes, particularly forming nano- and micro-filaments both in the absence of a solvent and in some solutions [1-3]. Determining of pKa shows that at pH=7 the four compounds exist mainly in their unionized form, which means that at physiological conditions (pH=7.4) they are again in a molecular (non-charged) form [5]. Studies of the solubility of these compounds in water and in octanol revealed a much higher (in orders) solubility in octanol than in water, defining high values of the partition coefficient (log P) that characterizes their distribution between water and lipid phase in the body [5].

Our previous studies established low *in vivo* oral and intraperitoneal toxicity (over 2000 mg/kg b.w.) and high therapeutic index for all studied substances (over 8). *In vitro* studies showed the lack of practical toxicity at concentrations 250 μ M -

toxicity is lower even than that of ascorbic acid (Vitamin C) [5]. Some changes in the orientation and nociception in white mice treated with the same substances were also established [5].

On the basis of all the data cited above we decided to study the neuropharmacological activities of these four peptide mimetics as potential pharmacological agents in rodents.

The aim of the study is to evaluate the ability of the used compounds to affect the cognitive functions of mice and to clarify some biochemical correlations in the rat brain after treatment with the compounds.

MATERIALS AND METHODS

Male ICR Albino mice were used for treatment with the targeted compounds in daily doses 125 and 250 mg/kg b. wt. intraperitoneally for 3 consecutive days. A control group has been treated with the same volume of solvent (Ol. Helianthi).

Several tests were performed to study the changes in the animals' cognition:

- for learning and memory (Step-through test) – on the 1st and 7th day,
- exploratory activity (Hole-board test) - on the 1st, 2nd and 3rd minute and
- muscular coordination (Rota-rod test).

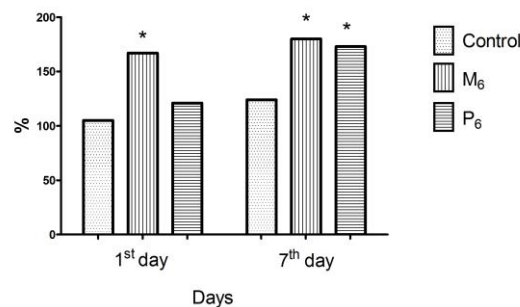
In parallel experiments the changes in biogenic levels in hippocampus of dopamine (DA), noradrenaline (NA) and serotonin- 5-hydroxytryptamine-(5-HT) were studied fluorimetrically 1 hour after single administration of M6 and P6 (250 mg/kg, b.wt. i.p). Experiments were performed on male Wistar rats, applying a method described by Jacobowitz et al (1978) [6].

The Student-Fisher test was used for statistical assessment of the experimental data.

RESULTS AND DISCUSSION

Our results demonstrate a significant improving effect of the pair of positional isomers with a longer spacer – both compounds M6 and P6 (125 mg/kg b wt, 3 days) - on all of the parameters studied: learning and memory, exploratory activity and muscular coordination.

As it is seen in Fig. 1, compound M6 has a positive influence on learning and memory in mice, evident both on the 1st and on the 7th days after treatment with the substances. Compound P6 has significant effect only on the 7th day, while the effect of M6 is well pronounced both on the 1st and on the 7th day (Fig. 1). It was established that the



* p<0.05

Fig. 1. Learning and memory after 3 days of treatment with M6 and P6 (125mg/kg, i.p.).

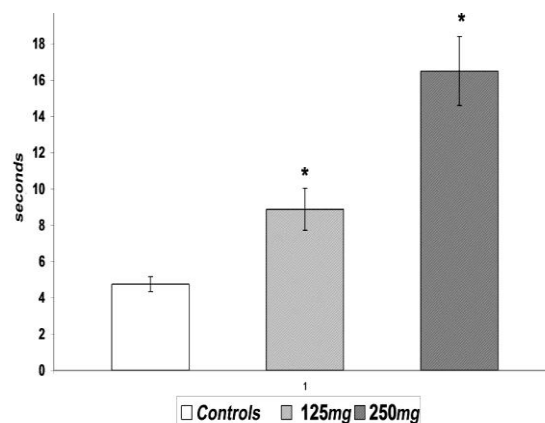


Fig. 2. Dose dependent effect of M6 on learning.

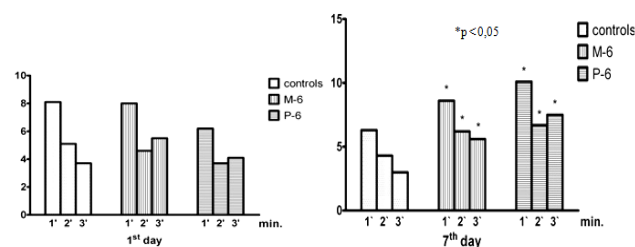


Fig. 3. Exploratory activity after 3-days of treatment with compounds M6 and P6.

positive effect of the compound M6 is dose-dependent (Fig. 2). Fig. 3 presents the effect of the active compound upon exploratory activity and it is well visible that both P6 and M6 compounds increase exploratory activity; although on the 1st day this influence was only slightly expressed, on the 7th day it had better expression. Neuromuscular coordination was improved significantly by M6 and P6 treatment and this effect was recorded not only on the 1st day, but also on the 7th day (Fig. 4).

The fact that the improving effect of the compounds lasts relatively long after the treatment-

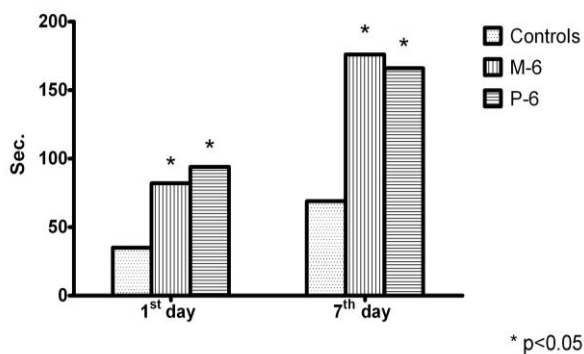


Fig. 4. Neuromuscular coordination (Rota rod test) after 3 days of treatment with M6 and P6

e.g. on the 7th day - is quite interesting and leads us to the suggestion of a slow metabolism and slow elimination of the studied compounds from the body.

The other two compounds – (M3 and P3), that contain 3 methylene groups in their spacer, did not affect significantly the processes of learning and memory (results are not presented) even though they increased moderately the exploratory activity of mice (Fig. 5a and 5b).

Both compounds decreased significantly motor coordination of the treated animals in comparison to the controls (with 22 % with M3 and 32 % with P3) (Fig. 6). Our experiments clearly demonstrated that the four used compounds can be divided into two groups on the basis of their investigated neuropharmacological activity, the first one including 6 methylene groups in their spacer –M6 and P6, which are positional isomers, and the second group: M3 and P3, another pair of positional isomers including 3 methylene groups in the molecule. The two groups affect cognitive functions of mice differently. All three parameters of the cognition (see above) were changed in a different way by the compounds with 6 methylene groups in the spacers in comparison to compounds with 3 methylene groups in the spacers. M6 and P6 increased them, as it is visible from Fig. 1 on the 1st, and with an enhanced effect on the 7th day; while M3 and P3 decreased them (they increased exploratory behavior as visible from the Hole-board test in Fig.5a and 5b).

The stable preventive effect of M6 and P6 on the cognitive processes, together with the physico-chemical analysis of compounds (water solubility and their partition coefficient), suggest a long half-life time and a slow metabolism of compounds in the body. Higher neuropharmacological activity of

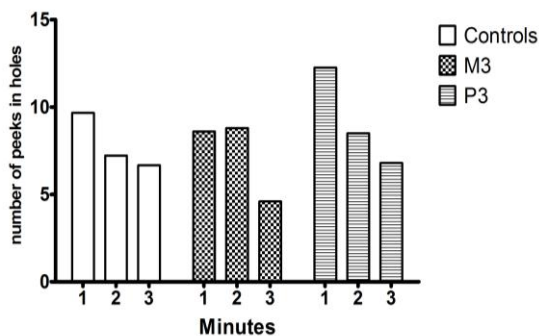


Fig. 5a. Hole-Board test for exploratory behavior in mice on the 1st day after 3 days of treatment with the compounds M3 and P3

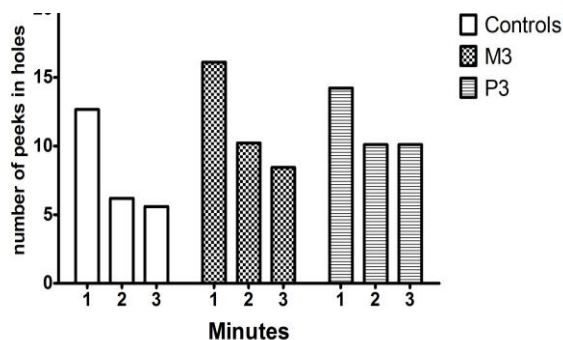


Fig. 5b. Hole-Board test for exploratory behavior in mice on the 3rd day after 3 days of treatment with the compounds M3 and P3.

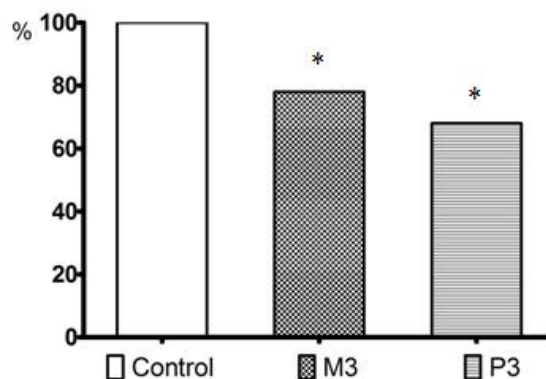


Fig. 6. Changes in neuromuscular coordination (Rota rod test) after 3 days of treatment with M3 and P3.

both compounds with 6 methylene groups spacer is probably related to their higher lipid solubility (higher log P) compared to shorter spacer ones [5]. Results obtained show that both compounds M6 and P6 influence the same cognitive functions, which is obviously due to the Val presence. The fact that the strength of their effect differs, we assume, is related to the different effects of the isonicotinic and nicotinic acid moieties, which are

positional isomers, contributing to the differences in the activity and pharmacokinetics of the compounds.

Biochemical studies in rat brain indicated significant changes in the levels of some neuromediators in the hippocampus after M6 and P6 treatment. Even after single administration both peptide mimetics with longer spacer increased significantly the serotonin (5-HT) levels in hippocampus in comparison to control levels. The isomer P6 increased significantly noradrenaline brain levels too.

The idea to use L- α -aminoacids and their derivatives for improving brain functions is not new. There are some publications in the literature revealing the important role of such substances for the better functioning of the CNS. The effects of several natural essential amino acids: branched-chain amino acids (BCAAs) and tryptophan, on the cognition of rodents and humans have been reported from other authors [7-9]. It has been reported in the literature that dietary BCAAs, including L-Val, ameliorated injury-induced cognitive impairment in mice [7], and also, supplementation with BCAAs in patients with severe traumatic brain injury improved recovery of cognition [8]. Dietary supplementation with tryptophan has been found to increase 5-HT levels in rat brain which correlated with a significant improvement in memory function of rats, as reported in a different study [9]. Also, a large body of research has documented memory-improving effects of the 5-HT uptake inhibitors, which are known to increase 5-HT-ergic neurotransmission by increasing 5-HT concentrations in the synaptic cleft [10].

Improving effects of the peptide mimetics containing L-Valine on some cognitive functions of rodents were also established in our experiment described here. Experimental results demonstrated positive effects of two of the newly synthesized peptide mimetics on cognitive functions and their biochemical correlates in rodents. Taking into account the important role of the hippocampus in cognition, we suggest that the increase of 5-HT level in this brain region by the compounds M6 and P6 may be one of the important neurochemical correlations of their nootropic effects.

The established changes in 5-HT and NA levels in rat hippocampus by P6 provided evidence for the realization of its CNS effect through changes in monoamine levels. P6 can modulate levels of

biogenic amines probably via regulation of the release of noradrenaline and serotonin.

We assume that the two new compounds with 6 methylene groups in the spacer can be useful as pharmacological modulators of declined cognitive functions, and they most probably exert their effects by influencing 5-HT metabolism in the brain.

CONCLUSIONS:

The neuropharmacological effects of M6 and P6 established in rodents can be related to the ability of compounds to modulate biogenic neurotransmitter levels in brain and especially 5-HT metabolism in hippocampus. The improving effect on cognitive functions of rodents is probably related to the presence of L-Valine, as well as of a nicotinic or isonicotinic residue, but the much stronger effect of the pair with a longer hydrophobic spacer is due to the better lipid solubility and is related to the possible transport to the brain cells.

Acknowledgements: This work was financially supported by University of Chemical Technology and Metallurgy (UCTM) - Sofia, under Scientific Project Grant No 10654/2008-2009

REFERENCES:

- 1 D. S. Tsekova, B. Escuder, J. F. Miravet, *Cryst Growth Des*, **8**, 11 (2008).
- 2 J. F. Miravet, B. Escuder, *Chem. Commun*, 5796, (2005).
- 3 D. S. Tsekova, J. A. Saez, B. Escuder, J. F. Miravet, *Soft Matter*, **5**, 3727 (2008).
- 4 L. Tancheva, V. V. Petkov, G. Karamukova, S. Abarova, Y. Chekalarova, D. Tsekova, B. Escuder, J. Miravet, K. Lyubomirova, *Bulg. Chem. Comm.*, **38**, 54 (2006).
- 5 D. S. Tsekova, E. Makakova, P. Alov, G. Gorneva, I. Pajeva, L. Tancheva, V. Petkov, A. Surleva, B. Escuder, J. Miravet, E. Katz, *Bulg. Chem. Comm.*, **41**, 133 (2009).
- 6 D.M. Jacobowitz, J.S. Richardson. *Pharmacol. Biochem. Behav*, **8**, 515 (1978)
- 7 J. T. Cole, C.M. Mitala, S. Kundu, A. Verma, J. A. Elkind, I. Nissim and A. S. Cohen, *PNAS*, **107**, 366 (2010)
- 8 R. Aqilani, P. Iadarola, A. Contardi, M. Boselli, M. Verri, O. Pastoris, F. Boschi, P. Arcidiaco, S. Viglio, *Arch. Phys. Med. Rehabil.*, **86**, 1729 (2005)
- 9 S. Khaliq, S. Haider, S. P. Ahmed, T. Perveen and D. J. Haleem, *Pak. J. Pharm. Sci.*, **19**, 11 (2006).
- 10 E. Nowakowska, K. Kus, T. Bobkiewicz-Kozłowska, H. Hertmanowska, *Pol. J. Pharmacol.*, **54**, 605 (2002)

НОВИ L-ВАЛИНОВИ ПЕПТИДОМИМЕТИЦИ КАТО
ПОТЕНЦИАЛНИ НЕВРОФАРМАКОЛОГИЧНИ АГЕНТИ

Л. П. Танчева¹, Е. Н. Енчева^{2*}, Д. С. Цекова³, Л. Г. Алова⁴, С. Л. Станчева⁴, В. В. Петков¹,
М. Т. Новоселски², Р. Ц. Клисуров²

¹*Поведенческа невробиология, Институт по невробиология, Българска академия на науките,
1113 София,*

²*Катедра по физиология, Медицински факултет, Медицински университет,
София 1431,*

³*Катедра „Органична химия“, Химикотехнологичен и металургичен университет,
Бул. „Климент Охридски“ № 8, 1756 София*

⁴*Радиоизотопна Лаборатория, Институт по невробиология, Българска академия на науките,
1113 София*

Постъпила на 10 юни, 2012 г.; приета на 7 август, 2012 г.

(Резюме)

Цел на настоящото изследване бе да се оцени ефекта на четири новосинтезирани пептидомиметика, производни на L-валин, съдържащи остатъци от никотинова/изоникотинова киселини, и хидрофобни спейсери с две различни дължини, върху когнитивни функции у гризачи. Бяха използвани мъжки лабораторни мишки, които бяха третираны с тези съединения в дневни дози по 125 и 250 mg/kg т.м. за три последователни дни. Техните памет и обучение бяха изследвани Step-through тест, изследователското им поведение - с Hole-board тест, а невро-мускулната им координация - с Rota-rod тест. Способността на изследваните вещества да повлияват метаболизма на биогенни амини в хипокамп, бе изследван при плъхове *Wistar*, 1 час след единична доза (250 mg/kg i.p.). Резултатите ни разкриха значителен дозо-зависим ефект на две от съединенията, които представляват позиционни изомери и съдържат по-дълъг хидрофобен спейсер. Ефектът им върху параметрите на обучение и памет, изследователска активност и невро-мускулна координация, бе добре изразен. Нивата на невромедиатори в хипокамп бяха значително променени след единично третиране. Серотониновите (5-НТ) нива бяха завишени значително и от двете съединения, едно от които увеличи също норадреналиновите нива. Подобряващият когнитивни функции у гризачи ефект на веществата най-вероятно е свързан с наличието на L-валинов, както и на никотинов или изоникотинов остатък. Много по-силното повлияване от страна на двойката с по-дълъг хидрофобен спейсер, за да могат да бъдат модулирани нивата на биогенни невромедиатори в плъшия хипокамп, се дължи на по-добрата липорастворимост на тези съединения, обуславяща възможния техен транспорт през кръвно-мозъчната бариера.

Thaumatococcus crystallization in hanging drop and in thin layer by vapour diffusion method

D.S. Tsekova

Department of Organic Chemistry, University of Chemical Technology and Metallurgy, 1756 Sofia

Received June 10, 2012; Accepted August 17, 2012

Crystallization of the protein Thaumatococcus in a drop and in a thin layer at hanging drop set up has been studied. Two main orientations of its tetragonal crystal were observed for crystals formed and grown on a flat foreign surface. They were well shaped inside the drop and show habitus changes as well as depression formations when growing in a thin layer. Crystals nucleated and grown at the end of the layer, often in agglomerates, also show specific morphology.

Keywords: Protein crystallization, Thaumatococcus, hanging drop method, solution layer, morphological (in)stability

INTRODUCTION

Crystallization of biological macromolecules is important for the X-ray diffraction studies, but it is also intensively exploited topic because of the efforts to understand the crystallization process. Biological macromolecules crystallize usually from complex aqua solutions with specific parameters like type and pH of the buffer, ionic strength, inorganic and organic additives and concentrations of all of the ingredients [1,2]. Developments in crystallization methodologies, protocols, and reagents are also facilitating crystallization efforts. The most often applied approach used for obtaining protein crystals is the vapour diffusion one, particularly as a hanging drop method. There are many publications relating to the application of this method and very few considerations of the processes that happen in such systems [3,4]. In this set-up several areas with different influence on the protein solution behaviour exist: bulk, contact of protein solution with the cover slide from one side and with the air – from the other side, as well as simultaneous contact of the protein solution with both solid surface and air. Studies of the influence of the cover slide surface, in some cases additionally treated to obtain new templates, as well as other solid foreign substrates, on the crystallization behaviour of proteins are published by many research groups [5]. It is well known that heterogeneous nucleation is easier than homogenous, so in case of attraction between a foreign surface and protein molecules,

crystallization is facilitated. Kaishev developed a model, to show that heterogeneous surface nucleation is easier than in the bulk, and also that the nucleation in a concave corner is easier than the surface one [6].

Here, crystallization of the protein Thaumatococcus in a hanging drop and in a solution layer again in the hanging drop set-up is presented. Solution layer, instead of hanging drop is a modification which is not recorded up to now in the literature. Results obtained concern microscope observations of the grown at these conditions crystals. Thaumatococcus is a sweet protein with molecular weight (Mw) of 22 kDa, 207 amino acids and isoelectric point of 12 [7]. Even it was crystallized in several different singonies, the most often used conditions for crystallization are from buffers with pH around 7 and the presence of tartaric acid or its sodium/potassium salts. Crystals grown and examined in this report were obtained also following this protocol and belong to the tetragonal space group P41212.

MATERIALS AND METHODS

Materials

Thaumatococcus from *Thaumatococcus daniellii* (T-7638.) was purchased from Sigma-Aldrich. Salts, buffers components, all used solvents were analytical-grade reagents (Sigma, Merck). Cover Glass 18x18 mm – Borosilicate glass, VWR (Cat No 631-0120).

Crystallization experiments were performed using 48 wells Linbro tissue boxes for vapour diffusion crystallization in hanging drop. Crystals

* To whom all correspondence should be sent:
E-mail: d_tsekova@uctm.edu

were observed by optical microscope Olympus BX51M equipped with a CCD video camera.

Cover slides cleaning

Glass slides were cleaned with a hot mixture of concentrated nitric and sulphuric acids (3:1 concentrated $H_2SO_4:HNO_3$) at 50–60 °C and then rinsed in deionized water until removing the acidic mixture. The washed slides were dried in an oven at 120 °C and after that cooled to room temperature.

Solutions used for protein crystallization

Thaumatococcus crystallization solutions were in 50 mM PIPES, pH=6.8, sodium potassium tartrate in the interval 0.34M to 1 M and Thaumatococcus from 16 to 75 mg/ml.

All solutions of protein and salts were prepared in appropriate buffer concentrations and were filtered prior to mixing for crystallization through 0.22 μ m porous filters.

Concentrations are defined according balance data for the solute and data for final solution volume presented in mg/ml, percent [%] or molar [M] units.

Hanging drop crystallization

The hanging drop method was performed in two variants – classical – protein solution is in the shape of a drop [1,2] and in a thin layer (see Figure 1).

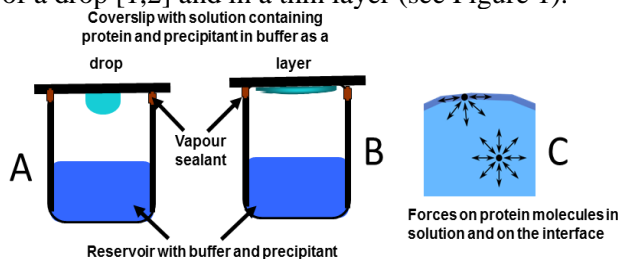


Fig. 1. Hanging drop crystallization set-up: **A.** in the classical (drop), and **B.** new modified variant (layer). **C.** Protein molecules in the bulk and on the interface. Intermolecular forces that arise between two equal molecules are demonstrated by arrows.

The set-up used consisted of 2-5 μ l protein containing solution placed on a clean or a salinized glass cover slide and stabilised over the reservoir solution of 200-500 ml. The reservoirs did not contain any protein. Crystallization occurs only in the protein solution on the cover slide. Normally, the initial relation of precipitant concentration in the protein solution (C_A) versus that in the reservoir ($2C_A$) is 1:2, which during the equilibrium leads to the protein solution volume shrinking twice (because of water evaporation) and adequate increasing of its supersaturation. In the classical

variant the protein solution is just dropped on the cover slide, which immediately is reversed and sealed over the reservoir.

A modification has been applied in the shape and the disposal of the protein solution for this study. Dropped by means of automatic pipette protein solution was purposely spared on the cover glass surface. In this procedure, the real spreading depended also on the hydrophobicity of the surface. The diameter of the layers in the described here experiments was in the range 5 – 8 mm and adequate layer thickness: 50–250 μ m.

In this set-up several important regions can be recognized (see Figure 1 C) – first - in the bulk, where the supersaturation is the main factor and second - on the interface, where solution contact either the surface of the cover slide or the air, and interactions with the foreign surface can have contribution to the process of crystal formation [5]. Besides these two cases of bulk and „solution-foreign surface“ interactions, we can distinguish a third possible location of protein molecules taking part in a nucleus formation – „solution-glass surface-air“, which is the circus line around the layer, laying on the cover slide. Interactions of the protein molecules situated exactly on this line differ from above commented cases – in the bulk and on smooth substrates. It is well known and also visible in the Figure 1 A and B that areas of contact of protein solution: „cover slide surface-solution“, „air-solution“ and „solution-glass surface-air“, in the solution layer variant are several times more extended than in the drop and it is on the account of the bulk interactions in the solution.

RESULTS AND DISCUSSIONS

Bulk crystallization of Thaumatococcus.

Crystals nucleated and grown at the conditions used and presented above, belong to the P41212 tetragonal space group. Typical habitus observed for such formed crystals is presented in the Figure 2. Bulk nucleated and grown crystals develop full number of faces typical for this space group, like it is presented in the Figure 2A. Of course, when crystal growth is hampered by different obstacles this shape is usually changed in various ways – faces smoothness violation, change in the number of appeared faces and so on.

Inside the droplet or the layer contacting with a flat foreign surface

The influence of solid surfaces, having different chemical composition and surface properties on the

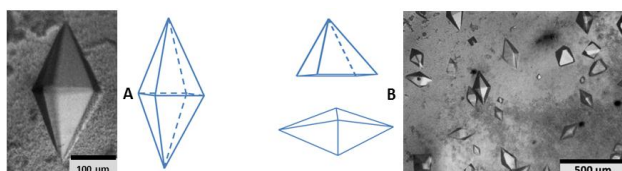


Fig. 2. Tetragonal Thaumatin crystals formed in a hanging drop. **A.** Bulk nucleated and grown crystal – photo and depicted crystal morphology. **B.** The most often revealed morphologies, containing reduced number of faces – depiction and photo. Crystals grown from 50 mM PIPES, pH=6.8, sodium potassium tartrate 0.5 M and Thaumatin 26 mg/ml.

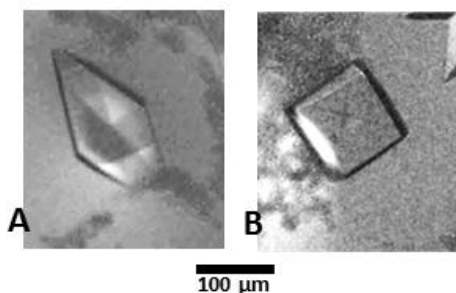


Fig. 3. Thaumatin crystals grown in a thin layer vapor diffusion. Two different orientations are shown, corresponding to these given in the Figure 2B. Crystals grown from Thaumatin of 16 mg/ml and sodium potassium tartrate 0.34 M in 50 mM PIPES, pH=6.8, solution layer on a glass slide covered by phenyl groups (see [8]).

crystallization of Thaumatin in consideration of number and sizes of crystals, was published as a different study [8]. Here attention is paid on the morphology of the crystals formed on an alien surface. Obviously the heterogeneously formed and grown on flat surfaces crystals develop reduced number or particularly developed faces like these ones presented in the Figure 2B. The same phenomena – growth of different orientations of crystals formed and grown on foreign surfaces was found for lysozyme and ferritin [9].

When the growth happens in a thin layer the lack of space reflects on the shape of the growing crystal. First of all, as it is visible from the Figure 3, apexes and edges necessary to have pyramidal constructions, like these presented in the Figure 2 miss here, instead new „faces“ parallel to the substrate tried to appear. Another important element in these crystals is the lack of smoothness of these „new faces“ and depression formations. This phenomena called „morphological instability“ was noticed before for other two proteins - lysozyme and ferritin crystals growing in a very thin (40 µm) glass cell [10] reaching during their growth a phase boundary. Actually papers concerning this polyhedral instability in case of

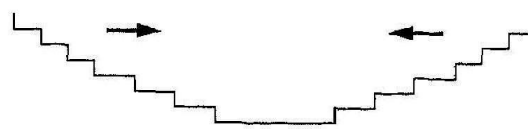


Fig. 4. Steps generated from the apexes that move towards the central part of a facet. The stability (flatness) of this face is determined by the step advance velocity and the step generation rate at the corners.

protein crystallization are limited in number [10,11]. More reports have been published for low molecular systems, where various attempts have been made to understand and predict morphological stability of growth of polyhedrons from solution [12].

When a polyhedral crystal grows from solution, the solute concentration around it is no uniform distributed, but the highest is around the edges and the lowest is in the central parts of the faces. That is why it is believed that 2D nucleation process of new layers is realized at the edges and continues propagation as new crystal layers towards the center of the face (see Figure 4). In the Figure 4 it is indicated how the steps generated from the two neighbouring corners are moving in opposite directions. When two steps meet, step annihilation occurs and a new facet is formed.

Chernov's theory for polyhedral stability [12a] is based on the idea, that the concentration inhomogeneity is compensated by the change of the kinetic coefficient in the center of the crystal face. He suggested: $\sigma_{corner}k_{corner} = \sigma_{center}k_{center}$, where σ is the supersaturation, given as a difference between real concentration in the corner (C_{corner}) or center (C_{center}) and equilibrium one (C_e); ($C_{corner} - C_e$ or $C_{center} - C_e$), and k is the kinetic coefficient. This compensation would work when the difference $C_{corner} - C_{center}$ is in a reasonable range, suggested to be lower than 10-20% [11]. If the solution becomes sufficiently thin, solute transfer along the growing face will be hampered and this difference will become higher, then the spreading speed of the steps will be low. As the steps are continuously generated from the corner of the crystal then the step density will be much higher around the corners decreasing toward the central part, so the face will lose the flatness and will develop depression in its center.

Depressions formed in these crystals, as it is well visible from the photos in the Figure 3, are polygonised and do not look as rough morphological defects, which is most probably a result from the slow kinetics of protein crystal growth.

*Crystals nucleated and grown on the contact area
„solid surface-protein solution-air“*

When a solution layer is used, often crystals formed on this border line (solid surface-protein solution-air) are many and sometimes agglomerate during their growth if they are very close each to other (see Figure 5). Reasons for that are more than one. According the theory, nucleation of crystals in

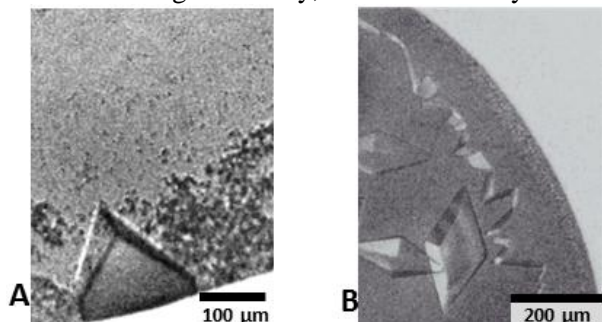


Fig. 5. Crystals nucleated and grown at the end of the solution layer. **A.** A monocrystal. Besides the reduced number of faces, the developed morphology also much differ than typical habitus of tetragonal Thaumatococcus crystals. **B.** Agglomerations surrounding the solution layer. Growing crystals merge and there is no visible boundary between different crystals.

a concave corner is even easier than on a smooth foreign surface [6] so many crystals are expected to be nucleated at this boundary. Although air cannot be considered as solid substrate, the forces acting on the interface solution-air favour increasing the concentration of molecules with hydrophobic regions on their surfaces [13,5h]. So to some extent the effect of the interphase can be expected to be similar to the hydrophobic surface. Therefore, the nuclei formed and grown on the border line – „substrate-solution-air“ most probably represent examples of crystals that nucleate in the concave corner [6], which are even smaller and have less number of faces than these formed on the surface. Also, right there it is expected the increasing in the local concentration (supersaturation) to be most pronounced because of the bevelling the layer, which causes additionally significant change in the morphology of growing there crystals.

CONCLUSIONS

The results obtained show that the crystallization of proteins is highly dependent on the presence of phase boundaries in the solution, e.g. solid substrates, air bubbles, solid impurities like dust, synthetic or natural fibres and so on. They can be used both to facilitate nucleation and to track the growth of crystals, which is important for

understanding the fundamental process of crystallization of proteins.

Depression formation on the surface of crystals growing at a phase boundary where the diffusion supply is hampered confirms that growth of the crystal face occurs by 2D nucleation and propagation of separate monolayers.

Results obtained reveal also that the equilibrium shape of crystals grown depends on where the nucleus was formed, as it was considered and derived by Kaischew [6]. Indeed, recent studies have shown that crystallization of some proteins and other low molecular compounds passes through two phases - liquid dense clusters and then solid nucleus inside the liquid phase [14], however, the observed phenomena clearly show that the surfaces have an impact on both the process of nucleation [5] and the shape of crystals further developed.

Acknowledgments: *The author thanks Dr Daryl R. Williams and Dr Jerry Y.Y. Heng, Imperial College, London for the opportunity to work in a collaboration with them and to use materials and facilities in their labs, so to conduct the experiments described in this work.*

REFERENCES:

- 1 A. McPherson, *Crystallization of Biological Macromolecules*, CSHL Press, Cold Spring Harbor, 1999.
- 2 R. Giege, A. Ducruix (Eds). *Crystallization of Nucleic Acids and Proteins : A Practical Approach*, Oxford University Press Inc., New York, pp 278-312, 1999.
- 3 (a) W. Fowles, L. J. DeLucas, P. J. Twigg, S. B. Hovard, E.J. Meehan, Jr & J.K. Baird, *J. Cryst. Growth* **90**, 117 (1988).
(b) V. Mikol, J.-L. Rodeau, R.Giege, *Anal. Biochem.* **186**, 332 (1990).
- 4 J.K. Baird, *Journal of Crystal Growth* 1999, 204, 553-562 *J. Cryst. Growth* **90**, 117 (1988).
- 5 (a) A.L. Grzesiak, A.J. Matzger, *Crystal Growth & Design* **8**, 347 (2008).
(b) T. Kubo, H. Hondoh, T. Nakada, *Crystal Growth & Design*, **7**, 416 (2007).
(c) G. Tosi, S. Fermani, G. Falini, J.A.G. Gallardo, J.M Garcia-Ruiz, *Acta Cryst. D* **64**, 1054 (2008).
(d) Y.-X .Liu, X.-J. Wang, J. Lu, C.-B. Ching, *J. Phys. Chem. B* **111**, 13971 (2007).
(e) E. Pechkova, C. Nicolini, *Nanotechnology* **13**, 460 (2002).
(f) C.N. Nanev, D. Tsekova Heterogeneous nucleation of hen-egg-white lysozyme-molecular approach. *Cryst. Res. Technol.* **35**, 189 (2000).
(g) L. Sun, J. Li, C. Xu, F. Yu, H. Zhou, L. Tang, J. He, *Acta Biochim. Biophys. Sin.* **42**, 332 (2010).
(h) D. Tsekova, S. Popova, C. Nanev, *Acta Cryst. D* **58**, 1588 (2002).

- (i) E. Saridakis, S. Khurshid, L. Govada, Q. Phan, D. Hawkins, G.V. Crichlow, E. Lolis, S.M.Reddy, N.E. Chayen, *PNAS* **108**, 11081 (2011).
6. R. Kaischew, *Comm. Bulg. Acad. Sci. (Phys.)* **1**, 100 (1950).
7. C.M. Ogata, P.F. Gordon, A.M. de Vos, S.-H. Kim, *J. Mol Biol.* **228**, 893 (1992).
8. D.S. Tsekova, D.R. Williams, J.Y.Y. Heng, *Chem. Eng. Sci.* **77**, 201 (2012).
- 9.(a) D.S.Tsekova, *Cryst. Growth Des.*, **9**, 1312(2009).
(b) D.S. Tsekova, *Bulg. Chem. Commun.* **38**, 67 (2006).
10. (a) D.S. Tsekova, PhD Thesis, Inst. Phys. Chem. Bulg. Acad. Sci., Sofia, 2002.
(b) C.N. Nanev, D.S. Tsekova, *Bulg. Chem. Commun.* **29**, 571 (1996/97).
11. C.N. Nanev, A.N. Penkova, *J. Cryst. Growth* **237–239**, 283 (2002).
12. (a) A.A. Chernov, S.R. Coriell, B.T. Murray, *J. Cryst. Growth* **132**, 405 (1993).
(b) C. N. Nanev, *J. Cryst. Growth* **140**, 381 (1994).
(c) M. Wang, R.-W. Peng, P. Bennema, N.-B. Ming, *Philos. Mag.* **71**, 409 (1995).
(d) W.R. Wilcox, *J. Cryst. Growth* **38**, 73 (1977).
13. R. Douillard, *Thin Solid Films*, **292**, 169 (1997).
14. (a) P.G. Vekilov, *Cryst. Growth Des.*, **4**, 671 (2004).
(b) D. Kashchiev, P.G. Vekilov, A.B. Kolomeiski, *J. Chem Phys.* **122**, 244706 (2005).

КРИСТАЛИЗАЦИЯ НА ТАУМАТИН ВЪВ ВИСЯЩА КАПКА И В ТЪНЪК СЛОЙ ЧРЕЗ ПРИЛАГАНЕ НА ПАРНО ДИФУЗИОННИЯ МЕТОД

Д.С. Цекова

Катедра по органична химия, Химикотехнологичен и металургичен университет, София 1756

Постъпила на 10 юни, 2012 г.; приета на 17 август, 2012 г..

(Резюме)

Изследвана е кристализацията на белтъка Тауматин в капка и в тънък слой по метода на висящата капка. Две основни ориентации на неговите кристали от тетрагоналната пространствена група са наблюдавани, типични за случаите на образуване и растеж върху плоска подложка. Кристалите са добре оформени, когато са нараствани в капка и с променен хабитус, често с образуване на вдлъбнатини, когато са нараствани в тънък слой. Образуваните и нарастнали в края на слоя кристали, рядко групирани в агломерати, също проявяват специфична морфология.

BULGARIAN CHEMICAL COMMUNICATIONS

Instructions about Preparation of Manuscripts

General remarks: Manuscripts are submitted in English by e-mail or by mail (in duplicate). The text must be typed double-spaced, on A4 format paper using Times New Roman font size 12, normal character spacing. The manuscript should not exceed 15 pages (about 3500 words), including photographs, tables, drawings, formulae, etc. Authors are requested to use margins of 3 cm on all sides. For mail submission hard copies, made by a clearly legible duplication process, are requested. Manuscripts should be subdivided into labelled sections, e.g. **Introduction, Experimental, Results and Discussion, etc.**

The title page comprises headline, author's names and affiliations, abstract and key words.

Attention is drawn to the following:

a) **The title** of the manuscript should reflect concisely the purpose and findings of the work. Abbreviations, symbols, chemical formulas, references and footnotes should be avoided. If indispensable, abbreviations and formulas should be given in parentheses immediately after the respective full form.

b) **The author's** first and middle name initials, and family name in full should be given, followed by the address (or addresses) of the contributing laboratory (laboratories). **The affiliation** of the author(s) should be listed in detail (no abbreviations!). The author to whom correspondence and/or inquiries should be sent should be indicated by asterisk (*).

The abstract should be self-explanatory and intelligible without any references to the text and containing not more than 250 words. It should be followed by key words (not more than six).

References should be numbered sequentially in the order, in which they are cited in the text. The numbers in the text should be enclosed in brackets [2], [5, 6], [9–12], etc., set on the text line. References, typed with double spacing, are to be listed in numerical order on a separate sheet. All references are to be given in Latin letters. The names of the authors are given without inversion. Titles of journals must be abbreviated according to Chemical Abstracts and given in italics, the volume is typed in bold, the initial page is given and the year in parentheses. Attention is drawn to the following conventions:

a) The names of all authors of a certain

publications should be given. The use of "*et al.*" in the list of references is not acceptable.

b) Only the initials of the first and middle names should be given.

In the manuscripts, the reference to author(s) of cited works should be made without giving initials, e.g. "Bush and Smith [7] pioneered...". If the reference carries the names of three or more authors it should be quoted as "Bush *et al.* [7]", if Bush is the first author, or as "Bush and co-workers [7]", if Bush is the senior author.

Footnotes should be reduced to a minimum. Each footnote should be typed double-spaced at the bottom of the page, on which its subject is first mentioned.

Tables are numbered with Arabic numerals on the left-hand top. Each table should be referred to in the text. Column headings should be as short as possible but they must define units unambiguously. The units are to be separated from the preceding symbols by a comma or brackets.

Note: The following format should be used when figures, equations, *etc.* are referred to the text (followed by the respective numbers): Fig., Eqns., Table, Scheme.

Schemes and figures. Each manuscript (hard copy) should contain or be accompanied by the respective illustrative material as well as by the respective figure captions in a separate file (sheet). As far as presentation of units is concerned, SI units are to be used. However, some non-SI units are also acceptable, such as °C, ml, l, etc.

The author(s) name(s), the title of the manuscript, the number of drawings, photographs, diagrams, etc., should be written in black pencil on the back of the illustrative material (hard copies) in accordance with the list enclosed. Avoid using more than 6 (12 for reviews, respectively) figures in the manuscript. Since most of the illustrative materials are to be presented as 8-cm wide pictures, attention should be paid that all axis titles, numerals, legend(s) and texts are legible.

The authors are asked to submit **the final text** (after the manuscript has been accepted for publication) in electronic form either by e-mail or mail on a 3.5" diskette (CD) using a PC Word-processor. The main text, list of references, tables and figure captions should be saved in separate files

(as *.rtf or *.doc) with clearly identifiable file names. It is essential that the name and version of the word-processing program and the format of the text files is clearly indicated. It is recommended that the pictures are presented in *.tif, *.jpg, *.cdr or *.bmp format, the equations are written using "Equation Editor" and chemical reaction schemes are written using ISIS Draw or ChemDraw programme.

The authors are required to submit the final text with a list of three individuals and their e-mail addresses that can be considered by the Editors as potential reviewers. Please, note that the reviewers should be outside the authors' own institution or organization. The Editorial Board of the journal is not obliged to accept these proposals.

EXAMPLES FOR PRESENTATION OF REFERENCES

REFERENCES

1. D. S. Newsome, *Catal. Rev.–Sci. Eng.*, **21**, 275 (1980).
2. C.-H. Lin, C.-Y. Hsu, *J. Chem. Soc. Chem. Commun.*, 1479 (1992).
3. R. G. Parr, W. Yang, *Density Functional Theory of Atoms and Molecules*, Oxford Univ. Press, New York, 1989.
4. V. Ponec, G. C. Bond, *Catalysis by Metals and Alloys (Stud. Surf. Sci. Catal., vol. 95)*, Elsevier, Amsterdam, 1995.
5. G. Kadinov, S. Todorova, A. Palazov, in: *New Frontiers in Catalysis (Proc. 10th Int. Congr. Catal., Budapest, 1992)*, L. Guzzi, F. Solymosi, P. Tetenyi (eds.), Akademiai Kiado, Budapest, 1993, Part C, p. 2817.
6. G. L. C. Maire, F. Garin, in: *Catalysis. Science and Technology*, J. R. Anderson, M. Boudart (eds), vol. 6, Springer-Verlag, Berlin, 1984, p. 161.
7. D. Pocknell, *GB Patent 2 207 355* (1949).
8. G. Angelov, PhD Thesis, UCTM, Sofia, 2001.
9. JCPDS International Center for Diffraction Data, Power Diffraction File, Swarthmore, PA, 1991.
10. *CA* **127**, 184 762q (1998).
11. P. Hou, H. Wise, *J. Catal.*, in press.
12. M. Sinev, private communication.
13. <http://www.chemweb.com/alchem/articles/1051611477211.html>.

CONTENTS

<i>B.A. Fil, A. E. Yilmaz, R. Boncukcuoğlu, S. Bayar</i> , Removal of divalent heavy metal ions from aqueous solutions by Dowex HCR-S synthetic resin.....	201
<i>D. Plachkova-Petrova, P. Petrova, St. Miloshev, Ch. Novakov</i> , Optimization of reaction conditions for synthesis of C-tetramethylcalix[4]-resorcinarene.....	208
<i>A.G. Chapkanov, B.B. Ivanova</i> , Structural and spectroscopic characterization of 2-amino-3, 5-dibromopyridin.....	216
EDITORIAL, 6 th Bulgarian Peptide Symposium, Sofia, 2011.....	221
<u>S. S. Pancheva</u> , <i>R. H. Kalauzka, E. S. Jovcheva, T.A.Dzimbova, E. P. Popgeorgieva, T. I. Pajpanova</i> , Novel cysteic acid S-amides substituted in the sulfonamide function. Synthesis and modifications.....	222
<i>A.G. Chapkanov, T.A. Dzimbova, B.B. Ivanova</i> , A facile synthesis and IR-LD spectral elucidation of <i>N</i> -acetyl amino acid derivatives.....	228
<i>S.Ts. Staykova, B.D. Mihaylova, I.G. Goshev, D.W. Wesselinova, L.T. Vezenkov, E.D. Naydenova</i> , Antioxidant capacity of new analogs of octreotide.....	233
<i>D.L.Danalev, R.N.Raykova, D.A.Marinkova, L.K.Yotova, S.G. Bayryamov, B.H.Hristova, V.S. Stoyanova</i> , Synthesis of new hybrid cell penetrating peptides-medical drugs molecules.....	238
<i>T. Dzimbova, R. Mavrevski, N. Pencheva, T. Pajpanova, P. Milanov</i> , Computer modelling of ligand-receptor interactions – enkephalin analogues and delta-opioid receptor.....	242
<i>R. Kalfin, E. Leventieva-Necheva, G. Sgaagli, F. Pessina</i> , Neuropeptides and urinary bladder ischemia-reperfusion injury.....	247
<i>P.V. Hadzhibozheva, T.K. Georgiev, R.E. Kalfin, A.N. Tolekova</i> , Angiotensin II and Vasopressin effects on motor activity of rat isolated tissue strips from urinary bladder and rectum	252
<i>R. Kalfin, R. Alexandrova</i> , Myocardial preconditioning by short ischemia-reperfusion cycles and levels of the peptide interleukin-8.....	258
<i>L. P. Tancheva, E. N. Encheva, D. S. Tsekova, L. G. Alova, S. L. Stancheva, V. V. Petkov, M. T. Novoselski, R. Klisurov</i> , New L- valine peptide mimetics as potential neuropharmacological agents.....	262
<i>D.S. Tsekova</i> , Thaumatin crystallization in hanging drop and in thin layer by vapour diffusion method.....	267
INSTRUCTIONS TO THE AUTHORS.....	272

СЪДЪРЖАНИЕ

<i>Б.А. Фил, А.Е. Йилмаз, Р. Бонджукджуюолу, С. Баяр</i> , Отстраняване на двувалентни йони на тежки метали от водни разтвори със синтетична йонообменна смола Dowex HCR-S.....	207
<i>Д. Плачкова-Петрова, П. Петрова, Ст. Милошев, Хр. Новаков</i> , Оптимизация на реакционните условия за синтез на С-тетраметилкаликс[4]-резорцинарени.....	215
<i>А. Г. Чапкънов, Б. Б. Иванова</i> , Структурно и спектроскопско охарактеризиране на 2-амино-3, 5-дибромопиридин.....	220
Редакционна: 6-ти български пептиден симпозиум, София, 2011.....	221
<i>С.С. Панчева</i> , <i>Р.Х. Калаузка, Е.С. Йовчева, Т.А. Дзимбова, Е.П. Попгеоргиева, Т.И. Пайпанова</i> , Нови S-амиди на цистеиновата киселина, заместени в сулфонамидната група. Синтез и модификации.....	222
<i>А. Г. Чапкънов, Т. А. Дзимбова, Б. Б. Иванова</i> , Синтез и ИЧ-ЛД спектрално определяне на N-ацетил аминокиселинни производни	228
<i>С. Ц. Стайкова, Б. Д. Михайлова, И. Г. Гошев, Д. В. Веселинова, Л. Т. Везенков, Е.Д. Найденова</i> , Антиоксидантен капацитет на нови аналози на октреотид.....	237
<i>Д. Л. Даналев, Р.Н. Райкова, Д.А. Маринкова, Л.К. Йотова, С.Г. Байрямов, Б.Х. Христова, В.С. Стоянова</i> , Синтез на нови хибридни молекули включващи мембранно проникващи пептиди и лекарствени молекули	241
<i>Т. Дзимбова, Р. Мавревски, Н. Пенчева, Т. Пайпанова, П. Миланов</i> , Компютърно моделиране на взаимодействието лиганд-рецептор – енкефалинови аналози и делта-опиоиден рецептор.....	246
<i>Р. Калфин, Е. Левентиева-Нечева, Дж. Сгарали, Ф. Песина</i> , Невропептиди и увреждане на пикочния мехур вследствие исхемия и реперфузия.....	251
<i>П. В. Хаджибожева, Ц. К. Георгиев, Р. Е. Калфин, А. Н. Толева</i> , Ефекти на Ангиотензин II и Вазопресин върху съкратителната активност на изолирани тъканни ивици от пикочен мехур и ректум на плъх	257
<i>Р. Калфин, Р. Александрова</i> , Нива на пептида интерлевкин-8 при прекондия на миокарда посредством кратки цикли на исхемия-реперфузия.....	261
<i>Л. П. Танчева, Е. Н. Енчева, Д. С. Цекова, Л. Г. Алова, С. Л. Станчева, В. В. Петков, М. Т. Новоселски, Р. Ц. Клисуров</i> , Нови L-валинови пептидомиметици като потенциални неврофармакологични агенти	266
<i>Д. С. Цекова</i> , Кристализация на Тауматин във висяща капка и в тънък слой чрез прилагане на парно дифузионния метод.....	271

NOTES TO CONTRIBUTORS

The journal BULGARIAN CHEMICAL COMMUNICATIONS publishes research papers and invited reviews in all branches of Chemistry: General and Inorganic, Analytical, Physical, Organic, Polymer, Theoretical, Chemical Engineering, and Biochemistry.

Manuscripts are submitted by e-mail or mail. They should be in a concise and clear style. The text must be typed double-spaced, on A4 format paper using Times New Roman font size 12, normal character spacing and should not exceed 15 pages (about 3500 words), including photographs, tables, drawings, formulae, *etc.* Authors are requested to use margins of 3 cm on all sides. Hard copies should be submitted in duplicate and reproduced by a clearly legible duplication process.

Manuscripts are published in English. All papers should be supplied with a summary. It has to be self-explanatory and clear, without reference to the text, and should not exceed 250 words.

Key words (up to 6) should be indicated on a separate line after the summary.

The first and the middle name of the authors are to be indicated by initials, the family name(s) of the author(s) are to be given in full. The name of the author to whom correspondence should be addressed is to be marked by an asterisk. The affiliation of the author(s) should be listed in detail (no abbreviations!).

References, quoted in the manuscript by Arabic numerals in square brackets set on the line, should be typed on a separate sheet. The names of all authors of a certain publication should be given. The use of “*et al.*” in the list of references is not acceptable. Titles of journals must be abbreviated according to Chemical Abstracts.

Figure captions and tables should be appended to the manuscript in separate files (sheets). Special attention is drawn to conciseness of captions. Author(s) name(s), title of the paper, number of drawings, photographs, diagrams, *etc.*, should be written on the back of the illustrative material in accordance with the list enclosed. Avoid using more than 6 (12 for reviews, respectively) figures in the manuscript.

The final text should be submitted by e-mail or on a 3.5” diskette (CD). The main text, list of references, tables and figure captions should be saved in separate files as *.rtf or *.doc of Word processor with clearly identifiable file names. Pictures should be presented in *.tif, *.jpg, *.cdr or *.bmp format, the chemical reaction schemes should be written using ISIS Draw or ChemDraw programme.

The authors are required to list three individuals and their e-mail addresses that can be considered by the Editors as potential reviewers. Please, note that the reviewers should be outside the authors’ own institution or organization. The Editorial Board of the journal is not obliged to accept these proposals.

Instructions about Preparation of Manuscripts can be found at:

<http://cl.bas.bg/hosted-journals-of-the-bulgarian-academy-of-sciences/bulgarian-chemical-communications/>

Manuscripts and enclosures should be sent to:

Prof. V. Beschkov
Editor-in-Chief
Bulgarian Chemical Communications
Institute of Chemical Engineering
Bulgarian Academy of Sciences
Acad. G. Bonchev St., Block 103
1113 Sofia
Bulgaria
E-mail: bioreac@bas.bg or vbeschkov@yahoo.com

or

Prof. D. Yankov
Editor
Bulgarian Chemical Communications
Institute of Chemical Engineering
Bulgarian Academy of Sciences
Acad. G. Bonchev St., Block 103
1113 Sofia
Bulgaria
E-mail: yanpe@bas.bg

ISSN 0324-1130